

MODIS VEGETATION INDEX (MOD13)

ALGORITHM THEORETICAL BASIS DOCUMENT

Version 2

Alfredo Huete¹
Chris Justice²
(Team Members)

and

Wim van Leeuwen¹
(Associate team member)

¹429 Shantz Bldg. #38
University of Arizona
Tucson, AZ 85721

²University of Maryland/ NASA - GSFC
Greenbelt, MD 20771

October, 1996

Table of contents

Table of contents	i
List of Figures	iii
List of Tables	v
 MODIS VEGETATION INDICES	 1
1.0 Introduction	1
1.1 Identification of Algorithms	2
2.0 Overview and background information	3
2.1 Experimental Objective	4
2.2 Historical perspective	5
2.2.1 NDVI limitations	8
2.2.2 Atmospheric effects	9
2.2.3 Angular considerations	10
2.2.4 Saturation problems	10
2.2.5 Canopy background contamination	12
2.2.6 Canopy structural effects	13
2.2.7 New and improved vegetation indices	14
2.3 Instrument characteristics	18
3.0 Algorithm Description	20
3.1 Theoretical Description	20
3.1.1 Linearity and Saturation Considerations	25
3.1.2 Vegetation - Background Interactions	31
3.1.3 Atmospheric aerosol corrections	34
3.1.4 Variance and Uncertainty Estimates	38
3.1.5 Temporal and spatial compositing of MODIS VIs (Level 3)	43
3.1.5.1 Angular, View and sun angle considerations	43
3.1.5.2 Maximum value composite (MVC) approach	45
3.1.5.3 Compositing period	49
3.1.6 Vegetation index composite algorithm	49
3.1.6.1 Description of Algorithm	49
3.1.6.2 Continuity vegetation index : NDVI compositing scenario	54
3.1.6.3 BRDF algorithm	54
3.1.6.4 MODIS BRDF product (MOD09B)	55
3.1.7 Vegetation index composite scenarios	56
3.1.7.1 Maximum value compositing scenario (MVC)	56
3.1.7.2 Minimum view angle composite scenario (MV-MVC)	56
3.1.7.3 View angle threshold composite scenario (TV-MVC)	57
3.1.7.4 Constraint view angle composite scenario (CV-MVC)	57
3.1.7.5 Three method composite scenario (TV-MVC/BRDF/MVC)	57
3.1.7.6 BRDF and MVC based composite scenario (BRDF/MVC)	57
3.1.7.7 Version 1 MODIS composite scenario (BRDF/CV-MVC/MVC)	58
3.1.7.8 Alternative composite approaches	59
3.1.7.9 Accuracy of BRDF models (PARABOLA)	61
3.1.7.10 Solar zenith angle effects on VI (PARABOLA)	63
3.1.7.11 BRDF models and VI compositing scenarios (ASAS)	66
3.1.7.12 Anisotropy of the enhanced VIs (ASAS)	71
3.1.7.13 Multi-temporal AVHRR Data, results for different composite scenarios	74
3.1.7.14 Continuity with AVHRR	78
3.2 Practical considerations	83
3.2.1 Numerical computation considerations (section from Trevor)	83

3.2.2 Programming/Procedural considerations	83
3.2.3 Calibration and Validation	84
3.2.3.1 Introduction	84
3.2.3.2 Validation criteria	85
3.2.3.3 Pre-launch algorithm test/development activities	89
3.2.3.4 Post-launch activities	92
3.2.4 Quality control and diagnostics	98
3.2.4.1 Level 2 vegetation indices	98
3.2.4.2 Level 3 vegetation index compositing	98
3.2.4.3 Run time data quality assurance (QA) evaluation	99
3.2.4.4 Run time Quality Control (QC) for daily and composited NDVI and SARVI	99
3.2.4.5 Run time product metadata QA considerations for Level 2 and Level 3	102
3.2.4.6 Post run time QA	102
3.2.4.7 DATA and Tools to be used	102
3.2.5 Exception handling	103
4.0 Constraints, Limitations, Assumptions	103
ACKNOWLEDGMENTS	104
REFERENCES	105

APPENDIX A: ERROR ANALYSIS

APPENDIX B: SWAMP REVIEW June 1994

APPENDIX C: SWAMP REVIEW May 1996

APPENDIX D: Response to review of 1994 and 1996

List of Figures

Figure. 2.1 Relationship between NDVI and fAPAR for wheat (From Asrar et al., 1984)	6
Figure. 2.2 Simplified seasonal - temporal vegetation index profile	7
Figure 2.3: Plot of biome-averaged integrated NDVI measurements versus published mean biome net primary productivity rates for North-America (From Goward et al.,1985)	8
Figure 2.4. Relationship between FPAR and NDVI based on observations and canopy modeling (From Moreau and Li, 1996).	11
Figure 2.5: Vegetation indices a) NDVI and b) SR derived from BRFs measured over a developing alfalfa for a range of LAIs (From Walter Shea et al., 1996).	15
Figure 3.1: Reflectance signatures for soil and leaves (From Tucker and Sellers, 1986)	21
Figure 3.2 Cloud of reflectance points in NIR-red waveband space for agricultural crops observed throughout the growing season (X-corn; O-cotton; *-wheat; A-alfalfa; S-soil).	22
Figure 3.3. Reflectance spectra from Landsat TM 5 plotted in red-NIR space for a wide range of land surface cover types.	22
Figure 3.4 Functional equivalency for NDVI and SR (a) and (b) the non functional equivalency between NDVI and DVI.	24
Figure 3.5 Vegetation index response (a-j) as a function of LAI for corn and cotton and different soil backgrounds	27-29
Figure 3.6 SR, NDVI and SAVI as a function of the NIR for a range of vegetation types (LANDSAT) .	30
Figure 3.7 Spectral reflectance signatures for conifer forest sites along the Oregon transect (NDVI and SARVI2 values are annotated for each spectral signature)	31
Figure 3.8 Vegetation index isoline in NIR-red reflectance space as modeled by the SR, NDVI, PVI, and SAVI	33
Figure 3.9 Simulated VI response as a function of Cedar LAI for different atmospheric aerosol conditions (Rayleigh and ozone corrected)	35
Figure 3.10: Illustration of the smoke correcting properties of the SARVI2 (a) along with the NDVI (b) and a color composite (c).	37
Figure 3.11 Comparison of VI absolute error (a) and vegetation equivalent noise (b) among various instrumental and environmental variables, based on simulated Cedar data.	42
Figure 3.12: Illustration of MODIS data acquisition on the EOS-AM platform. The bidirectional reflectance distribution function (BRDF) changes with view and sun geometry. Notice the shadow caused by clouds and canopy.	44
Figure 3.13: Illustration of the increasing IFOV (pixel size) as a function of the MODIS scan angle. . .	44
Figure 3.14: Flow diagram of pre-processing steps and quality flag evaluations that feed into the daily	

and composite VI algorithms	52
Figure 3.15: Diagram of the version 1 VI composite algorithm for 250 m and 25 km resolution	53
Figure 3.16: Version 1 monthly VI composite algorithm for 250 m and climate modeling grid.	53
Figure 3.17: Diagram of the coarse grid monthly composite scenario that would standardize view and solar zenith angles	60
Figure 3.18: Nadir Red and NIR reflectance and NDVI and SAVI as a function of solar zenith angle for a range of vegetation types (PARABOLA data).	65
Figure. 3.19: BRDF for MODIS bands red (R) and near-infrared (N) [FIFE Grassland, HAPEX Tigerbush site and BOREAS Black Spruce site; ASAS data in solar principal plane]	67
Figure 3.20: Effect of surface anisotropy on NDVI for a range of vegetation types.	67
Figure. 3.21 : a) Mean difference between measured and modeled nadir red and NIR reflectance factors for four BRDF models and 5 different view angle distributions of 14 vegetation cover sites. b) mean error in the predicted nadir vegetation index values of 14 vegetation covers, for five different view angle distributions and 4 different BRDF models using the measured nadir VI value as a reference; the error due to the MVC approach (MVC-NADIR) and the maximum error due to non standardization of the NDVI (MAX-MIN) is plotted as well.	70
Figure 3.22 Examples of the anisotropic effects on the SARVI (a), SAVI (b), WdVI (c), and SR (d) for a range of vegetation types. (Derived from ASAS data collected in the principal plane)	73
Figure 3.23: a) Mean NDVI response per continent for 7 different composite scenarios using 16 days of AVHRR data; b) Relative difference between the MVC and the other 6 composite scenarios (Table 4) for each continent.	75
Figure 3.24: Global frequency distribution for 10° view angle intervals and seven composite scenarios (see Table 4 for explanation of the legend)	76
Figure 3.25: a) Pseudo color NDVI image produced with the version 1 composite scenario (BRDF/CV-MVC/MVC); b) Global distribution of quality control flags including information on the applied composite method and clouds (input data: 16 days of AVHRR red and NIR reflectance and QC; 8 km, August 2-17, 1988).	77
Figure 3.26: Relationships between AVHRR and MODIS for NDVI, NIR, and Red using Rayleigh corrected data..	80
Figure 3.27: Relationships between AVHRR and MODIS for NDVI, NIR, and Red using '6S' corrected data..	81
Figure 3.28: Relationships between AVHRR and MODIS for NDVI, NIR, and Red using '6S' corrected MODIS data and Rayleigh corrected AVHRR data..	82

List of Tables

Table 1. MODIS sensor characteristics in support of the vegetation index algorithm products	19
Table 2. Variations in reflectances and vegetation indices across the spectral signatures encountered at the OTTER site	26
Table 3. Seasonal differences in solar zenith angle during MODIS overpass times for different latitudes (GMT 10.30h.;Longitude= 0°).	43
Table 4. Overview of the evaluated composite scenarios	58
Table 5. Information on the PARABOLA data sets with Leaf area index (LAI) and Plant area index (PAI)	61
Table 6. Number of land cover types for which the mean absolute error in the resulting VI, computed from the nadir reflectances, was within 0.005 of the lowest mean absolute error for a given land cover, solar zenith angle and sampling sector combination.	62
Table 7. Number of land cover types for which the mean relative error in the resulting VI, computed from the nadir reflectances, was the lowest or was within 0.01 of the lowest. Results are given as a function of land cover.	63
Table 8. Average coefficient of variation (CV) and relative difference (RD) in the red and NIR reflectance and albedo value and the associated NDVI and SAVI values as a function of solar zenith angle for the 9 vegetation types as measured by the Parabola instrument (where CV = 100 std/mean and RD=100 (max-min)/mean; computed for each vegetation cover type)	64
Table 9. Mean and standard deviation (std) of the difference between VIs derived from nadir reflectances and from albedo's for all sun angles and vegetation cover types	64
Table 10. Overview of errors in the NDVI due to BRDF and MVC composite scenarios (ASAS data)	71
Table 11. The number of times the error in the NDVI was larger then 0.01 , for 5 view angle distributions of the reflectance data for each vegetation type and BRDF model; H-HAPEX, F-FIFE, B-BOREAS, O-OTTER, pp-principal plane, op-orthogonal azimuthal plane).	71
Table 12. Average NDVI value (x10000) per continent and composite method	78
Table 13. Relative difference (%) between MVC and other vegetation index composite approaches (VICA) [100* (MVC-VICA)/VICA]	78
Table 14. Linear regression equations that relate NDVI, NIR, and Red between AVHRR and MODIS.	79
Table 15. Summary of pre-launch validation activities	90
Table 16. Intensive Field and Airborne Campaigns	93
Table 17. Proposed EOS/MODIS Field Mini-Campaigns	93
Table 18. Time line for vegetation index validation activities.	94
Table 19. Definition of quality control bits per pixel and daily vegetation indices (250 m) (level 2).	100

Table 20. Definition of quality control bits per pixel for 8 and 16 day composite (level 3).	100
Table 21. Definition of quality control bits per pixel for a monthly composite @ 250 m resolution (level 3).	101
Table 22. Definition of quality control bits per pixel for 25 km monthly composite (level 3).	101

MODIS VEGETATION INDICES

ALGORITHM THEORETICAL BASIS DOCUMENT

Version 2 (October 1996)

The plans for the MODIS instrument include the generation of improved global data sets. Vegetation Indices are simple, robust, empirical measures of vegetation activity at the land's surface. They are widely utilized for global monitoring of both spatial and temporal variations in vegetation at high precision. The MODIS VI products will improve upon currently available indices and will be used to more accurately monitor and detect changes in the state and condition of the Earth's vegetative cover. This document describes the theoretical basis for the development and implementation of vegetation indices and demonstrates the requirements for the characterization of their performance. **THIS IS A WORKING DOCUMENT WHICH CONTINUES TO EVOLVE IN RESPONSE TO THE PEER REVIEW PROCESS.** Using the progress made to date, the spectral vegetation index products are made globally robust with enhanced vegetation sensitivity and minimal variations associated with external and internal influences (atmosphere, view and sun angles, clouds, canopy background) in order to more effectively serve as a 'precise' measure of vegetation 'change'.

Vegetation indices will also play a role, as 'intermediaries' in the derivation of vegetation biophysical parameters, such as leaf area index (LAI), percent green cover, and fractional absorption of photosynthetically active radiation (fAPAR). In this ATBD we propose the use of two vegetation indices; (1) the NDVI and (2) an 'enhanced' VI to complement global studies of vegetation biophysical parameters. The NDVI will be utilized in fAPAR studies while the 'enhanced' VI will be used in canopy structure studies, including LAI and canopy morphology. Relationships between vegetation indices and vegetation biophysical parameters are being developed for globally representative data sets of ground, aircraft, and satellite measurements. These data sets are used for pre-launch assessment of vegetation index algorithm performance as well as to provide a preliminary set of 'translation' coefficients to convert the vegetation index products into measures of canopy biophysical properties. The use of biophysical data forms an integral component of the vegetation index validation plan.

1.0 Introduction

One of the primary interests of the NASA Earth Observing System (EOS) program is to study the role of terrestrial vegetation in large-scale global processes with the goal of understanding how the Earth functions as a system. This requires an understanding of the global distribution of vegetation types as well as their biophysical properties and spatial/temporal variations. Remote sensing observations offer the opportunity to monitor, quantify, and investigate large scale changes in vegetation in response to human actions and climate. Vegetation influences the energy balance,

climate, hydrologic, and bio-geochemical cycles and can serve as a sensitive indicator of climatic and anthropogenic influences on the environment.

The MODIS vegetation indices (VIs) will provide consistent, spatial and temporal comparisons of global vegetation conditions which will be used to monitor the Earth's photosynthetic vegetation activity for phenologic, change detection, and biophysical interpretations. The MODIS vegetation index (VI) products will play a major role in several EOS studies as well as be an integral part in the production of most global and regional biospheric models. Currently, satellite-derived vegetation indices are being integrated in interactive biosphere models as part of global climate modeling (Sellers et al., 1994) and production efficiency models (Prince et al., 1994; Prince, 1991). They are also used for a wide variety of land applications, including operational famine early warning systems (Prince and Justice, 1991; Hutchinson, 1991). This latter example is one of the few examples where derived satellite data are currently being used to drive policy decisions.

1.1 Identification of algorithm(s)

Two vegetation index (VI) algorithms are to be produced globally for land, at launch. One is the standard normalized difference vegetation index (NDVI), which is referred to as the 'continuity index' to the existing NOAA-AVHRR derived NDVI. At the time of launch, there will be an 18-year NDVI global data set (1981 - 1998) from the NOAA- AVHRR series, which could be extended by MODIS data to provide a long term data record for use in operational monitoring studies. The other is an 'enhanced' vegetation index with improved sensitivity to differences in vegetation from sparse to dense vegetation conditions. The two VIs compliment each other in global vegetation studies and improve upon the extraction of canopy biophysical parameters.

The daily, level 2, VIs will be available 'on demand' and will be computed from bidirectional surface reflectances, generated from level 1b, calibrated 'at sensor' radiances, masked for clouds and cloud shadow, and atmospherically corrected for aerosols, Rayleigh scattering and ozone absorption. MODIS bands 1 and 2 (centered at 648 nm, and 858 nm, respectively) will be used in the generation of the vegetation index products at 250 m spatial resolution (Table 1). These are currently listed as the following Level 2 product in the Earth Observing System (EOS) MODIS product summary document;

MODIS Product No. 13, Vegetation Indices (Level 2)

Normalized Difference Vegetation Index (NDVI), Parameter No. 2749

Spatial/Temporal Coverage and Characteristics: daily at 250 m for the global land surface.

Processing Level: 2

Product Type: Standard, fully operational at launch

Key Science Applications: Global vegetation monitoring on a daily basis; anthropogenic change detection, fire scars, agricultural activities, volcanic, and other landscape disturbances.

The level 3, spatial & temporal gridded vegetation index products are composites of daily bidirectional reflectances. The gridded VIs are 8, 16, and 30 day spatial and temporal, re-sampled products designed to provide cloud-free, atmospherically corrected, and nadir-adjusted vegetation maps at nominal resolutions of 250 m and 0.25°. The compositing algorithm utilizes the bidirectional reflectance distribution function of each pixel to normalize the reflectances to a nadir view and standard solar angular geometry. The 8 and 16 day VI composites will be archived at 250 m resolution and will include the selected, nadir-adjusted VI value, the nadir-adjusted red and NIR surface reflectances, median solar zenith, relative azimuth, and quality control parameters. These are currently listed as the following Level 3 products in the Earth Observing System (EOS) MODIS product summary document;

MODIS Product No. 34, Gridded Vegetation Indices (Level 3)

Normalized Difference Vegetation Index (NDVI), Parameter No. 2749a
'Enhanced', Soil and Atmosphere Resistant Vegetation Index (SARVI), Parameter No. 4334a.

Spatial/Temporal Coverage and Characteristics:

8 day, 16 day, and monthly at 250 m for the global land surface;
8 day, 16 day, and monthly at 0.25° for the global land surface.

Processing Level: 3

Product Type: Standard, fully operational at launch

Key Science Applications: Global vegetation monitoring; Global bio-geochemical and hydrologic modeling; Global and regional climate modeling, land cover characterization. The VIs are used as input in the land cover and land cover change products, and play an important role in the derivation of the fAPAR, LAI, and thermal products (Fire).

2.0 Overview and Background Information

2.1 Experimental Objective

The overall objective is to design an empirical or semi-empirical robust vegetation measure applicable over all terrestrial biomes of the earth. Vegetation indices are dimensionless, radiometric measures of vegetation activity exploiting the unique spectral signatures of canopy elements, particularly in the red and NIR portions of the spectrum. Their principal advantage is their simplicity. They require no assumptions, nor additional ancillary information other than the measurements themselves. The goal becomes, how to effectively combine these bands in order to minimize non-vegetation related signals while enhancing the 'green' vegetation signal.

The VI compositing objectives are to provide accurate and cloud free VI imagery over set temporal intervals. The task is to design an algorithm that is able to combine multiple single day images into a single, cloud-free image, taking into account the varying states of the atmosphere (aerosols, clouds) as well as the variable sensor view and sun angle conditions. The VI products will be capable of depicting spatial variations in vegetation across scales as well as depict temporal variations for phenologic studies (intra-annual) and change detection studies (inter-annual).

Specific tasks and experimental objectives include:

- ▶ develop precise, empirical measures of vegetation, depicting both spatial and temporal variations in vegetation composition, condition, and photosynthetic activity.
- ▶ continuity with current, global NOAA-AVHRR series, NDVI data fields.
- ▶ improved and complementary measures of vegetation for enhanced vegetation sensitivity and more accurate quantitative analysis.
- ▶ develop near-linear measures of vegetation parameters in order to maintain sensitivity over as wide a range of vegetation conditions as possible and to facilitate scaling and extrapolations across regional and global resolutions.
- ▶ provide estimates of biophysical parameters, including LAI, %green cover, and fAPAR comparable for insertion into global biome and climate models.
- ▶ maximize global and temporal land coverage at the finest spatial and temporal resolutions possible within the constraints of the instrument characteristics and land surface properties.
- ▶ minimize the effects of residual clouds, cloud shadow, and atmospheric aerosols.
- ▶ standardize variable sensor view and sun angle (BRDF effects) of the cloud-free pixels to a nadir view angle and nominal sun angle.

- ensure the quality and consistency of the composited data.

2.2 Historical Perspective

Many studies have shown how red and near-infrared (NIR) reflected energy are related to the amount of vegetation present on the ground (Colwell, 1974). Reflected red energy decreases with plant development due to chlorophyll absorption in an actively photosynthetic plant. Reflected NIR energy, on the other hand, will increase with plant development as most of this energy is reflected and transmitted with very little absorbed in healthy leaves. Unfortunately, because the amount of radiation reflected from a plant canopy and reaching a satellite sensor varies with solar irradiance, atmospheric conditions, non-photosynthetic vegetation (NPV), canopy background, and canopy structure/ composition, one cannot use a simple measure of light to quantify plant biophysical parameters. To date, individual band data are difficult to implement for vegetation studies on a global, operational basis, due to the intricate radiant transfer processes at both the leaf level (cell constituents, leaf morphology) and canopy level (leaf elements, orientation, NPV, and background). This problem has been circumvented somewhat by combining 2 or more bands into an equation or 'vegetation index' (VI).

The ratio vegetation index (RVI) or simple ratio (SR) was the first VI to be used (Jordan, 1969; Tucker, 1979). This index was formed by dividing the NIR radiance, digital count, or reflectance by the corresponding 'red' band output,

$$RVI = SR = X_{nir} / X_{red} . \quad (1)$$

However, for densely vegetated areas, the amount of red light reflected approaches very small values and this ratio, consequently, increases without bounds. Deering (1978) normalized this ratio from -1 to +1, by ratioing the difference between the NIR and red bands by their sum:

$$NDVI = (X_{nir} - X_{red}) / (X_{nir} + X_{red}) , \quad (2)$$

where X can be digital counts, at- satellite radiances, top of the atmosphere apparent reflectances, land leaving surface radiances, surface reflectances, or hemispherical spectral albedos. For terrestrial targets the lower boundary became approximately zero. Each method of computation is correct and has been utilized, although they yield different results for the same surface conditions.

Global-based operational applications of the NDVI have utilized digital counts, at-sensor radiances, 'normalized' reflectances (top of the atmosphere), and more recently, partially atmospheric corrected (ozone absorption and molecular scattering) reflectances. Thus, the NDVI has been able to evolve with improvements in measurement inputs. Currently, a partial atmospheric correction for Rayleigh scattering and ozone absorption is used operationally for the generation of the AVHRR Pathfinder

and the IGBP Global 1km NDVI data sets (James and Kalluri 1994; Townshend et al. 1994). In contrast to the heritage AVHRR-NDVI product, the MODIS NDVI algorithm will utilize complete, atmospherically corrected, surface reflectance inputs.

The normalized difference vegetation index (NDVI) is a very robust and sensitive vegetation measure, utilizing the spectral contrast in vegetation canopy reflected energy in the red and near-infrared portions of the electromagnetic spectrum. It is currently the only operational, global-based vegetation index utilized. This is in part, due to its 'ratioing' properties, which enable the NDVI to cancel out a large proportion of signal variations attributed to changing irradiance conditions that accompany changing sun angles, topography, clouds/shadow and atmospheric conditions.

Many studies have shown the NDVI to be related to LAI, green biomass, and fAPAR (Asrar et al., 1984; Tucker et al., 1981; Curran, 1980) (Fig. 2.1). Some relationships between fAPAR and NDVI have been shown to be near linear (Pinter, 1993; Begué, 1993; Wiegand et al., 1991; Daughtry et al., 1992), in contrast to the non-linear and saturation problems experienced when the NDVI is used to derive LAI. Gallo et al. (1985) observed polynomial relationships between NDVI and fAPAR in corn.

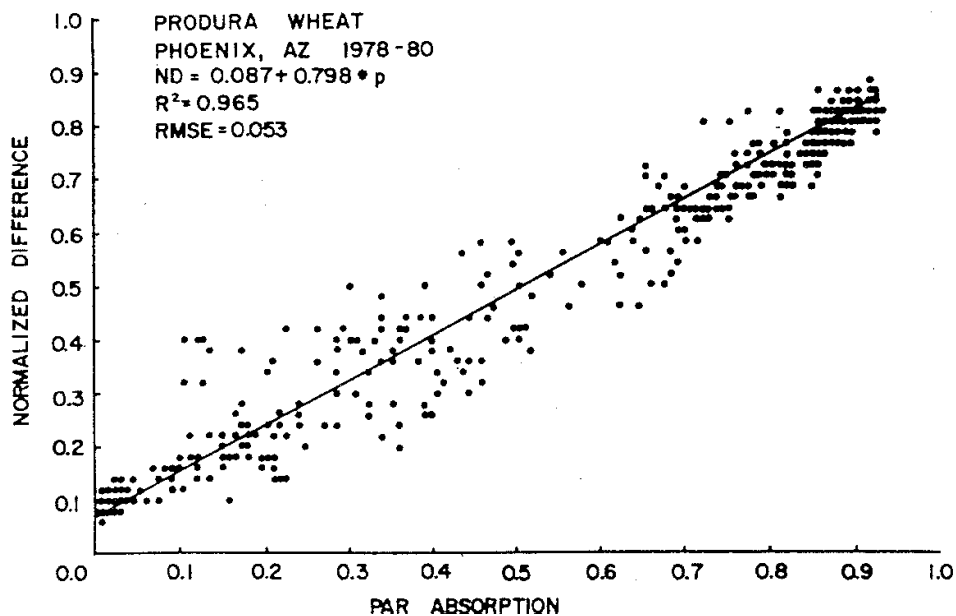


Fig. 2.1 Relationship between NDVI and fAPAR for wheat (From Asrar et al., 1984)

The temporal profile of the NDVI has been shown to depict seasonal and phenologic activity (Fig. 2.2) and the time integral of the NDVI over the growing season has been correlated with NPP (Justice et al., 1985; Goward et al., 1991; Tucker and Sellers, 1986) (Fig. 2.3). Other studies have shown the NDVI to be related to canopy resistance, potential evapotranspiration, and carbon-fixation, allowing its use as input to models of ecosystem productivity (Sellers, 1985; Asrar et al., 1984; Running et al.,

1989; Running, 1990; IGBP, 1992).

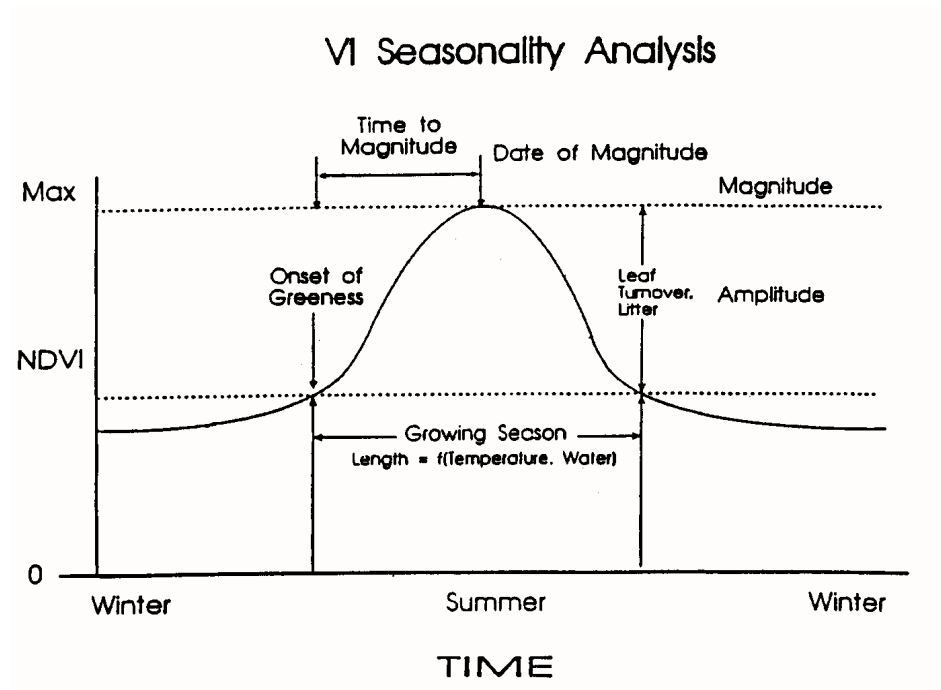


Fig. 2.2 Simplified seasonal - temporal vegetation index profile

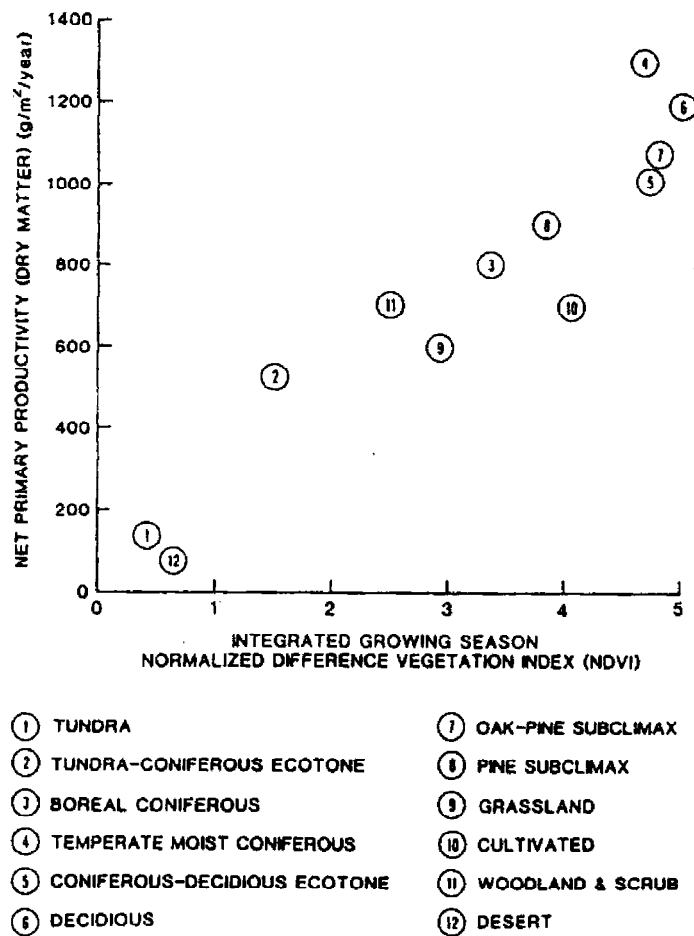


Figure 2.3: Plot of biome-averaged integrated NDVI measurements versus published mean biome net primary productivity rates for North-America (From Goward et al.,1985)

2.2.1 NDVI limitations

The global use of the NDVI requires that it not only be calculated in a uniform manner, but that the results be comparable over time and location. Although the NDVI has been shown useful in estimating many biophysical vegetation parameters, there is a history of vegetation index research identifying limitations in the NDVI, which may impact upon its utility in global studies. These include:

1. atmospheric effects due to variable aerosols, water vapor, and residual clouds.
2. sun-target-sensor geometric configurations and the resulting interactions of surface and atmospheric anisotropies on the angular dependent signal.
3. saturation problems whereby NDVI values remain invariant to changes in the amount and type of dense vegetation.
4. non-linearity in biophysical coupling of NDVI with fAPAR and/ or LAI.

5. canopy background contamination in which the background reflected signal alters the NDVI value. This includes surface wetness, snow, litter, roughness, and soil type.
6. canopy structural effects associated with leaf angle distributions, clumping and non-photosynthetically-active components (woody, senescent, and dead plant materials). Thus for a given quantity of green vegetation, the NDVI will vary with changes in the structure and orientation of the canopy.

2.2.2 Atmospheric Effects

The atmosphere degrades the NDVI value by reducing the contrast between the red and NIR reflected signals. The red signal normally increases as a result of scattered, upwelling path radiance contributions from the atmosphere, while the NIR signal tends to decrease as a result of atmospheric attenuation due to scattering and water vapor absorption. The net result is a drop in the NDVI signal and an underestimation of the amount of vegetation at the surface. The degradation in NDVI signal is dependent on the aerosol content of the atmosphere, with the more turbid atmospheres resulting in the greatest decreases in the NDVI signal. The impact of atmospheric effects on NDVI values is most serious with aerosol scattering (0.04 - 0.20 units), followed by water vapor (0.04 - 0.08), and Rayleigh scattering (0.02 - 0.04) (Goward et al. 1991; Teillet, 1989).

The atmosphere problem may be corrected through direct and indirect means (Kaufman and Tanré, 1996). Atmospheric effects on the MODIS-NDVI will become minimal as a result of the atmospheric correction algorithms being developed. However, since the resolution of the aerosol product will be much coarser (~10 km resolution) (Vermote et al., 1995) than the NDVI product (250 m), some residual aerosol contamination will be expected in the NDVI product. Of particular concern will be spatial variations in smoke, gaseous and particulate pollutants, and light cirrus clouds, which are present at finer spatial resolutions. The accuracy of atmospheric correction will also vary with the availability of 'dark-objects', which are needed for the best corrections.

Kaufman and Tanré (1992) developed the atmospherically resistant vegetation index (ARVI) as an example of an indirect approach to atmosphere correction. The ARVI reduces the dependence of the vegetation index to atmospheric properties by utilizing the difference in the radiance between the blue and the red channels to cancel out and correct the radiance in the red channel. Myneni and Asrar (1993), in a sensitivity study with simulated data, found the ARVI to reduce atmospheric effects and to mimic ground-based NDVI data. Pinty and Verstraete (1992) have proposed an AVHRR-specific, global environment monitoring index (GEMI), which minimizes atmospheric effects in AVHRR data.

2.2.3 Angular Considerations

The NDVI has been shown to be affected by variations in bidirectional reflectances resulting from differences in sun-target-sensor geometries (Walter-Shea et al., 1996). MODIS viewing angles will vary $\pm 55^\circ$ cross-track accompanied by solar illumination angle differences of up to 20° from edge to edge of the MODIS swath. In addition sun angles will vary with latitude and time of the year. This resulting variability in view and sun angles is important for the intercomparison of vegetative covers on a global basis. The current NDVI compositing procedure tends to select off-nadir and larger solar zenith angles (Moody and Strahler, 1994; Cihlar et al., 1994; Gutman, 1991) which contain greater amounts of atmospheric contamination and spatial distortion of the pixels. This angular-induced anisotropy is expected to become more pronounced following atmospheric correction and thus must be considered in derivation of the vegetation index products.

At the same time there is considerable research and understanding of bidirectional reflectances with the development of physical, semi-empirical, and empirical BRDF models (Wanner et al., 1995). Consequently, both empirical and MODIS-MISR BRDF products will be evaluated for use in the level 3 vegetation index compositing scheme in order to generate near-nadir vegetation index maps with minimal angular variations.

2.2.4 Saturation and non-linearity problems

The NDVI is shown here, as in other studies (Gitelson et al., 1996), to 'saturate' over densely vegetated areas, whereby the NDVI no longer responds to variations in green biomass. Others have reported the NDVI to be an insensitive measure of LAI when values exceed 2 or 3. This is attributed to the high sensitivity of the NDVI to the red (chlorophyll) absorption band, which also saturates quickly. Maximum sensitivity to chlorophyll-*a* (Chl-*a*) pigment absorption is at 670nm. For Chl-*a* concentration beyond $3\text{--}5\ \mu\text{g}/\text{cm}^2$, the inverse relationship of reflectance at 670nm vs. chlorophyll concentration 'saturates' and is no longer sensitive despite a global range in chlorophyll concentrations from 0.3 to $45\ \mu\text{g}/\text{cm}^2$ (Vogelmann et al. 1993; Buschmann and Nagel 1993).

Recent work by Moreau and Li (1996) (Fig. 2.4) have shown non-linearity between the NDVI and FPAR over a wide range of experimental and modeled data sets. In this figure, the NDVI is seen to saturate before FPAR does (i.e., $\text{NDVI}=0.8$ for FPAR values greater than 0.7). Myneni et al. (1992) have also suggested that the non-linearity is due to the NDVI saturating earlier than canopy absorptance.

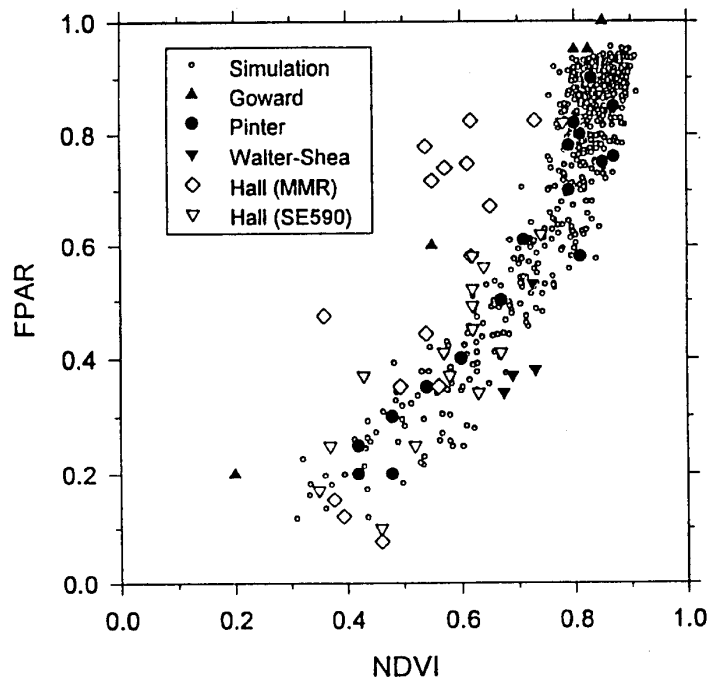


Figure 2.4. Relationship between FPAR and NDVI based on observations and canopy modeling (From Moreau and Li, 1996).

Gitelson et al. (1996) reported enhanced sensitivity could be achieved by replacing the red channel with a green channel, which was found to remain sensitive to chlorophyll-a over a wider range of concentrations. They proposed a green NDVI equation which was five times more sensitive to Chl-a concentration. Yoder and Waring (1994) similarly have used a green NDVI for improved estimates of photosynthetic activity in Douglas-fir trees. As further discussed in the 'Theory' section, 'saturation' issues in the NDVI result mainly from the non-linear transform process from the NIR/red ratio which render the NDVI overly sensitive to the red reflected signal.

This is of concern to the MODIS-NDVI equation because the MODIS red channel is much narrower (620 - 670nm) than that of the AVHRR (580 - 680nm) and may thus saturate more quickly. Land use change detection, vegetation monitoring, net primary production, and scaling studies cannot be carried out in an NDVI 'saturated' mode (Townshend et al., 1991). The potential, however, for improved vegetation analysis with narrower-band channels is well demonstrated (Elvidge and Chen, 1995).

2.2.5 Canopy Background Contamination

Numerous ground-, air-, and satellite-based observations have shown the NDVI to be overly sensitive to the brightness of the underlying canopy background (Elvidge and Lyon, 1985; Huete et al., 1985; Heilman and Kress, 1987; Huete and Warrick, 1990; Qi et al., 1993a). The backgrounds of canopies exhibit spatial and temporal reflectance variations resulting from rain events, snowfall, litter fall, roughness, and the organic matter content and mineralogy of the soil substrate material. In all of these studies there is a systematic increase in the NDVI value as the reflectance or 'brightness' of the background decreases. This systematic change in NDVI with background brightness is also confirmed with canopy radiative transfer models including the SAIL, Myneni, and two-stream approximation models (Baret and Guyot, 1991; Baret et al., 1989; Myneni and Asrar, 1993; Sellers, 1985; Choudhury, 1987).

A common misconception is that canopy background considerations are only important in sparsely vegetated, arid and semi-arid areas, where spectral variations in background are the greatest. However, most studies and simulations show NDVI background sensitivity to be greatest at intermediate levels of vegetation, comparable to humid and sub-humid land cover types, including open forest stands. Bausch (1993) and Huete et al. (1985) showed the influence of canopy background reflectance on NDVI values to be 0.20 units at LAI=0; and 0.30 units at LAI=1; and 0.20 units at LAI=2 for background reflectances which varied from 0.06 to 0.33 in the red. Background influences disappear at LAI > 2, which is where 'saturation' begins. The range in background reflectances becomes greater when snow, wetlands, and irrigated rice paddy fields are included. The errors presented above are reduced by one-half if only surface moisture influences on background reflectance are considered.

Several approaches have been proposed to minimize background influences on vegetation indices. Richardson and Wiegand (1977) introduced the perpendicular vegetation index which utilized a 'soil line' concept for site specific background corrections. The soil line is a 'baseline' value of zero vegetation over a wide 'brightness' range of soil backgrounds, from which vegetation can be measured in NIR-red space, relative to the baseline. Huete (1988) developed the soil adjusted vegetation index (SAVI) which offered a 'global' first-order correction for background. This was further improved by Baret et al. (1989) yielding the transformed soil adjusted vegetation index (TSAVI) and by Qi et al. (1993b) with the modified SAVI (MSAVI). Clevers (1989) found the weighted difference vegetation index (WDVI) to greatly improve upon the estimation of LAI while minimizing background effects. Elvidge and Chen (1995) showed how narrower-band channels, as input to vegetation indices, reduce background-related problems present in broad-band vegetation indices. Similarly, Hall et al. (1990) and Demetriades-Shah et al. (1990) have discussed the value of narrow-band, derivative spectra for reducing background effects.

In a sensitivity study of both atmosphere and canopy background influences on vegetation indices, Huete and Liu (1994) found background influences on the NDVI to

decrease greatly with increases in atmospheric aerosol contents and that at a horizontal visibility of 5km (turbid atmosphere), background influences became nearly zero. This was also observed with satellite imagery (Qi et al., 1993). Consequently, we anticipate canopy background problems to become more pronounced in MODIS-NDVI imagery due to the improved atmospheric correction algorithms being implemented. A feedback problem is evident whereby the improvement of one form of noise (atmosphere) increases other forms of noise (background). Liu and Huete (1995) developed a feedback-based approach to correct for the interactive canopy background and atmospheric influences. Incorporating both background adjustment and atmospheric resistance concepts into a feedback-based equation, resulted in a modified normalized difference vegetation index (MNDVI).

2.2.6 Canopy Structural Effects

Sellers (1985) calculated the variation of the NDVI with canopy greenness fractions and demonstrated how the presence of dry and dead plant material severely alters the relationship between NDVI and LAI. He showed the NDVI to vary greatly with leaf angle and solar zenith angles, which alters the optical thickness of the canopy. He also showed that due to the non-linear nature of the NDVI-LAI relationship, the contribution of the bare ground fraction to the NDVI is disproportionately strong when equal amounts of greenness (LAI) are distributed differently, such as in clumps. The same LAI in smaller cover fractions yielded the lowest NDVI. Clevers and Verhoef (1993) used the SAIL canopy and PROSPECT leaf models to show how the main variable that influences vegetation indices is the leaf inclination angle distribution. The more planophile a canopy the greater the vegetation index value for a given LAI.

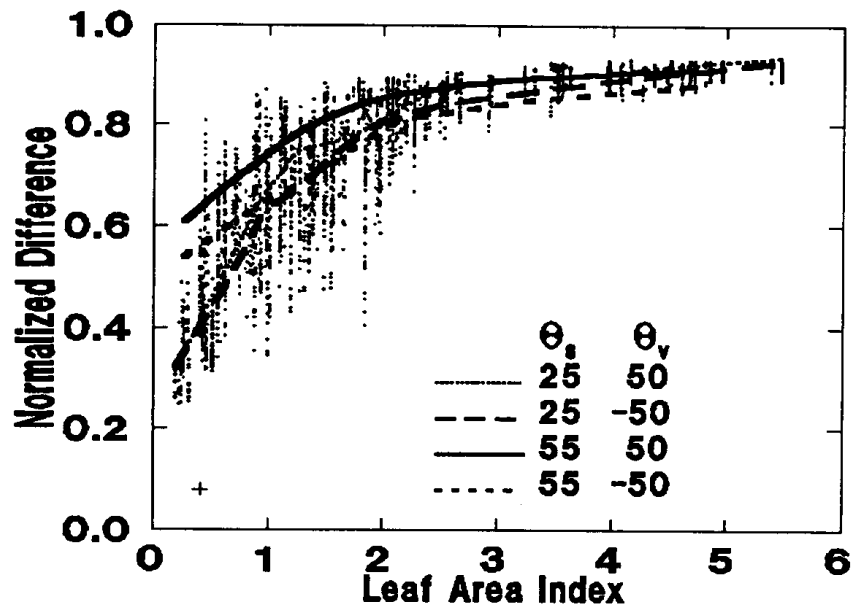
Because of the overwhelming influence of canopy structure on spectral reflectances and vegetation indices, it is very difficult to derive biophysical plant parameters directly from the NDVI. Many of the NDVI to biophysical parameter relationships involve site specific, regression plots which are subject to variability associated with canopy background, atmosphere, instrument calibration, sun angle, and view angle. It is necessary to accommodate the effects of the different factors when interpreting NDVI values, especially if we are to detect deviations in behavior indicative of directional or 'global' change (Wickland, 1989; Prince and Justice, 1991). A direct approach would be to utilize a canopy radiative transfer model to handle the radiative transfer processes within the structure of the canopy. Alternatively, an indirect approach may be utilized whereby 'land cover type' empirical parameters are used in the translation from NDVI to LAI, green cover, or fAPAR.

2.2.7 New and Improved Vegetation Indices

The MODIS VI's are envisioned as improvements over the current NOAA-AVHRR NDVI as a result of both improved instrument design and characterization and the significant amount of VI research conducted over the last decade. Many new indices have been proposed to further improve upon the ability of the NDVI to estimate biophysical vegetation parameters (Prince et al., 1994). Many of these indices have more linear responses with vegetation biophysical parameters and do not saturate so readily. Their extended linear sensitivity in more densely vegetated areas is due to their NIR sensitivity which can penetrate the canopy leaf layers. These indices are more useful in monitoring LAI and associated canopy structure variations. The NDVI, on the other hand, responds to the highly absorbed visible reflectances, and thus is more closely related with fAPAR. Epiphanio and Huete (1995) showed how the SAVI and NDVI responded to different properties of an alfalfa canopy due to the strong relationship of SAVI with NIR, and NDVI with red. This suggests that two vegetation indices may be complementary in global vegetation studies. Figure 2.5, from Walter-Shea et al. (1996), is a good example of how the non-linearity and saturation in the NDVI is readily removed in using a more NIR-sensitive vegetation measure, in this case the simple ratio.

However, the robustness and global implementation of these indices have not been tested and one must be cautious that a new index not create new errors in the process of improving upon a specific source of noise. On one hand there is a need for continuity, while on the other hand improvements to make the NDVI more quantitative are needed. In the algorithm description of this document, a comparative analysis of potential indices are made along with the NDVI as a first step in determining the feasibility of improving upon the NDVI.

a)



b)

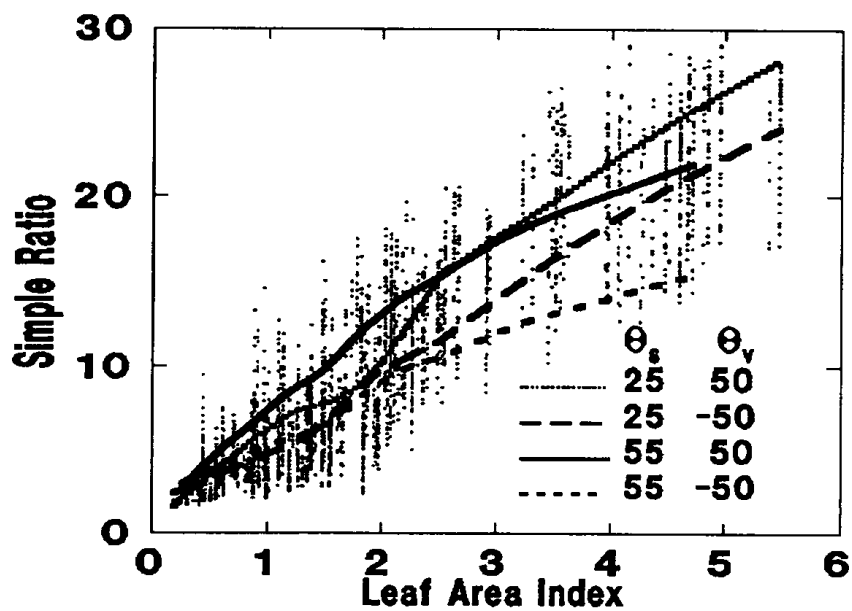


Figure 2.5: Vegetation indices a) NDVI and b) SR derived from BRFs measured over a developing alfalfa for a range of LAIs (From Walter Shea et al., 1996).

The following NIR sensitive vegetation indices (two-band) will be tested for MODIS use and compared with the NDVI:

- the weighted difference vegetation index (WDVI) (Clevers, 1989),

$$WDVI = \rho_{nir} - k \rho_{red} , \quad (3)$$

where k is the generalized ratio of NIR background reflectance to that of the red.

- the soil-adjusted vegetation index (SAVI) (Huete, 1988),

$$SAVI = [(\rho_{nir} - \rho_{red}) / (\rho_{nir} + \rho_{red} + L)] (1 + L), \quad (4)$$

with a 'global' soil adjustment factor, L, included in the denominator. The L term is related to Beer's Law and accounts for the differential red and NIR canopy spectral extinction through a photosynthetically-active canopy.

- the perpendicular vegetation index (PVI) (Richardson and Wiegand, 1977),

$$PVI = [1/(a^2 + 1)^{0.5}] (WDVI - b), \quad (5)$$

where a and b are the soil line slope and intercept, respectively in NIR-red space (Baret and Guyot, 1991).

- the global environment monitoring index (GEMI) (Pinty and Verstraete, 1992),

$$GEMI = \eta (1 - 0.25 \eta) - [(\rho_{red} - 0.125) / (1 - \rho_{red})], \quad (6)$$

$$\text{where } \eta = [(2(\rho_{nir}^2 - \rho_{red}^2) + 1.5 \rho_{nir} + 0.5 \rho_{red}) / (\rho_{nir} + \rho_{red} + 0.5)].$$

In addition, a few indices which utilize the green and/or blue band will be analyzed:

- the 'green' NDVI_g (green and NIR channels),

$$NDVI_g = [(\rho_{nir} - \rho_{green}) / (\rho_{nir} + \rho_{green})], \quad (7)$$

- the atmospherically resistant vegetation index (ARVI) (blue, red, NIR channels),

$$ARVI = (\rho_{nir}^* - \rho_{rb}^*) / (\rho_{nir}^* + \rho_{red}^*), \quad (8)$$

$$\text{where } \rho_{rb}^* = \rho_{red}^* - \gamma (\rho_{blue}^* - \rho_{red}^*).$$

The ARVI mainly accounts for atmosphere aerosol scattering and assumes that

atmospheric correction of molecular scattering and ozone absorption be performed prior to its use (ρ^*).

- the enhanced, soil and atmosphere resistant vegetation index (SARVI) (blue, red, NIR channels) (Huete et al., 1996):

$$\text{SARVI} = 2 [(\rho_{\text{nir}} - \rho_{\text{red}}) / (L + \rho_{\text{nir}} + C_1 * \rho_{\text{red}} - C_2 * \rho_{\text{blue}})], \quad (9)$$

where ρ is 'apparent' (top-of-the-atmosphere) or 'surface' directional reflectances with a canopy background adjustment term, L , and C_1 and C_2 weighs the use of the blue channel in aerosol correction of the red channel.

In summary, the criteria for and definition of a global vegetation index includes:

- the index should maximize sensitivity to plant biophysical parameters, preferably with a linear response in order that some degree of sensitivity be available for a wide range of vegetation conditions and to facilitate validation and calibration of the index,
- the index should normalize or model external effects such as sun angle, viewing angle, and atmosphere for consistent spatial and temporal comparisons,
- the index should normalize canopy background variations in reflectances (brightness) for consistent spatial and temporal comparisons,
- the index should be applicable to the generation of a global product, allowing precise and consistent, spatial and temporal comparisons of vegetation conditions,
- the index should be coupled to key biophysical parameters such as LAI and fAPAR as part of the validation effort and quality control.

Improved vegetation sensitivity will be achieved with improved MODIS sensor characteristics and from the optimal utilization of MODIS sensor wavebands (Table 1). An 'improved' index could increase sensitivity by enhancing the reflected signal from vegetation and further normalize internal and external 'noise' influences, thus improving the vegetation signal to noise ratio. Or a second index may provide new, unique information for vegetation analysis. Atmospheric correction algorithms and atmospheric resistant versions of the NDVI will greatly minimize atmospheric sources of noise. Angular concerns (view and sun angles) will be handled through the use of BRDF models and improved compositing methods.

2.3 Instrument Characteristics

This section identifies those aspects of the instrument critical to the VI parameters. The normalized radiances of MODIS bands 1 and 2 are directly input into the NDVI equation (Table 1). For the enhanced VI, band 3 may be utilized for correction of residual aerosol, and band 4 is being tested to minimize chlorophyll saturation problems. Critical to the quality of the NDVI product will be the co-registration of the red and NIR 250m channels, spectral stability of the red channel, and pixel registration and calibration over time. The MODIS NDVI will not be completely the same as that derived from the NOAA-AVHRR instrument due to different sensor characteristics. An example is the narrower spectral widths of the MODIS bands, which eliminates the water absorption region in the NIR (Table 1) and also renders the red band more sensitive to chlorophyll absorption.

The MODIS repeat cycle is sixteen days, during which each point on the earth will be viewed with a range of view angles between $\sim 55^\circ$ in the forward and backscatter direction. The scan angle is slightly lower than the view zenith angle due to the curvature of the earth. Complete coverage of the earth may further be attained within a scan angle of 20° in an 8-day period. Since the repeat cycle is 16 days, it is suggested to make the compositing period half of this time, thus 8 days. This number seems appropriate since it gives a consistent distribution of view angles and a possibility to cover all latitudes within small viewing angles, providing the best spatial resolution (250 m NDVI) and most accurate atmospheric correction.

Geolocation accuracy is very important for temporal composites. The geometry of the detector (weighted triangular response) and the scan geometry determine the accuracy of the Earth location. The MODIS Land team requires the Earth location accuracy to be 0.1 pixels (for 1 km pixels) to support image registration for change detection and temporal compositing. Actual day to day registration accuracy over a 16 day period will be determined post-launch.

Table 1. MODIS sensor characteristics in support of the vegetation index algorithm products.

#	Bandwidth (nm)		IFOV (m)	Spectral Radiance ¹	Required SNR	Bandwidth Tolerance
1	620	670	250	21.8	128	+/- 4.0 nm
2	841	876	250	24.7	201	4.3
3	459	479	500	35.3	243	2.8
4	545	565	500	29.0	228	3.3
5	1230	1250	500	5.4	120	7.4
6	1628	1652	500	7.3	275	9.8
7	2105	2155	500	1.0	110	12.8
¹ =Watts/m ² /μm/sr Quantization: 12 bits Scan width: 2330 km by 10 km (track) at 705 km platform altitude +/-550 cross track Absolute Calibration: +/-5%; +/-2% Reflectance Spectral Stability: stable to < 2nm; Co-registration: +/-20% along and off track at 1km with +/-10% goal.						

3.0 Algorithm Description

Vegetation indices are empirical measures of vegetation activity. Our primary goal is to formulate as precise a measure of spatial/ temporal differences in vegetation as possible and maintain an equation that is robust. Sensitivity over a global range of vegetation conditions is best achieved through linear equations. The vegetation index equations presented here are designed to isolate and enhance the red and NIR reflected signals from the 'green', photosynthetically-active vegetation component of a given pixel. The level 3, spatially and temporally gridded vegetation index products are radiometrically calibrated, and are cloud-free vegetation maps, corrected for view angle influences and surface anisotropy, via use of bidirectional reflectance distribution models. The level 3 products will consist of 8-, 16-, and 30-day composites, constructed from daily, level 2 reflectances, adjusted to nadir. In the following sections the theory and physical principles from which the VI products are derived are presented and also how they are developed into precise, global robust measures of vegetation activity.

3.1 Theoretical Description

Two vegetation indices will be produced at launch. The normalized difference vegetation index, NDVI;

$$NDVI = (\rho_{nir} - \rho_{red}) / (\rho_{nir} + \rho_{red}) , \quad (10)$$

and an 'enhanced' VI; the soil and atmosphere resistant vegetation index, SARVI;

$$SARVI = 2 [\rho_{nir} - \rho_{red}] / (L + \rho_{nir} + C_1 * \rho_{red} - C_2 * \rho_{blue}), \quad (11)$$

where ρ_{nir} , ρ_{red} , and ρ_{blue} are the atmospherically-corrected, surface bidirectional reflectances in the near-infrared (MODIS band 2), red (MODIS band 1), and blue (MODIS band 3), respectively; $L = 0.6$ is the canopy background adjustment factor; and $C_1 = 3.3$ and $C_2 = 4.5$ are the coefficients for atmospheric aerosol resistance, using the blue band to adjust the red band for residual aerosols.

The theoretical basis for 'empirical-based' vegetation indices is derived from examination of typical spectral reflectance signatures of leaves (Fig. 3.1). We see that reflected energy in the visible is very low as a result of pigment absorptions with maximum sensitivity in the blue (470 nm) and red (670 nm) wavelengths. Nearly all of the near-infrared radiation is scattered (reflected and transmitted) with very little absorption, in a manner dependent upon the optical and structural properties of a canopy (LAI, LAD, leaf morphology). As a result, the contrast between the red and

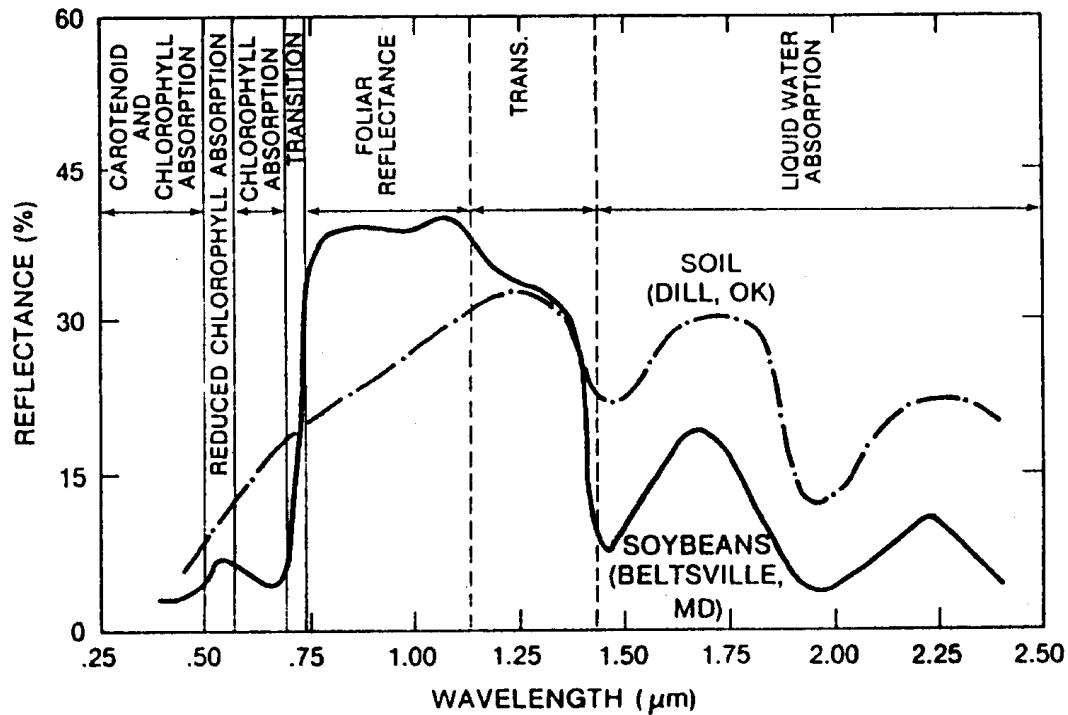


Figure 3.1: Reflectance signatures for soil and leaves (From Tucker and Sellers, 1986)

near-infrared bands is a very sensitive measure of vegetation amount and this contrast can be enhanced through the use of ratios (NIR/red), differences (NIR-red), linear combinations of the two bands ($x_1 \cdot \text{red} + x_2 \cdot \text{NIR}$), or combinations of the above. In general, a vegetation index is a measure of this contrast and is a function of both canopy structural (LAI, LAD) and physiological (fAPAR) parameters.

The contrast between the red and NIR reflectances is also efficiently depicted in graphical form, using the red and near-infrared reflectances as axes. When terrestrial-based reflectances are plotted in red-NIR waveband reflectance space, a well defined, triangular, cloud of points is encountered with well-defined boundaries, whether the data represents ground-based reflectances of agricultural crops over the growing season (Fig. 3.2) or TM derived reflectances of natural landscapes from desert to forests (Fig. 3.3).

In both cases there is a lower 'baseline' of pixels close to the 1:1 line, representing the lower boundary condition of vegetation activity. This baseline of zero or near-zero vegetation was defined by Richardson and Wiegand (1977) as the 'soil line', since it primarily depicts soil spectral variations extending outward from the origin with increasing brightness. Alternatively, water (dark) and snow (bright) may define the lower 2 apices. The third apex represents dense vegetation and is at very low red values (chlorophyll-absorption) but high NIR values.

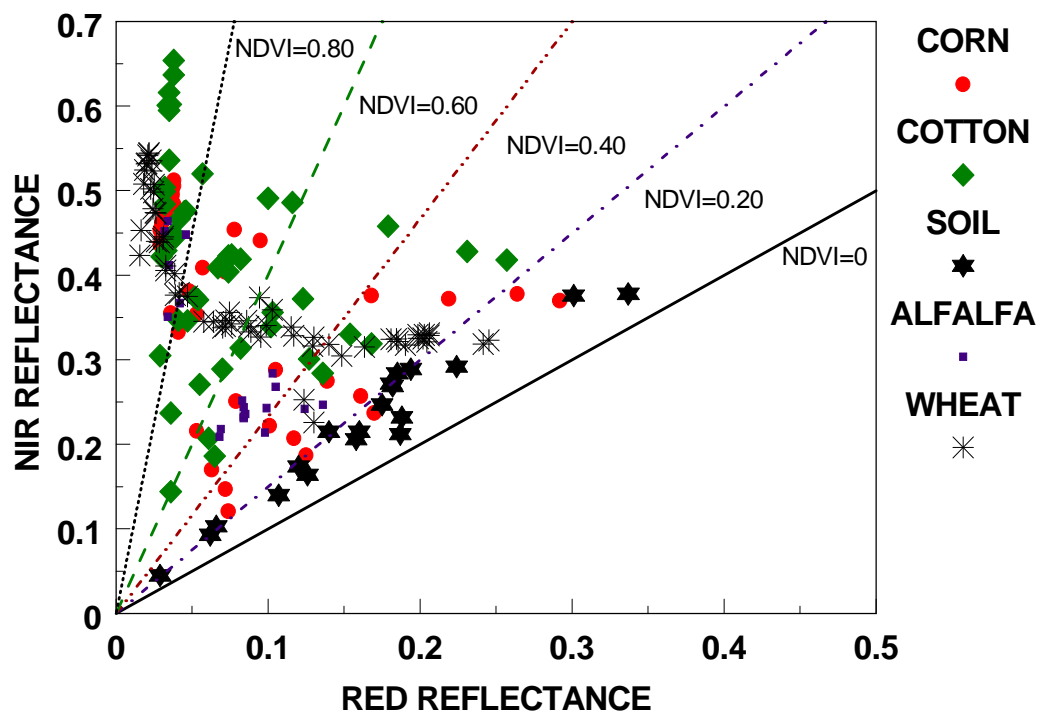


Figure 3.2 Cloud of reflectance points in NIR-red waveband space for agricultural crops observed throughout the growing season.

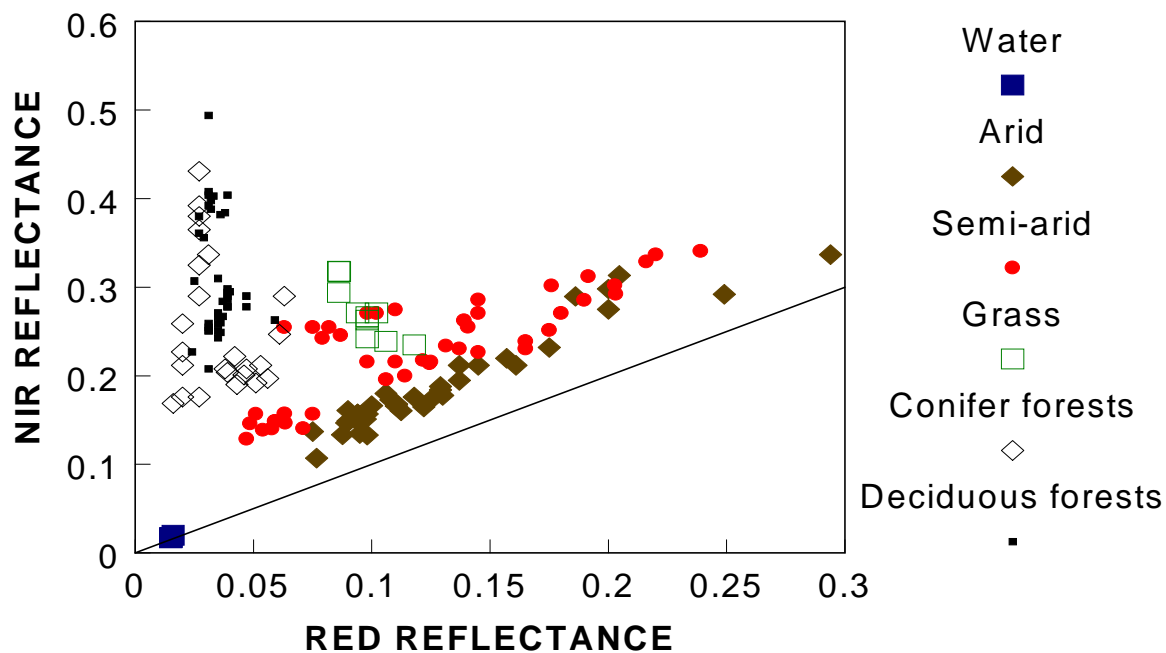


Figure 3.3. Reflectance spectra from Landsat TM 5 plotted in red-NIR space for a wide range of land surface cover types.

Vegetated pixels shift away from this lower baseline and toward an apex of maximum NIR and minimum red reflectance. The greater the amount of 'green', photosynthetically active vegetation present over a soil, the greater will be the red-NIR contrast, and thus the shift away from the soil line. In Figs. 3.2 and 3.3, pixels shift away from the 'background' baseline and toward the apex of maximum NIR and minimum red reflectances with increasing presence of vegetation. Desert regions fall near the lower zero 'baseline', followed by semi-arid and grassland pixels. Forested pixels occupied the extreme left-hand portion, being 'saturated' in the red with increasing values in the NIR (Fig. 3.3). The behavior of pixels within the NIR-red space is a function of the optical properties of the leaves, the quantity of vegetation present, and canopy structural parameters. Vegetation indices are designed to model the behavior and boundary conditions of terrestrial-based pixels in NIR-red space and their associated variations in time and space.

The NDVI is a 'normalized' transform of the NIR to red reflectance ratio, $\rho_{\text{nir}}/\rho_{\text{red}}$, or simple ratio (SR = NIR/red):

$$\begin{aligned}\text{NDVI} &= [(\rho_{\text{nir}}/\rho_{\text{red}}) - 1] / [(\rho_{\text{nir}}/\rho_{\text{red}}) + 1] \\ &= [\text{SR} - 1] / [\text{SR} + 1],\end{aligned}\tag{12}$$

and thus is functionally equivalent to the ratio i.e., no scatter (Fig. 3.4a). The advantage of the NDVI is its simplicity. Ratios create simple vegetation isolines (Fig. 3.2) graphically displayed in red-NIR space by isolines of increasing slopes diverging out from the origin. Since soil reflectance spectra fall on or close to the 1:1 line, the NDVI can ratio out a significant portion of background spectral variations as indicated by the 'zero' isoline. Furthermore, pixels will tend to shift toward the origin as a result of variations in irradiance, cloud shadows, and topography, thus maintaining constant ratio and NDVI values. The extent to which this holds true is dependent upon minimal effects from direct/diffuse irradiance variations as well as to which degree the ground surface exhibits Lambertian behavior. As mentioned previously, the difference of the 2 bands, NIR-red, is also a measure of the contrasting vegetation red and NIR reflectances and is thus a vegetation measure. Figure 3.4b, however shows the DVI to not be functionally equivalent to the NDVI and thus depicts different or unique information about the vegetated pixels.

In the following sections, we analyze in more detail the limitations of the NDVI both for the purpose of assessing product performance as well as to explore potential methods for improvement while maintaining a robust and operational algorithm.

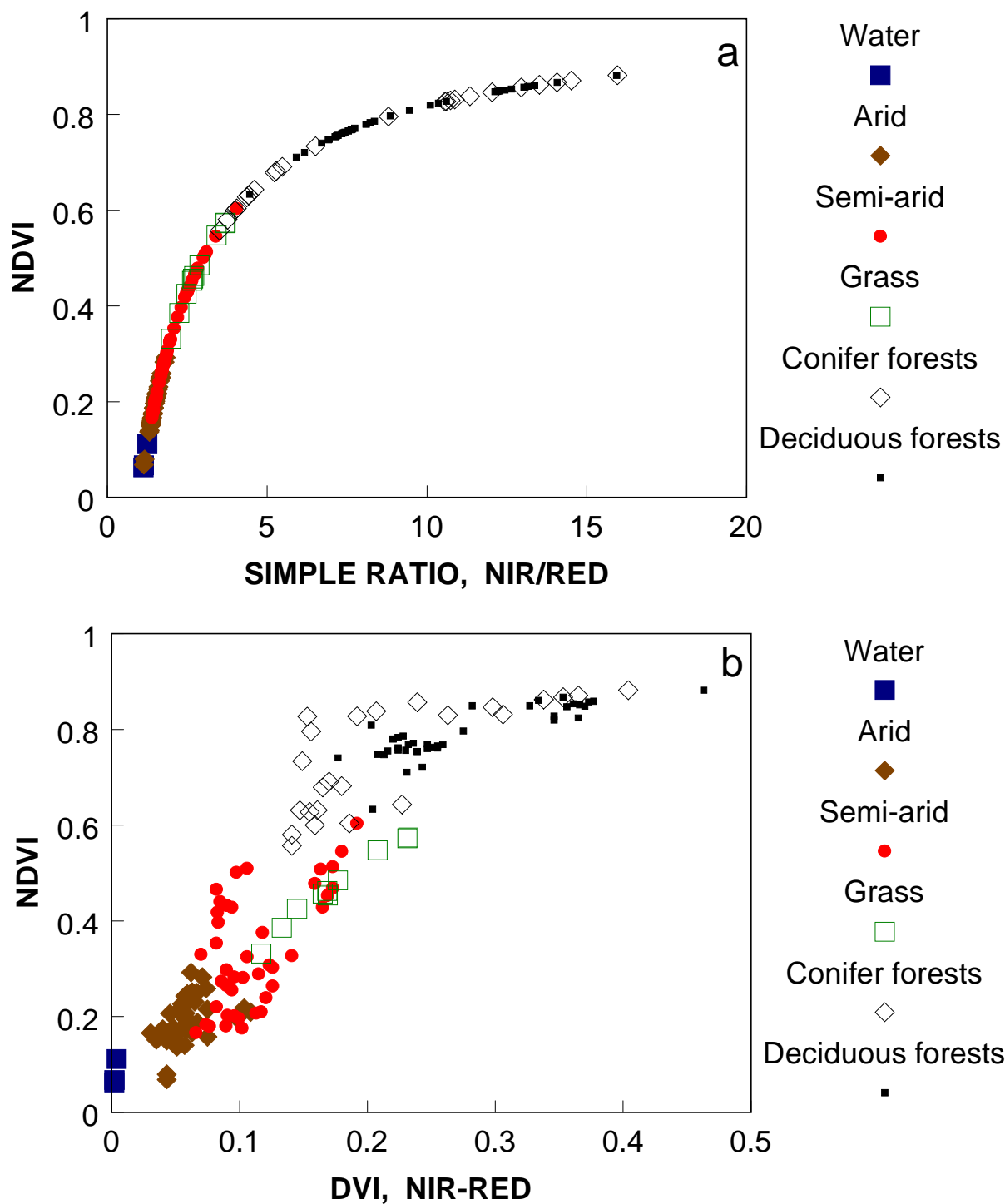


Figure 3.4 Functional equivalency for NDVI and SR (a) and (b) the non functional equivalency between NDVI and DVI.

3.1.1 Linearity and Saturation Considerations

Of the NDVI limitations given in section 2.2.1, improvements to the 'saturation' and linearity issues would yield the greatest benefits to global vegetation studies. As mentioned earlier, changes in land use, land cover, and net primary production are more difficult to detect in a 'saturated' mode (Townshend et al., 1991). Land cover classification based on multi temporal NDVI profiles would similarly be hampered. As a ratio, the NDVI enhances the contrast of the red and NIR portions of vegetation spectra. However, the NDVI is a non-linear 'stretch' of the simple ratio in order to confine its values from -1 to +1. The stretch has the effect of enhancing low ratio values while compressing higher ratio values (Fig. 3.4a). As ratio values increase from 5 to 10 and 15, the corresponding NDVI values shift from 0.67 to 0.82 (20% increase), and 0.87 (6% increase). A further increase in the NIR/red ratio to a value of 20 yields very little change in the NDVI (0.90). The non-linear stretch has the apparent effect of improving vegetation discrimination under low biomass conditions, but results in very low sensitivity to variations in densely vegetated areas.

The NDVI values can be compared with the NIR/red ratios for the agricultural and global TM land cover type data sets (Figs. 3.5 & 3.6). The simple ratios are fairly linear with LAI and do not saturate to the extent encountered in the NDVI with LAI values exceeding 2 (Fig. 3.5a,b). The scatter in these data sets is due to differences in canopy backgrounds with the darkest (or wettest) backgrounds resulting in both the highest NDVI values for a given LAI and the greatest degree of non-linearity. This is more strongly demonstrated in the data sets of Walter-Shea et al. (1996) (see Fig. 2.5). It is interesting to note that the difference between the two bands, the 'difference vegetation index' ($DVI = NIR - red$) also does not saturate (Fig. 3.5c). The same is observed with the TM derived spectra over a set of land cover types (Fig. 3.6). A clear NDVI plateau is seen over forested areas (needle leaf and broadleaf) despite the large variations observed in NIR reflectances (Fig. 3.6b). The NIR/red ratio does not saturate and remains sensitive to vegetation differences (Fig. 3.6a). The SAVI and SARVI2 similarly do not saturate and remain sensitive within the forested vegetation canopies (Figs. 3.6c, 3.6d).

The NDVI compression of the vegetation signal at the higher end of vegetation densities is also demonstrated in plots with the respective spectral reflectance signatures of forested canopies (Fig. 3.7). The red band, being sensitive to chlorophyll, is relatively constant and has saturated across the range of needle leaf evergreen forests at the OTTER transect site, where LAI values vary from 3 to 7 (Runyon et al., 1994). The NIR reflectances which are sensitive to canopy structural properties, such as LAI, have not saturated and vary more than 2-fold as a result of the scattering (reflective and transmissive) and penetrating capability of the NIR band. The NDVI has primarily responded with the red band and has saturated also, only varying from 0.80 to 0.88. The NDVI may thus be a more useful measure of the chlorophyll content of a canopy, useful for fAPAR studies. Table 2 depicts the respective VI values for the OTTER spectral signatures shown in Fig. 3.7. Of all 10 indices calculated, the NDVI is

the least sensitive to the differences within the forest vegetation canopies, varying only 0.08 units, 10% relative difference. Maximum discrimination differences were encountered with the 'orthogonal-based' indices which varied slightly more than the NIR reflectances themselves (Table 2). The enhanced SARVI2 had an absolute range of 0.40 units, a 100% relative range.

Table 2. Variations in reflectances and vegetation indices across the spectral signatures encountered at the OTTER site.

	OLD GROWTH (C.R.)	DOUG. FIR (CASC.)	DOUG FIR (C.R.)	SUB- ALPINE (CASC)	OLD GROWTH (C.R.)	ABS. DIFF.	% REL. DIFF.
RED	0.027	0.027	0.020	0.020	0.027	0.01	35.0
NIR	0.431	0.325	0.259	0.176	0.392	0.26	144.9
SR	15.71	11.86	13.20	9.00	14.29	6.71	74.60
NDVI	0.880	0.844	0.859	0.800	0.869	0.08	10.0
NDVI _{green}	0.833	0.824	0.808	0.765	0.818	0.07	8.9
DVI	0.404	0.298	0.239	0.157	0.365	0.25	157.3
WDVI	0.401	0.295	0.237	0.155	0.362	0.25	158.7
PVI	0.258	0.186	0.146	0.089	0.231	0.17	189.9
SAVI	0.632	0.524	0.461	0.338	0.595	0.29	87.0
ARVI	0.864	0.804	0.833	0.731	0.852	0.13	18.2
SARVI2	0.795	0.642	0.561	0.398	0.747	0.40	99.7
GEMI	0.887	0.761	0.674	0.532	0.844	0.36	66

A possible option for alleviating some of the NDVI saturation is to employ the green band in place of the red in the NDVI equation (Gitelson et al., 1996). However, we found no improvement when the green NDVI was computed over the forest canopies where only a 0.07 unit absolute difference was found (Table 2). A plot of the green NDVI over the agricultural canopies similarly showed little improvement in saturation (Fig. 3.5d).

Figure 3.5 (e-j) show the respective VI-LAI relationships for the remaining vegetation indices, including WDVI, PVI, SAVI, ARVI, SARVI2, and GEMI. Most of the other indices have an extended, linear response over a wider range of vegetation conditions which would not only minimize the 'saturation' problem, but also allow for more accurate aggregation and scaling of multi-resolution data sets.

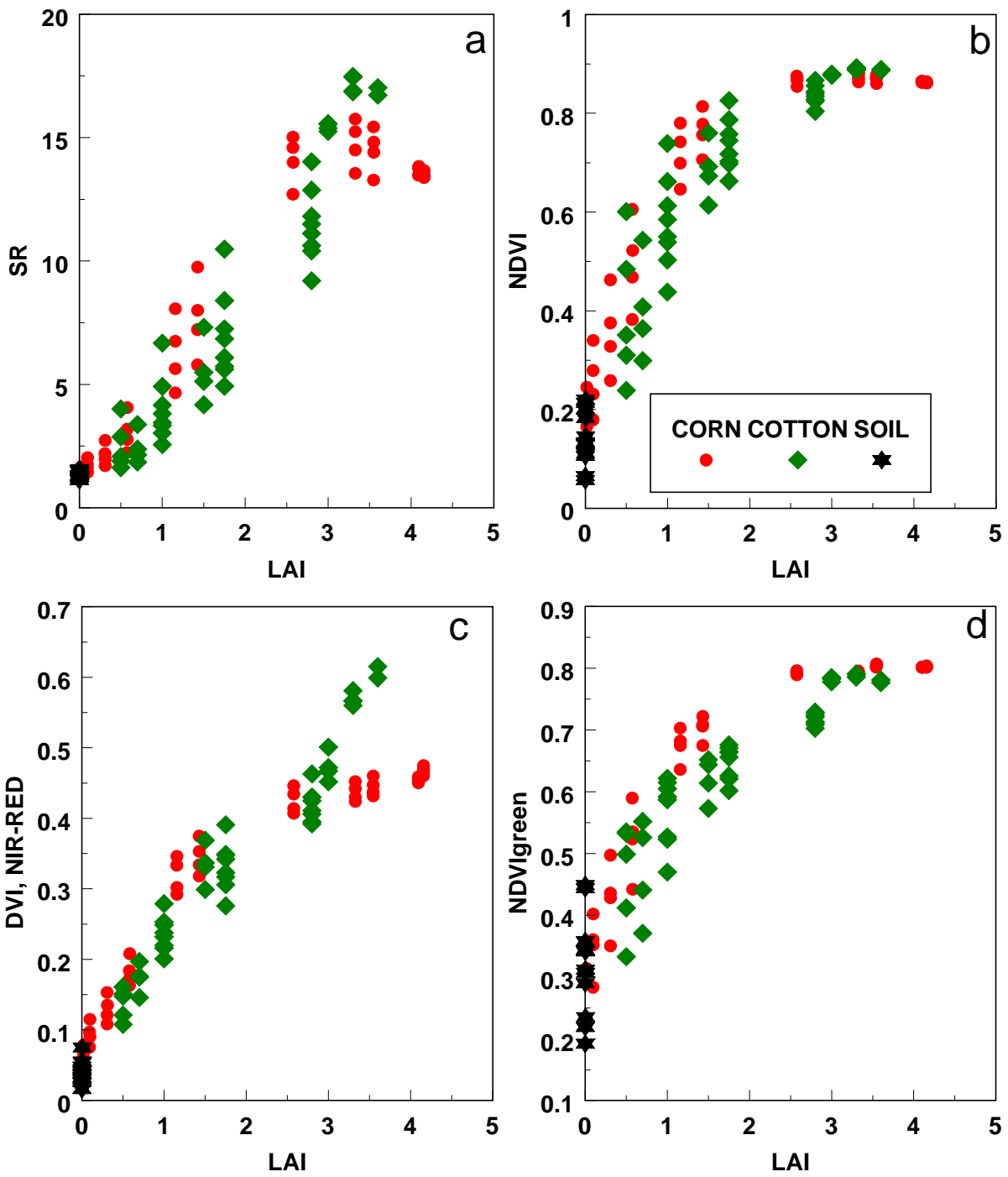


Figure 3.5 a-d

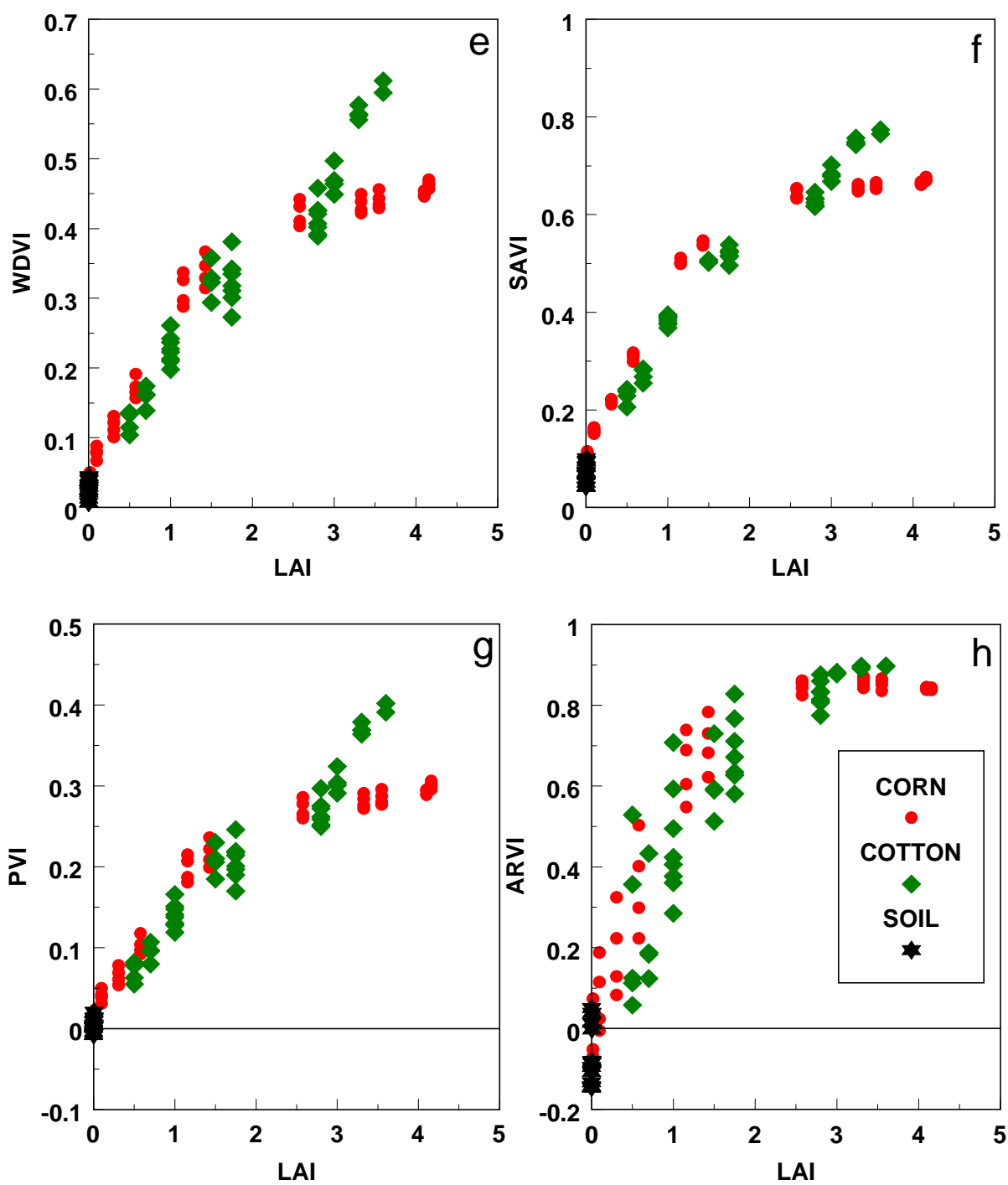


Figure 3.5e-h

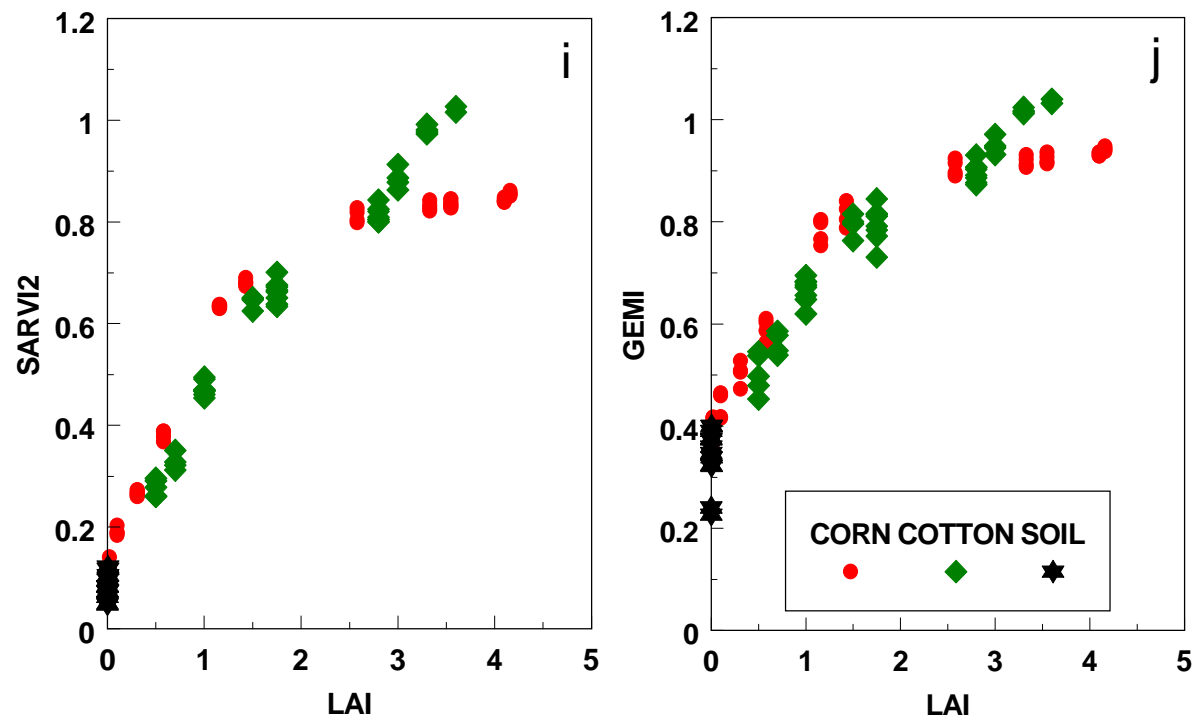


Figure 3.5 Vegetation index response (a-j) as a function of LAI for corn and cotton and different soil backgrounds

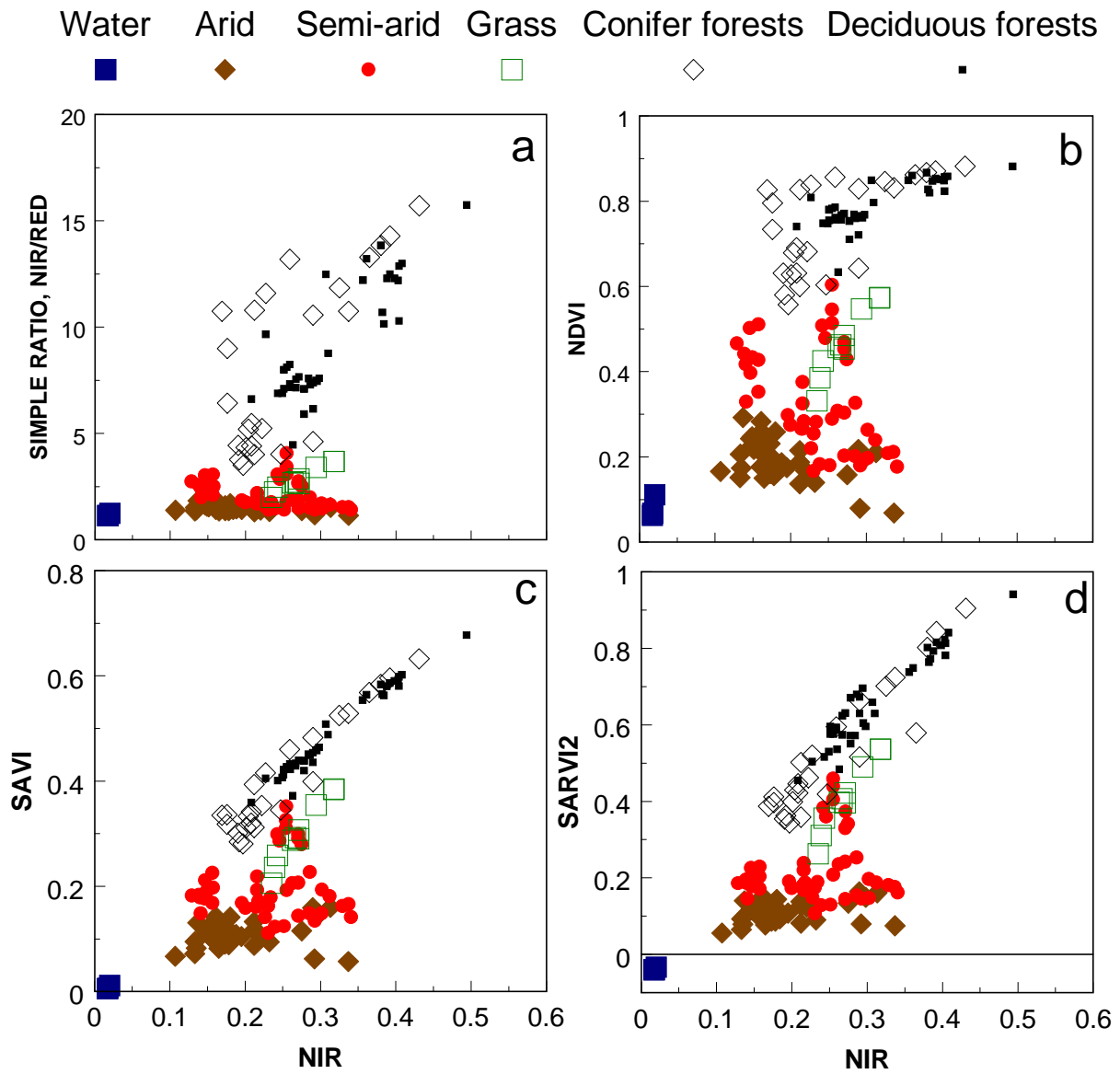


Figure 3.6 SR, NDVI and SAVI as a function of the NIR for a range of vegetation types. (LANDSAT)

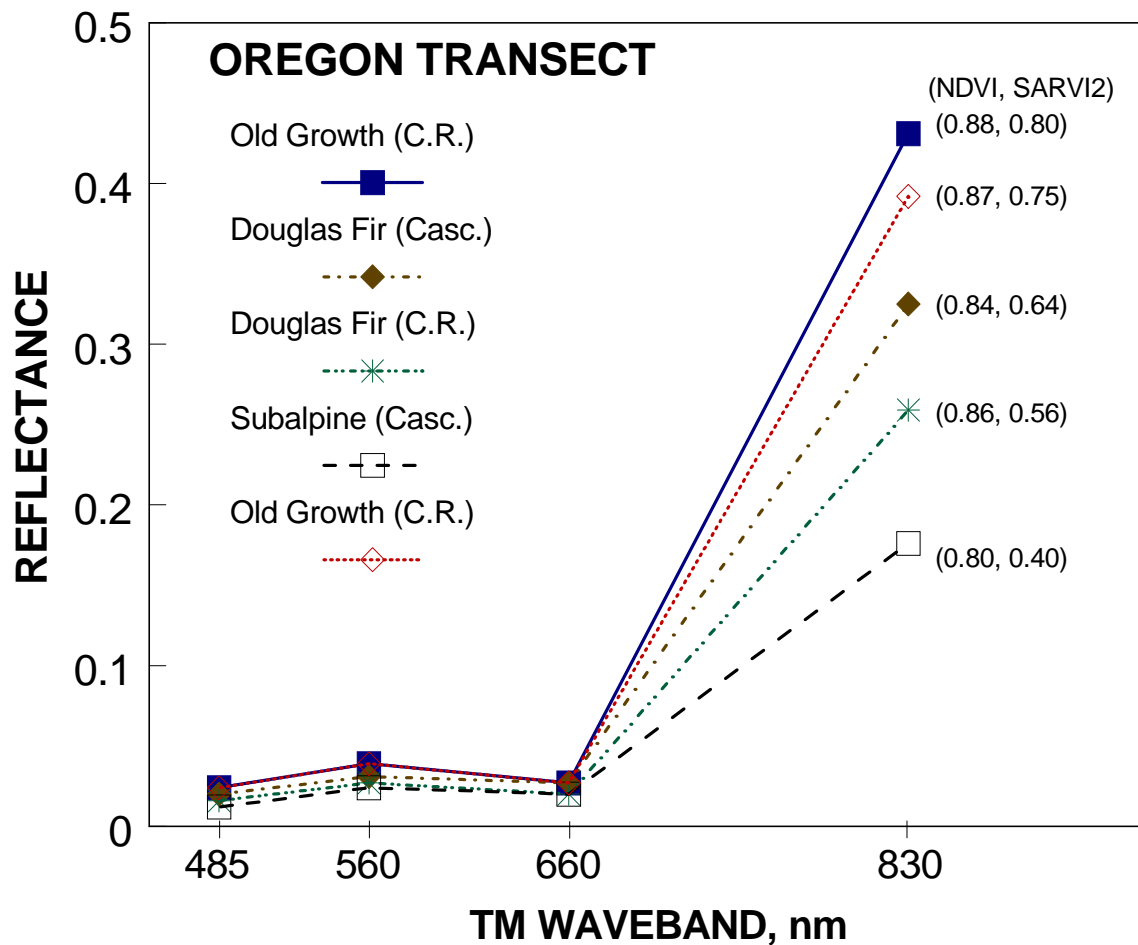


Figure 3.7 Spectral reflectance signatures for conifer forest sites along the Oregon transect (NDVI and SARVI2 values are annotated for each spectral signature)

3.1.2 Vegetation - Background Interactions

The first attempt made to model pixel behavior in multispectral space and its boundary conditions was by Kauth and Thomas (1976) with the Tasseled Cap model. A soil brightness vector in MSS 4-band space was created to describe the lower boundary condition or soil baseline. An orthogonal vector was then created orthogonal to the soil brightness vector and oriented toward the green apex or dense vegetated pixels, and named the 'Green Vegetation Index' (GVI). A third vector further described the senescence process or yellowing of the vegetation and was made orthogonal to the first two vectors. This was simplified to the soil line index and perpendicular vegetation index by Richardson and Wiegand (1977) in two-band (NIR-red) space. In both cases, the model uses the orthogonal distance of a pixel from the soil baseline as the quantitative measure of green vegetation.

From a theoretical point of view, the orthogonal-based indices such as the GVI, PVI, DVI, and WdVI assume canopy components to be opaque to solar radiation and spectrally independent. This is a simple mixing model of non-interacting components (vegetation and background) and results in isolines parallel to the soil line (Fig. 3.8), in contrast to isolines converging at the origin as was the case with the NDVI and SR. A more physically-based model is to take into account the transmissive and extinction properties of a canopy, which are spectrally dependent, i.e, canopy leaf components may be opaque or highly absorbing to red radiation allowing very little penetration but, at the same time allow significant amounts of scattered and transmitted NIR radiation to penetrate and interact with the canopy background.

This is demonstrated through Beer-Lambert (Bouguer's) law:

$$E_s(\lambda) = E_o(\lambda) \exp[-k(\lambda) \text{ LAI}], \quad (13)$$

$$T(\lambda) = \exp [-k(\lambda) \text{ LAI}], \quad (14)$$

where E_o is the global (diffuse + direct) irradiance entering the canopy medium, E_s is the irradiance at the soil surface after passing through a canopy optical path length (LAI), k is the 'global' canopy extinction coefficient (leaves, gaps, openings, etc.), $k \cdot \text{LAI}$ is the extinction optical thickness, T is transmittance through the canopy medium, and λ is wavelength. Canopy extinction becomes the slope obtained in plotting $-\ln T$ against LAI. A photosynthetically active canopy is characterized by pigment (chlorophyll) absorption in the red portion of the spectrum, resulting in a relatively high k_{red} and low T_{red} compared with k_{NIR} and T_{NIR} , respectively. Since red extinction through a canopy exceeds that in the NIR, more NIR energy is reflected off the canopy background relative to the red. This spectrally-dependent, secondary signal is not amenable to simple ratioing and a 'background' correction becomes necessary.

The slope and intercept of the vegetation isolines in NIR-red space are related to the optical properties of the canopy medium, such that when $k_{\text{red}} = k_{\text{NIR}}$ (a dormant canopy), the slope of the isolines remain constant and equal to the soil line slope. However, when $k_{\text{red}} > k_{\text{NIR}}$, which represents a photosynthetically active canopy, the slope of the isolines becomes greater than the soil line slope and increases with increasing amounts of LAI. The greater the difference between red and NIR extinction through a canopy, the steeper the isolines become. Ground-based observational data sets (Heilman and Kress, 1987; Bausch, 1993; Huete et al., 1985) and SAIL model simulations based on canopy radiant transfer theory (Baret et al., 1989; Huete and Liu, 1994) show vegetation isolines to both increase in slope and intercept with increasing amounts of vegetation.

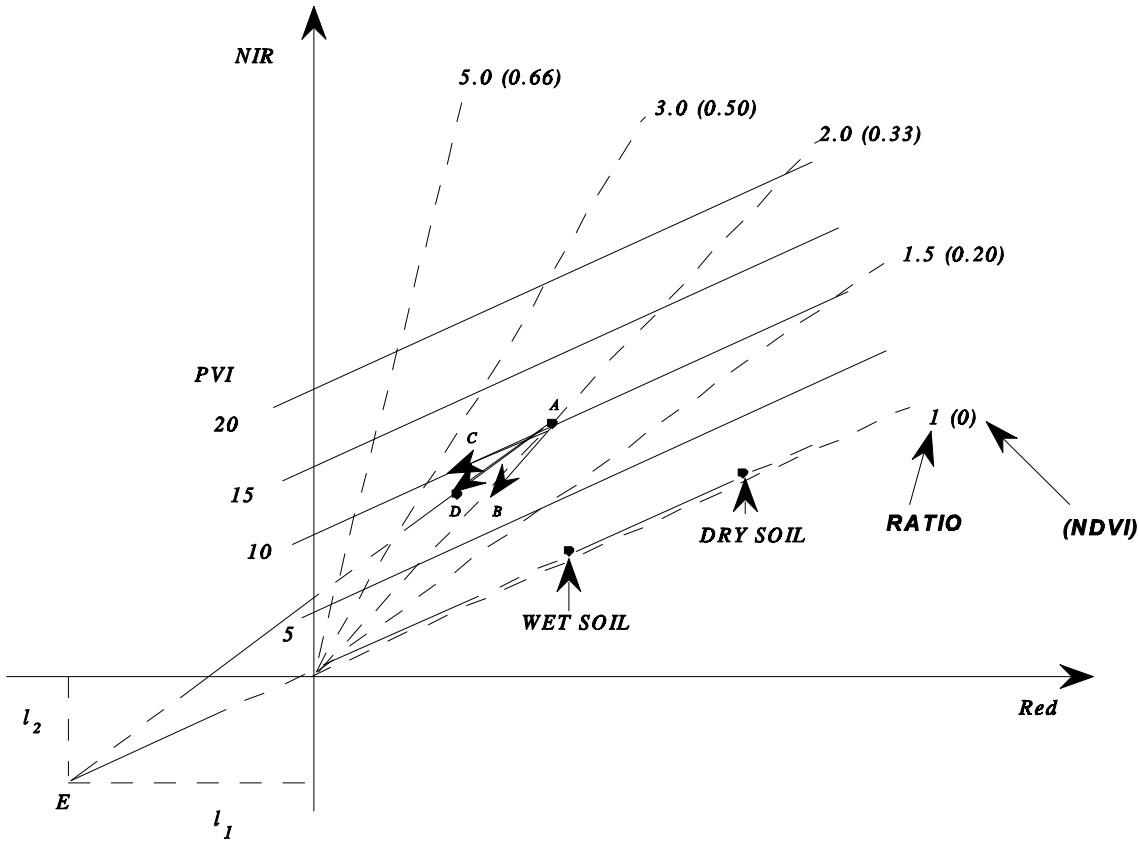


Figure 3.8 Vegetation index isoline in NIR-red reflectance space as modeled by the SR, NDVI, PVI, and SAVI (Huete, 1988)

This is the basis of the soil adjusted vegetation index (SAVI) in which an 'L' term is inserted into the NDVI equation to account for differential red and NIR extinction through the canopy medium and the resulting spectral interactions of the vegetation with canopy background;

$$SAVI = (1 + L) [(\rho_{nir} - \rho_{red}) / (L + \rho_{nir} + \rho_{red})]. \quad (15)$$

By shifting the origin to where the isolines converge, one considerably minimizes canopy background influences (Fig. 3.8). An 'L' value of 0.5 was found to minimize background variations throughout the full range (sparse to dense) of vegetation covers, producing vegetation results more independent of canopy background. As seen in Fig. 3.5f, the SAVI minimized canopy background variations relative to the orthogonal-based indices (PVI, DVI, WDI) and the ratio-based indices (NDVI, SR). The scatter in Fig. 3.5, at any LAI, is due to background variations in the corn and cotton canopies. Background contamination in the NDVI is greatest at LAI = 1 where the NDVI varied from 0.42 to 0.74 (50% increase) due to darker and wetter canopy backgrounds.

Background contamination was also strong in the SR, the green NDVI (especially at LAI=0) and the ARVI.

The 'L' factor also helps linearize the SAVI and sensitivity is maintained over dense levels of vegetation, as also seen in the TM results (Fig. 3.6c). In this figure one can also observe that the SAVI values for the lower boundary condition, representing arid regions, is nearly horizontal or invariant to background brightness. The NDVI shows an increase in values with darker desert substrates. Thus, dark soil backgrounds may be falsely interpreted as 'chlorophyll' absorption with higher than expected NDVI values. The NIR/red ratio has good baseline behavior with arid region values invariant to background variance, but has poor discriminating capability between arid and semiarid regions. The NDVI has better discrimination potential but has the systematic background bias whereby darker substrates yield higher NDVI values. The SAVI and SARVI have both stable baseline behavior and discrimination potential due to their more linear functions. Baseline behavior is deemed important for the final calibration of the VI product.

Further work by Qi et al. (1993b) and Baret et al. (1989) have resulted in further modification to the SAVI, by accounting for secondary vegetation - background interactions (modified SAVI or MSAVI) and through better baseline calibration (transformed SAVI or TSAVI). In summary, vegetation and canopy background spectral interactions are readily removed. As Fig. 3.5 shows, many indices minimize the background problem, relative to the NDVI, SR, and ARVI. These three indices, however, can be fixed through insertion of the 'L' term, including the SR which would become: $[(\text{NIR} + L) / (\text{red} + L)]$. The selection of an optimal index depends in part on how important background effects are in a 'global' sense and if new problems are created by removing the 'ratioing' properties of the NDVI or SR. Goward and Huemmrich (1992) noted how difficult it is to observe or quantify background effects in global scale imagery, although snow background was deemed to be of particular concern, introducing errors in the estimation of fAPAR in excess of 50% relative to more typical canopy backgrounds (soil & litter), where errors were in excess of $\pm 15\%$. The 'ratioing' properties of the NDVI were extremely vital when the NOAA-AVHRR production of the NDVI first began, particularly with un-normalized, uncalibrated, and uncorrected for atmosphere data sets. Since the MODIS NDVI product will utilize well-calibrated, atmospherically corrected, surface reflectances, one will need to re-assess the continued importance and benefits of 'ratios'.

3.1.3 Atmospheric aerosol corrections

Aerosol scatters solar radiation before it reaches the surface and absorbs it again after it is reflected by the surface and before it reaches the satellite sensor (Kaufman and Tanré, 1996). Atmospheric aerosols (smoke, dust, and air pollution particles) have a significant effect on all of the vegetation indices, reducing the contrast between red and NIR reflectances, thus lowering vegetation index values, whether they are based on the NIR-red difference or the NIR/red ratio. In Fig. 3.9 some of the

vegetation index - LAI relationships are shown for a set of simulated atmospheres. The NDVI and SAVI are very sensitive to atmospheric effects and these influences become more pronounced at higher densities of vegetation. Atmospheric correction of MODIS data will alleviate these effects and improve upon attaining consistent VI values. The atmospheric - resistant vegetation indices (ARVI & SARVI2), on the other hand, are able to minimize atmospheric aerosol variations and are thus less dependent on atmospheric correction.

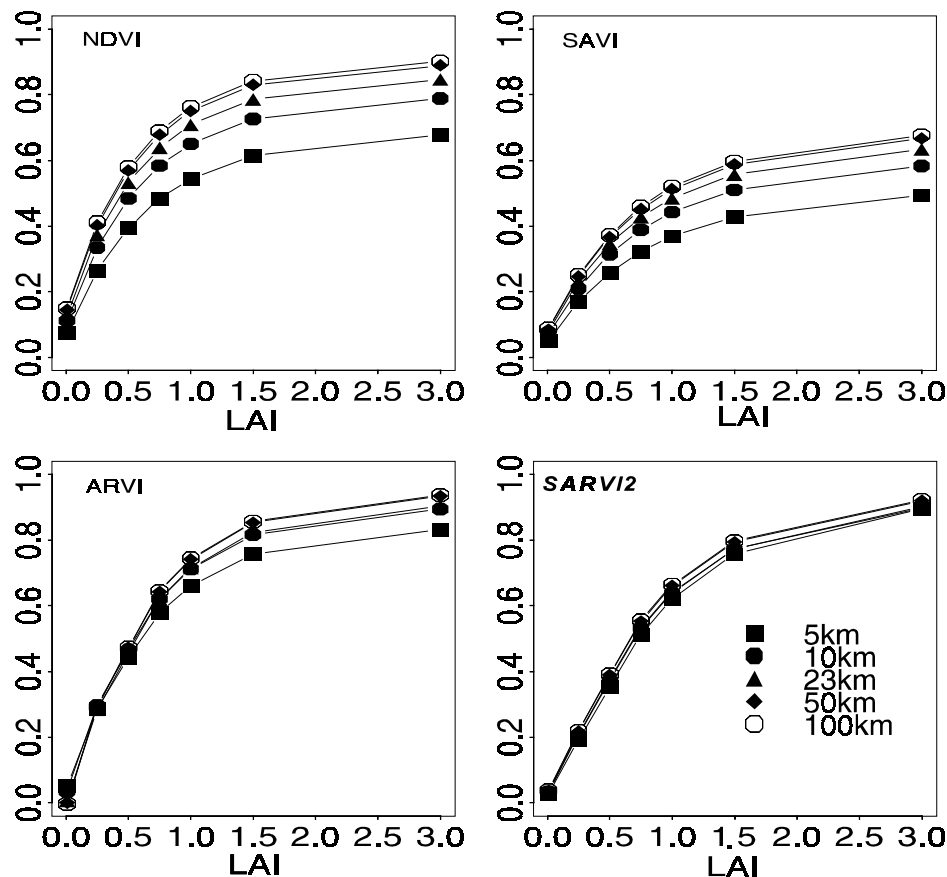


Figure 3.9 Simulated VI response as a function of Cedar LAI for different atmospheric aerosol conditions (Rayleigh and ozone corrected)

There exists both direct and indirect atmospheric correction methods, involving ground-based measurements, radiative transfer models, climatology, and dark object subtraction approaches. As it may not be possible to implement a globally consistent, atmospheric correction scheme utilizing climatology and dark object subtraction methods, atmospherically resistant vegetation index equations have been developed which minimize aerosol influences indirectly on a pixel by pixel basis. This would be useful in smoke-filled areas, where the spatial variability of aerosols will exceed the

resolution grid size of the aerosol products. Kaufman and Tanré (1992) developed the atmospherically resistant vegetation index (ARVI) to minimize atmospheric-induced variations in the VI on a pixel by pixel basis. The ARVI utilizes the difference in radiance between the blue and the red channel, via a γ function, to correct the radiance in the red channel and stabilize the index to temporal and spatial variations in atmospheric aerosol content:

$$\rho_{rb}^* = \rho_{red}^* - \gamma (\rho_{blue}^* - \rho_{red}^*), \quad (16)$$

and ρ^* are reflectances with prior correction for molecular scattering and ozone absorption (Fig. 3.9).

The atmospheric resistance concept may also be incorporated into the SAVI to form a soil and atmospherically resistant vegetation index or SARVI (Kaufman and Tanre, 1992). Liu and Huete (1994), however, found soil and atmospheric influences to be interactive such that the removal of one source of noise increased the presence of the other. Consequently, a feedback term was utilized for simultaneous correction, resulting in a SARVI2 formula written as:

$$SARVI2 = 2 [(\rho_{nir} - \rho_{red}) / (L + \rho_{nir} + C_1 \rho_{red} - C_2 \rho_{blue})]. \quad (17)$$

Thus the SARVI2 is a modified NDVI with a soil adjustment factor, L , and two coefficients, C_1 and C_2 , which describe the use of the blue band in correction of the red band for atmospheric aerosol scattering (Fig. 3.9). An example of the smoke correcting capabilities of the SARVI2 formula is shown with TM imagery (Fig. 3.10). Continued work is currently in progress to ensure that implementation of an atmospheric resistant vegetation index does not alter the quality and integrity of the data set, nor create new sources of variance and uncertainty. The main disadvantage in the atmospheric resistant vegetation indices is the 500 m resolution of the blue band which may either degrade the resolution of a final VI product from 250 to 500 m or require 'sharpening' and co-registration of the blue band with the red and NIR.

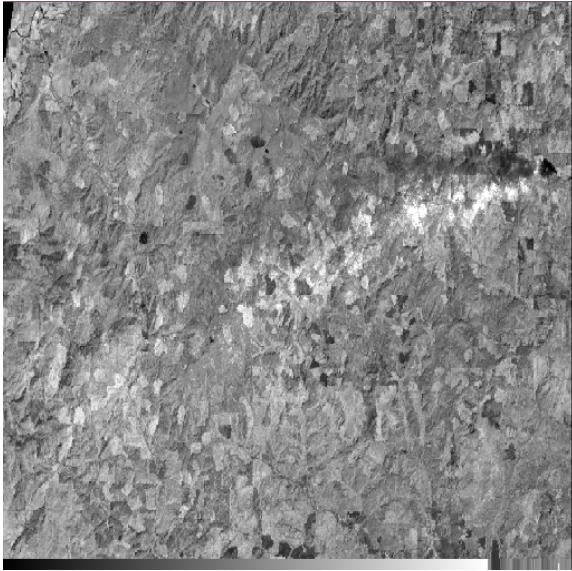
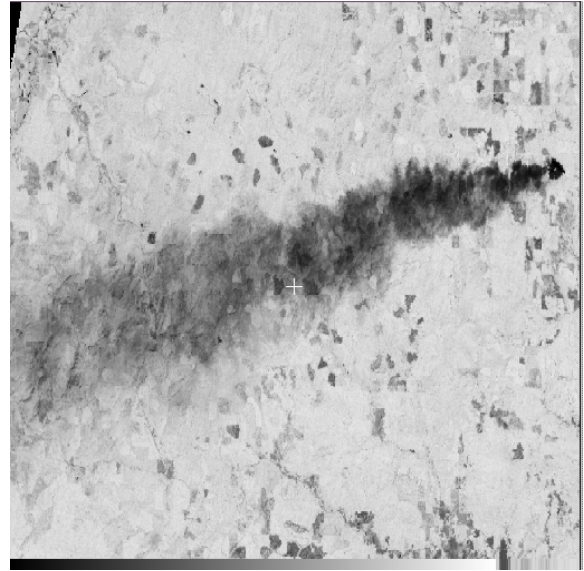
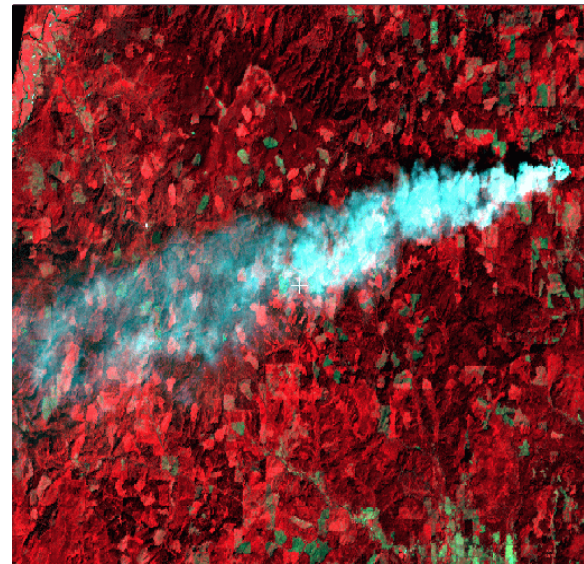
a**SARVI2****b****NDVI****c**

Figure 3.10: Illustration of the smoke correcting properties of the SARVI2 (a) along with the NDVI (b) and a color composite (c). (Oregon coastal forest, LANDSAT 5, August 29, 1993; 983x660 30 m pixels; atmospherically corrected with the dark object subtraction (DOS) technique)



3.1.4 Variance or uncertainty estimates

There are many sources of noise and uncertainty present in VIs, associated with instrument -related characteristics as well as uncertainties arising within the algorithm itself, due to environmental factors, such as canopy structure, atmosphere, canopy background, and sun-target-sensor geometry variations. Many sensitivity studies have documented vegetation index uncertainties resulting from the above perturbation factors. These studies include atmosphere and canopy radiative transfer models as well as observational data sets (see, e.g., Goward and Huemmrich, 1992; Huete and Liu, 1994). Since vegetation indices have two major uses; (1) a precise radiometric measure of vegetation, and (2) an estimator of vegetation biophysical parameters; two approaches will be utilized to assess VI performance and uncertainty. The absolute or relative change in VI units as a function of the degree of perturbation is one approach, giving a radiometric estimate of uncertainty. The second is based on plotting the perturbed response of the VI as a continuous function of a vegetation biophysical parameter, such as LAI or %cover, thus providing an estimate of error in biophysical units.

Instrument-related sources of noise include:

- error associated with a 5% absolute sensor calibration accuracy in bands 1, 2, and 3.
- error associated with a 20% band to band co-registration requirement in the cross- and along-track directions, and that associated with the 10% goal.
- error associated with a spectral band output change due to a shift in center wavelength. This varies from 0.5% (bands 1,2) to 2% (bands 3, 4) as shown in the MODIS CAL ATBD, Version 0 (Barker et al., 1993; p.12).

The primary issues of most concern in the level 3 compositing of the vegetation index are:

- the geolocation of images and accurate geometric registration, preferably to within 0.1 pixel;
- spatial resampling of the data to minimize radiometric degradation and;
- the accuracies and uncertainties present in the cloud screening, atmospheric correction, and BRDF products, as these have a direct impact on the generation of level 3 VI composited products.

Environmental sources of noise, which affect the intercomparison of vegetation index values on a global basis include:

- error and uncertainty associated with non-linearity and saturation.
- error and uncertainty associated with canopy structural effects, which affect the derivation of LAI, fAPAR, etc.
- error and uncertainty due to atmospheric variations.
- error and uncertainty associated with sun and view angle differences.
- error and uncertainty associated with background variations.

Several measures of sensitivity and error can be implemented. The dynamic range in a vegetation index is insufficient in characterizing its sensitivity to vegetation, as the ability of a VI to detect changes and differences in vegetation must also consider 'noise' and linearity. One can 'amplify' a vegetation signal through a log function or multiplicative term, however, this would also amplify noise in the equation. Thus a vegetation signal to noise ratio (S/N) or percent relative error are better methods to compare the performance of several VI's to spatial and temporal changes in vegetation.

The absolute error in the VI due to an instrument or environmental related perturbation may be described by:

$$e_a = VI_p - VI, \quad (18)$$

where VI is the 'true' VI value and VI_p is the perturbed VI response resulting from instrument error. The absolute error is a good measure of the resolution or uncertainty within each VI equation, but it is not necessarily a good basis for comparison of differences among VIs, since each VI has its unique dynamic range of values from bare soil to a full cover. The percent relative error forms a better basis for comparison and is defined as:

$$e_r (\%) = 100 \times (VI_p - VI) / (VI - VI_b), \quad (19)$$

where VI_b is the VI response over bare soil (lower boundary condition for the VI dynamic range). Thus the % relative error standardizes the VI by first subtracting the lower VI baseline value (bare soil, VI_b) from all VI terms, and then dividing by the true VI. A measure of vegetation sensitivity is the reciprocal of the relative error or signal to

noise ratio (S/N):

$$S/N = (VI - VI_b) / (VI_p - VI), \quad (20)$$

where the numerator is the 'signal' at any level of vegetation amount and the denominator is the 'noise'. The 'vegetation signal to noise ratio' encompasses both the desire to maintain as large a dynamic range as possible as well as to minimize all external, internal, and sensor variations.

A further measure of VI performance is the 'vegetation equivalent noise' (VEN):

$$VEN = (VI_p - VI) / d(LAI), \quad (21)$$

where $d(LAI)$ is the slope, $dVI/dLAI$, of the VI-LAI curve at a specific LAI. The VEN and percent relative error are different measures of sensitivity, as % relative error describes uncertainty along the 'y' axis (VI), while the VEN describes uncertainty along the 'x' axis (biophysical parameter; %cover or LAI). These 2 terms may differ considerably, especially if the VI-biophysical parameter relation is non-linear.

Figure 3.11 is a limited and preliminary example of the above equations, showing the average absolute error and average VEN values for each VI over a range of simulated cedar, LAI values (Huete and Liu, 1994). The error and noise terms are separated into the individual canopy background and atmospheric components as well as the combined total. Soil and atmospheric error are of similar magnitudes, but vary for each VI. Soil noise and error are much higher in the ARVI and NDVI and lowest in the SAVI and SARVI2. The inclusion of the blue band (atmospheric-resistant versions) can aggravate the soil noise problem as the soil noise in the ARVI exceeds that of the NDVI. The atmospheric-resistant variants (ARVI and SARVI2), on the other hand, have lower atmospheric noise and error than the NDVI and SAVI.

For comparison purposes, the absolute error due to different instrument characteristics is also shown in Fig. 3.11. The derivation of the error analyses is included in Appendix A. The largest source of instrument error considered here was an anticipated 5% radiometric calibration accuracy of the MODIS bands 1, 2, and 3. Calibration error is approximately one-half that due to 'total' (soil/atmosphere) error. Nevertheless, calibration error is of the same order of magnitude as individual soil and/or atmosphere error. For the most part, the band shift error and band to band co-registration (20%) error are much smaller than the calibration error except in the case of the SAVI and ARVI, where co-registration error is of the same magnitude as calibration error. Further analysis is needed to couple all sources of error in an end-to-end (sensor to ground) model.

Error and uncertainty measures for the level 3 VI compositing algorithm are evaluated in the BRDF and composite sections. The uncertainty due to sun angle variation is illustrated in section 3.1.7.10 in this document. The Maximum VI value

composite scenario (MVC) was compared with alternative composite scenarios using nadir-equivalent VIs as a reference in sections 3.1.7.13. Errors in the NDVI due to standardization of nadir-equivalent reflectance values with BRDF models were evaluated in 3.1.7.9 and 3.1.7.11.

In conclusion, this very limited sensitivity and error analysis has shown the interrelationships of environmental and instrument sources of noise and has laid out a basis for assessment of the performance of the MODIS VI products.

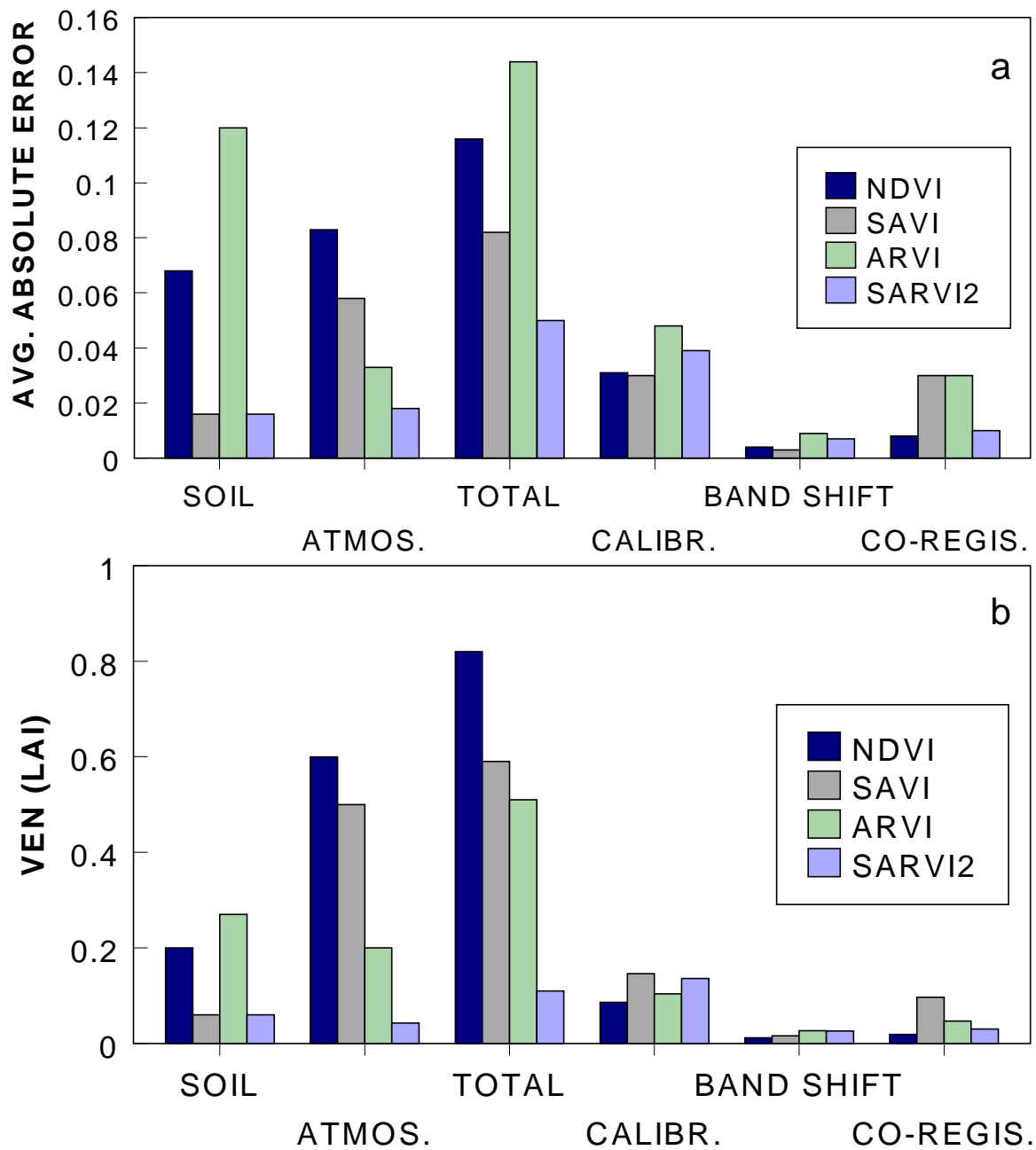


Figure 3.11 Comparison of VI absolute error (a) and vegetation equivalent noise (b) among various instrumental and environmental variables, based on simulated Cedar data.

3.1.5 Temporal and Spatial Compositing of MODIS VIs (Level 3)

3.1.5.1 Angular, View and Sun Angle Considerations

Vegetation indices are affected by variations in bidirectional reflectances which vary greatly as a function of sun-target-sensor geometries (Walter-Shea et al., 1996). Figure 3.12 gives a schematic diagram of the position of the sun and MODIS sensor for the EOS-AM1 morning overpass time. MODIS will image the earth's surface over a swath width of 2330 km over sensor viewing angles of $\pm 55^\circ$ cross-track with the effective view angle on the ground being slightly larger owing to the earth's curvature. Solar zenith angles across MODIS imagery may vary up to 20° from edge to edge of the 2330 km swath and also vary spatially with latitude and seasonally over the growing season (Table 3). The sun-target-sensor geometric configuration of EOS-AM1 (descending node, morning overpass) will be somewhat constrained with the backscatter direction of the MODIS swath having larger solar zenith angles than the forward scatter (Fig. 3.12). The resulting variability in both view and solar zenith angles are important for intercomparison of vegetative covers at different latitudes and in different seasons and must be accounted for in the VI compositing algorithm if we are to maintain 'global' VI robustness.

Table 3. Seasonal differences in solar zenith angle during MODIS overpass times for different latitudes (GMT 10.30h.; Longitude = 0°).

DOY	Latitude(N)					
	1°N	15°N	30°N	45°N	60°N	75°N
1	33°	44°	58°	71°	85°	no sun
90	24°	26°	34°	46°	59°	72°
180	20°	24°	22°	29°	40°	53°
270	33°	26°	37°	50°	64°	78°

The influence of variable sun-target-sensor configurations on derived vegetation indices can be standardized in various manners, including (1) standardize reflectances to nadir view angle at representative solar zenith angle; (2) standardize reflectances to nadir view angle and constant (smallest) solar zenith angle; (3) use of spectral (hemispherical) albedos; or (4) adjust to a constant 'off-nadir' view angle with constant sun angle. For the standard MODIS VI products, we propose to use the first two methods and examine the other two approaches post-launch. Preliminary analysis suggests that both the third and fourth approaches may enhance vegetation detection over a limited range of land cover conditions (Privette et al., 1996a), but will result in overall decreased sensitivity from desert to forest, and present greater saturation problems in more densely vegetated canopies.

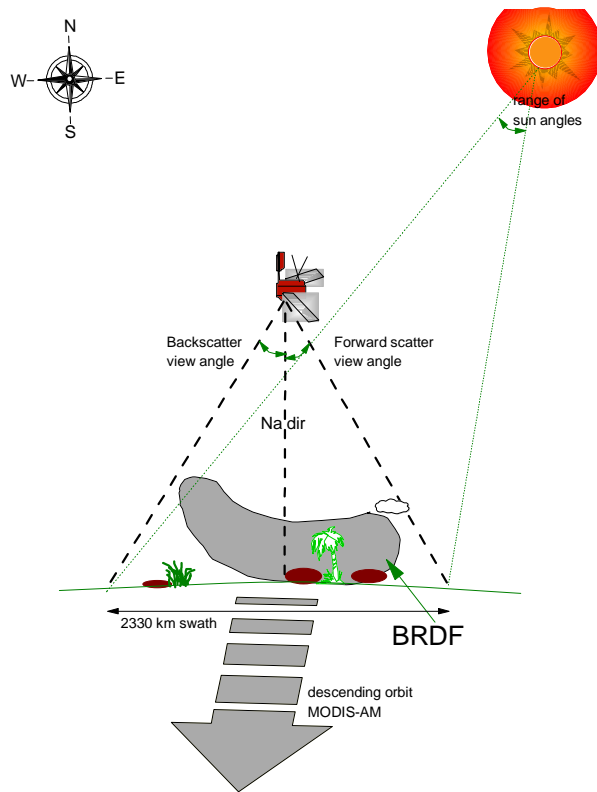


Figure 3.12: Illustration of MODIS data acquisition on the EOS-AM platform. The bidirectional reflectance distribution function (BRDF) changes with view and sun geometry. Notice the shadow caused by clouds and canopy.

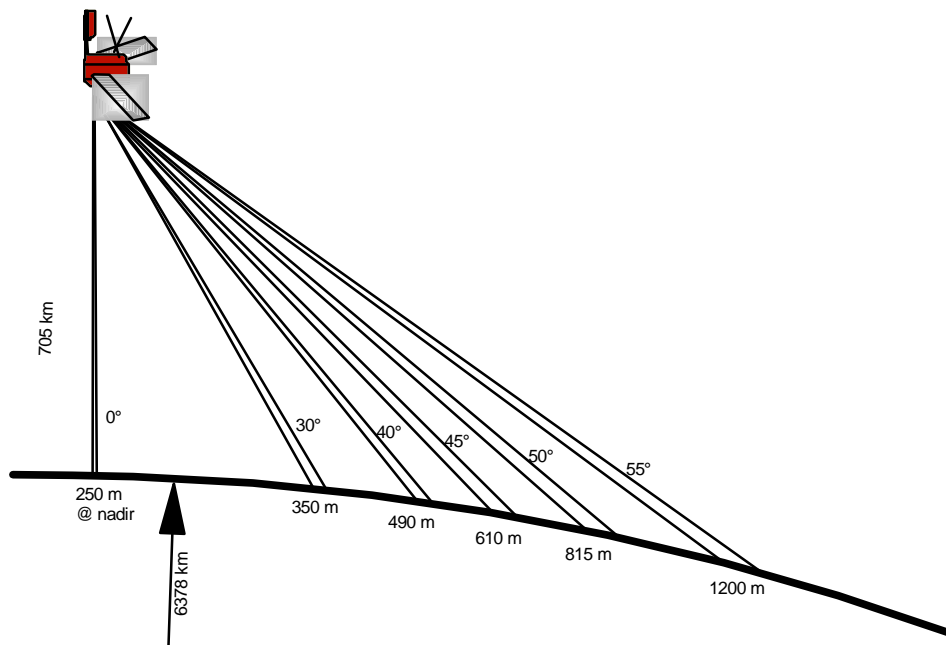


Figure 3.13: Illustration of the increasing IFOV (pixel size) as a function of the MODIS scan angle.

The advantages of standardizing the VI to the smallest, near-nadir view and smallest solar zenith angles include:

- The pixels with the smallest view zenith angle will have the finest spatial resolution. This is 250 m for the red and NIR reflectances. This allows one to preserve the finest detail available with the MODIS sensor, which will allow for the computation of VIs at the finest detail. The 250 m pixel size will increase to over 1 km at the edges of the scan angle and up to 500 m along track (Fig 3.13).
- The pixels with the smallest view and solar zenith angles will have the most accurate atmospheric correction (least path length; Fig 3.13). Furthermore, since BRDF and atmospheric correction are coupled, one can achieve the best atmospheric correction and BRDF extraction at the smallest viewing angles.
- Established biophysical parameter relationships with vegetation indices are based upon nadir-viewing angles.
- Vegetation index “saturation” problems become greater with off-nadir view and larger solar zenith angles.
- Spatial degradation and blurring increase greatly with off-nadir view angles (Moody and Strahler, 1994) and off-nadir pixels will thus be more difficult to register than nadir pixels.
- The bowtie effect, in which several pixels overlap for a given area on the ground, is more pronounced with increasing off-nadir view angles, making it more difficult to assign the right values to one pixel.
- Solar zenith angle differences are minimal within a composite period for observations measured at close to nadir view zenith angles.
- Less cloud shadow is measured for the smallest solar zenith angle and in the backscatter view direction since the cloud and cloud shadow areas are more likely to overlap.
- Near nadir view angles allow for a wider range of VI validation efforts with nadir viewing sensors, e.g. ASTER, LANDSAT-7.

3.1.5.2 Maximum value composite (MVC) approach

The currently accepted procedure for generation of composited AVHRR-NDVI products is the maximum value compositing (MVC) technique in which several NDVI images are merged to create a single cloud-free image with minimal atmospheric effects (Holben, 1986). This is accomplished by selecting, on a pixel by pixel basis, the highest NDVI value as output to the composited product. The procedure generally

includes cloud screening and data quality checks (Goward et al., 1994; Eidenshink and Faundeen, 1994).

The maximum NDVI compositing approach is based on theory and logic and is primarily formulated to reduce residual cloud cover not accounted for in the cloud masking procedure, and atmospheric sources of contamination, both of which cause lower NDVI values (see atmosphere section 3.1.3). Since the influence of atmospheric contamination increases with optical path length, the maximum NDVI criterion has a tendency to select not only the 'clearest' (lowest optical depth) atmosphere, but also the most near-nadir view and smallest solar zenith angle pixels (least optical path length). Therefore, in an ideal case, a maximum NDVI would exclude the most cloud-affected and atmospheric contaminated pixels, if there are clear and cloud-free pixels available. This favors a final, cloud-free product with reduced view and sun angle effects (Holben 1986; Goward et al., 1991 Cihlar et al., 1994a). The anisotropy of atmospheric scattering tends to produce the highest NDVI value with the clearest atmosphere and at near-nadir and small solar zenith angles (least path lengths).

The MVC approach is attractive due to its simplicity, however, its major shortcoming is that the bi-directional influences of the surface are not adequately considered. Ratioing of the NIR and red spectral bands to compute vegetation indices does not remove surface anisotropy (Walter-Shea et al., 1996). This is a result of the spectral dependence of the BRDF with the NIR reflectance response generally more anisotropic than the red reflectance response (Gutman, 1991; Roujean et al, 1992). Many studies and experience have shown the maximum NDVI approach to select pixels with large view and sun angles which are not always cloud-free or atmospherically clear (Goward et al., 1991; Moody and Strahler, 1994; Cihlar et al., 1994b). Since residual clouds and the view angle alter the surface reflectances and thus the VIs, comparisons of global vegetation types would not be consistent throughout the year. The MVC works nicely over near-Lambertian surfaces where the primary source of pixel variations within a composite cycle is associated with atmosphere contamination and path length. However, the bidirectional spectral behavior of numerous, 'global' land cover types and terrestrial surface conditions have been widely documented and shown to be highly anisotropic due to canopy structure, shadowing, and background contributions.

When a Lambertian surface is replaced with an anisotropic scattering surface (see section on ASAS data, 3.1.7.11 and 3.1.7.12), the MVC selection becomes unpredictable and has a tendency toward selection of off-nadir, larger solar zenith angle pixels. The forward scatter (more shaded) direction produces the highest NDVI values, with the NDVI values lowest in the more 'sunlit' backscatter view angles. The nadir view direction is normally close to a minimum, although the NDVI tends to decrease and increase slightly about nadir for the backscatter view angles. The atmosphere counteracts and dampens the surface BRDF signal, mainly through the increasing path lengths associated with off-nadir view angles and sun angles.

The maximum NDVI value selected is related to both the bidirectional properties of the surface and the atmosphere, which in turn vary with atmospheric optical depth and canopy density and structure. This is the primary reason for the inconsistencies observed in the selection of maximum NDVI values. Depending on the structure and density of the canopy, the anisotropy results in higher and lower NDVI values about nadir. As atmospheric correction algorithms improve, however, the bidirectional profiles of the VIs will be less a function of atmospheric optical properties and more related to the bidirectional properties of the surface. Surface anisotropy and bidirectional reflectances will thus become more pronounced in the EOS era as a result of improved atmospheric removal algorithms, which will accentuate differences in surface bidirectional reflectances resulting from canopy structural influences (Cihlar et al., 1994a).

Several deficiencies in the MVC approach need to be resolved for the generation of consistent MODIS global data sets with sufficient accuracy for vegetation monitoring:

1. The maximum value NDVI favors the forward scattering direction at off-nadir pixels (Gutman, 1991; Moody and Strahler, 1994) and thus does not account for surface anisotropic behavior, which generally produces higher NDVI values off-nadir, where more vegetation and less canopy background is 'effectively' viewed by the sensor.
2. There are significant solar zenith angle variations across an image which also influence the maximum NDVI pixel selected. Most studies have shown a near linear increase in NDVI with increasing solar zenith angles (Sellers 1985; Begué 1993; Huete et al. 1992; Leeuwen et al. 1994; Qi et al. 1994; Jackson et al., 1990). Singh (1988) and Middleton (1991) showed sun angle effects on the NDVI to be of concern at solar zenith angles greater than 30 degrees. This effect was particularly strong in canopies with low LAI values (Goward and Huemmrich, 1992). Sellers et al. (1994) found the opposite effect for the FASIR algorithm, but this was based on data uncorrected for atmosphere. Thus, as with viewing angles, the surface optical properties exhibit sun angle patterns which may run counter to those of the atmosphere.
3. There remains residual cloud contamination and atmospheric variability within a compositing cycle. As the MVC does not separate the relative effects of view angle and sun angle on the NDVI, it is difficult to state with certainty that the clearest pixel has been selected, since off-nadir pixels with residual clouds may produce higher NDVI values than nadir and clear pixels.
4. Selection of the maximum NDVI at off-nadir view and large solar zenith angles produces higher NDVI values than at nadir and results in an overestimation of vegetation, contributing more to the NDVI saturation problem. Tests with AVHRR data, using only Rayleigh corrected apparent reflectances, showed that on a continental scale the selected maximum NDVI value (MVC) was 5 to 15 % higher than the NDVI derived from near nadir reflectances.

5. The compositing procedure does require individual AVHRR images to be corrected geometrically, resampled, and registered as precisely as possible. Further research on the resampling method is needed with the goal of minimizing the affected radiometry of the output image (IGBP, 1992). For this reason the NDVI is normally calculated prior to resampling.

The MVC method works best for data uncorrected for atmosphere (Cihlar et al, 1994a), although numerous inconsistencies result (Gutman, 1991; Goward et al., 1991, 1994; Cihlar et al., 1994b). The MVC favors cloud free pixels, but does not necessarily pick the pixel closest to nadir or the least atmospheric contamination. The NDVI tends to increase for atmospherically corrected data, but this does not mean that the highest NDVI is an indication of the best atmospheric correction. We conclude that the primary benefit of the MVC is to reduce atmospheric sources of contamination and produce cloud-free imagery. The MVC thus is not necessarily appropriate for the atmospherically-corrected surface reflectance data to be generated by MODIS for the following reasons:

- VIs computed from atmospherically-corrected surface reflectances are strongly biased toward off-nadir viewing and larger solar zenith angles, where more vegetation is viewed or illuminated by the sensor.
- Off-nadir viewing angles result in pixels having more distortion and are coarser in size, i.e., less detail.
- Atmospheric correction is less reliable at off-nadir viewing and larger solar zenith angles where atmospheric path lengths are greatest.
- The MVC method will overestimate NDVI values which will result in an overestimation of vegetation biophysical parameters and will contribute to the saturation of the NDVI.
- Because of the above biases toward selection of off-nadir and larger solar zenith angle pixels, there is a higher probability of residual cloud and smoke being selected.

The MVC criterion applied to MODIS data will thus result in the selection of off-nadir, distorted and less radiometrically accurate pixels and deviate from the primary objective of working with the finest (nominal) resolution 250m NDVI data sets. We propose to resolve angular considerations of sensor view and solar illumination effects on the VIs through BRDF corrections to nadir viewing angles. BRDF corrections of AVHRR reflectances to a standard nadir view angle have been shown to improve the accuracy of the composited NDVI (Roujean et al., 1992; Cihlar et al., 1994a; Wu et al., 1995)

Consequently, the MVC algorithm will be used as a last resort composite scenario if the MODIS atmospheric correction and the cloud mask are inaccurate and a BRDF correction cannot be applied. A minimum of four to five 'good' observations will

be needed to invert a simple BRDF model to derive nadir-equivalent reflectance values representative of the composite time interval.

3.1.5.3 Compositing period

Variable composite periods have been used to obtain cloud free NDVI data on a global scale. The minimum compositing period is limited by cloud cover frequency and may vary from every 5 days at higher latitudes to as long as 30 days or more in some humid tropical areas. NDVI composite periods have varied among 7, 9, 10, 11 and 14 days and monthly intervals with variable (1 km to 1°) spatial resolutions (Townshend, 1994). The composite period depends on its application and the availability of cloud free data on a global scale. Shorter compositing periods will pick up more dynamic land cover changes and allows one to combine compositing periods to monthly or bi-weekly periods. However, the shorter the compositing period, the greater the likelihood of cloud-affected or missing pixels in the composited image. The proposed temporal resolution for the MODIS compositing algorithm is 8 days, 16 days, and monthly, and is partly based on attaining a symmetric view angle distribution over the 16-day MODIS repeat cycle.

3.1.6 Vegetation Index Compositing Algorithm

3.1.6.1 Description of Algorithm

The goal of the MODIS compositing algorithm is to preferentially select near-nadir view, cloudless pixels since this will optimize the spatial resolution, atmosphere correction and BRDF correction of angular effects. The VI compositing objectives are to :

- minimize effects and presence of residual clouds and cloud shadow, atmospheric aerosols, and BRDF effects (view angles standardized to nadir),
- maximize global and temporal land coverage at the finest spatial and temporal resolutions possible within the constraints of the instrument characteristics and land surface properties,
- ensure the quality and consistency of the composited data.

Two, level 3 gridded vegetation indices will be produced, the Normalized Difference Vegetation Index (NDVI) and the enhanced Soil and Atmospheric Resistant Vegetation Index (SARVI) with quality control (QC) values that indicate the quality of the data.

The gridded VIs will be produced at 8-day, 16-day and monthly temporal resolutions. They will be spatially and temporally resampled products, designed to provide cloud free vegetation index maps at nominal resolutions of 250 m and 0.25° global circulation grid cell size. The 8 and 16-day cycles are designed according to the EOS-AM1 16-day repeat cycle and consequent attainment of the full array of viewing angles.

The compositing algorithm will rely on information from the cloud mask, atmospheric correction, view zenith angle, solar zenith angle, relative azimuth angle and on surface BRDF normalization. The algorithms utilize the information in the reflectance-QC (MOD-09), partially derived from the MODIS cloud mask product (MOD-06), to pre-process the atmospherically corrected reflectance data of MODIS bands 1, 2, and 3 (red, NIR, blue). Land pixels with clouds, shadow, and bad data integrity will be excluded from the VI composite. A flowchart of this process is shown in figure 3.14.

The logic of the compositing algorithm is based on the MODIS specific input data and theoretical knowledge of radiative transfer and surface reflectance anisotropy. The compositing algorithm will optimize the choice of the best VI representative for each composite period (8, 16 days, or month), spatial resolution and global land extent.

The composite algorithm for an 8-day and 16-day cycle:

1. If five or more observations are "good" from an 8-day or 16-day cycle, the bidirectional reflectance data for each band will be fitted with a BRDF model. The fitted model will then be used to interpolate the surface reflectance at nadir view angle. The prevalent sun angle and VIs will be computed from the composited and normalized surface reflectances. Since a minimum of 5 surface reflectance observations are required for a stable BRDF model (Walthall's) inversion, the primary composite method will only be applied if 5 or more good observations are available.
2. If the number of cloud-free observations is smaller than 5 or the results of the BRDF inversion are unrealistic (e.g. negative reflectances, $NDVI_{BRDF} > NDVI_{MVC}$), the two reflectance observations with the smallest view angles will be selected, the VIs calculated, and the maximum value selected.
3. If the data over all 8 or 16 days is "bad", then the VI will be calculated for all days and the best pixel will be chosen based on the MVC approach (the 3rd criterion). The output composited reflectance data and corresponding QC for all three bands is stored in a separate file and used to produce the aggregate (climate modeling grid - CMG) VI composite. Sun angle information for each tile will be stored in the metadata. This processing scheme is depicted in 3.15.

The aggregated 0.25° NDVI and SARVI composites are calculated from cloud-free and atmospherically corrected, composited and gridded surface reflectances which were used to produce the VIs at 250 m resolution. The output for the composited NDVI and SARVI for the different spatial and temporal resolutions will be 16 bit integers for the VIs and 1 byte for quality (QC) control which will contain information on data integrity, composite method used and cloud cover. The number of cloudy or unusable pixels are counted for each CMG pixel to compute the percentage cloud cover.

The monthly VI products are created by a weighted average of the stored reflectance files representing the 16-day composites that fall within a particular month and the ones that overlap in the beginning and end of each calendar month (Fig. 3.16). The QC will indicate which composite periods were used in the monthly products. The preprocessing steps and algorithms are schematically represented in Figures 3.14, 3.15 and 3.16.

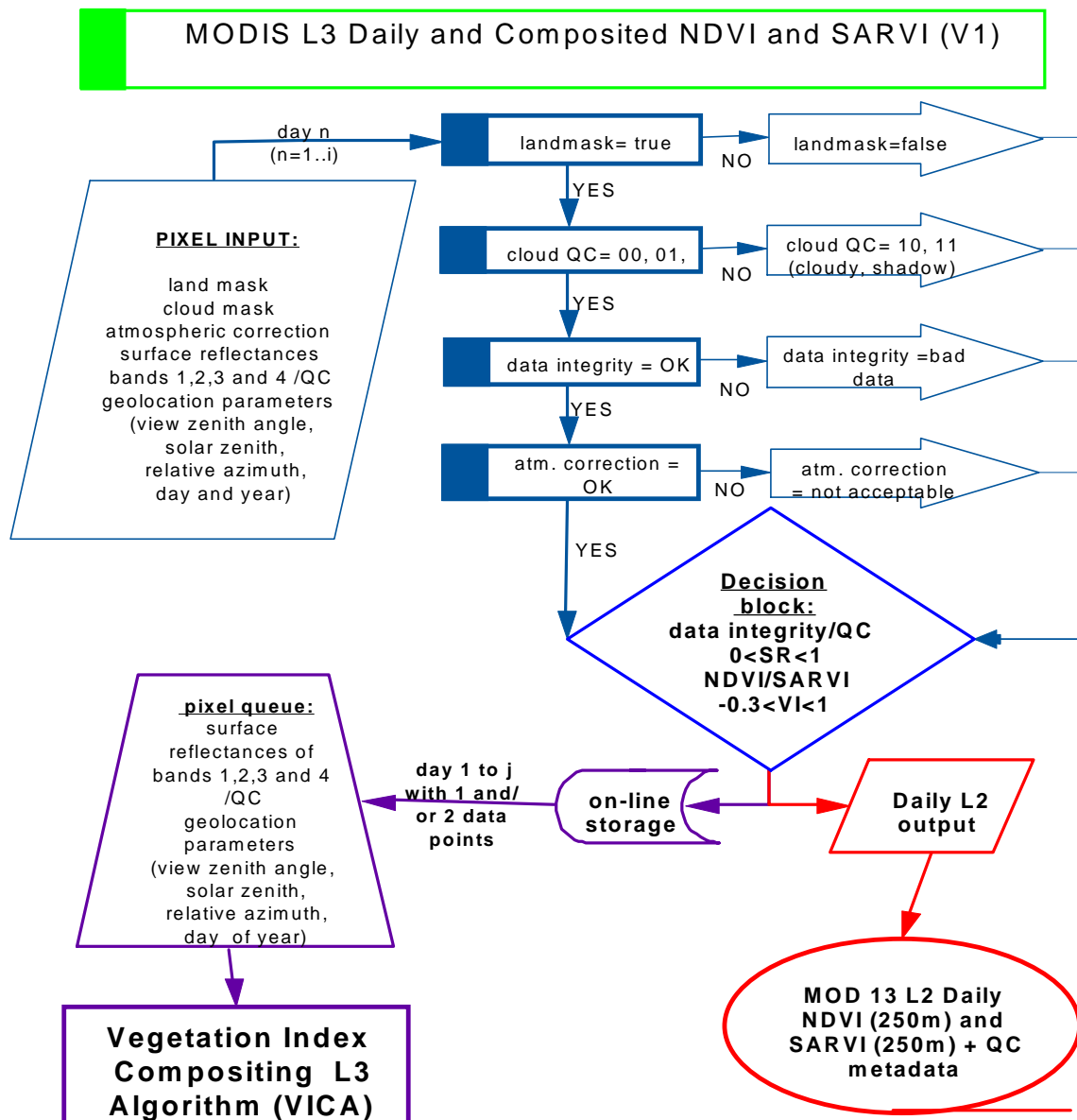


Figure 3.14: Flow diagram of pre-processing steps and quality flag evaluations that feed into the daily and composite VI algorithms.

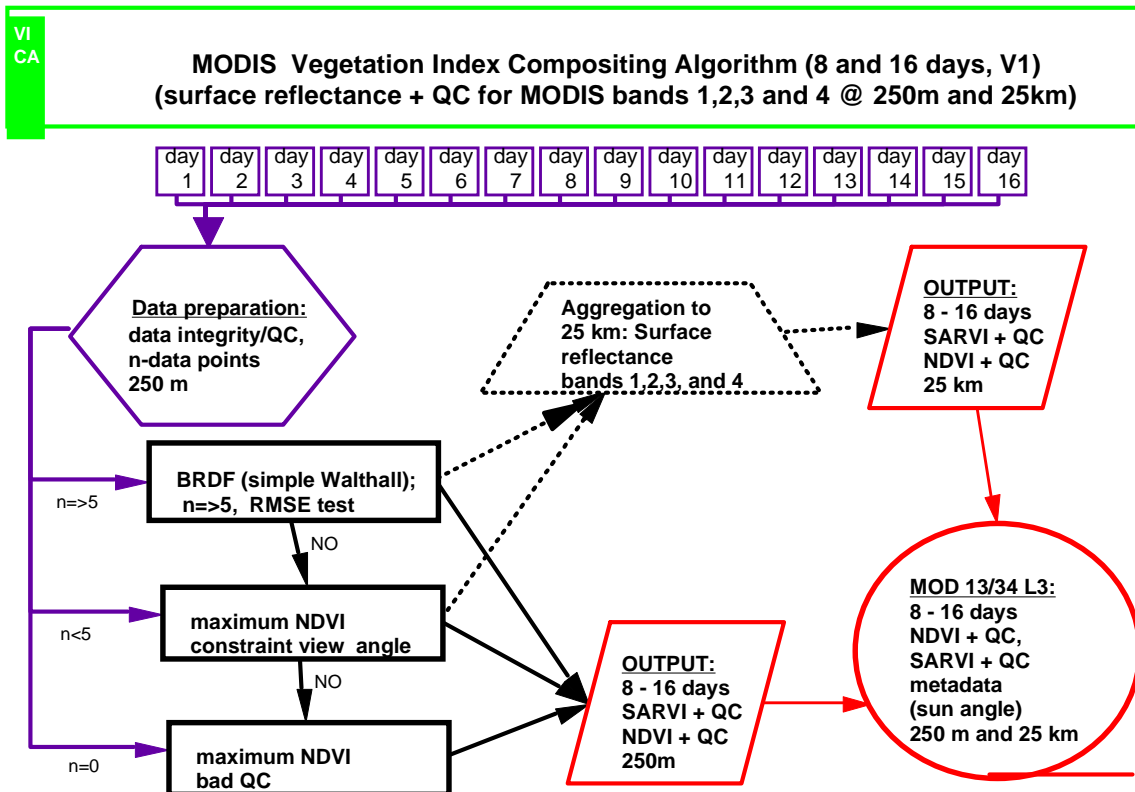


Figure 3.15: Diagram of the version 1 VI composite algorithm for 250m and 25km resolution.

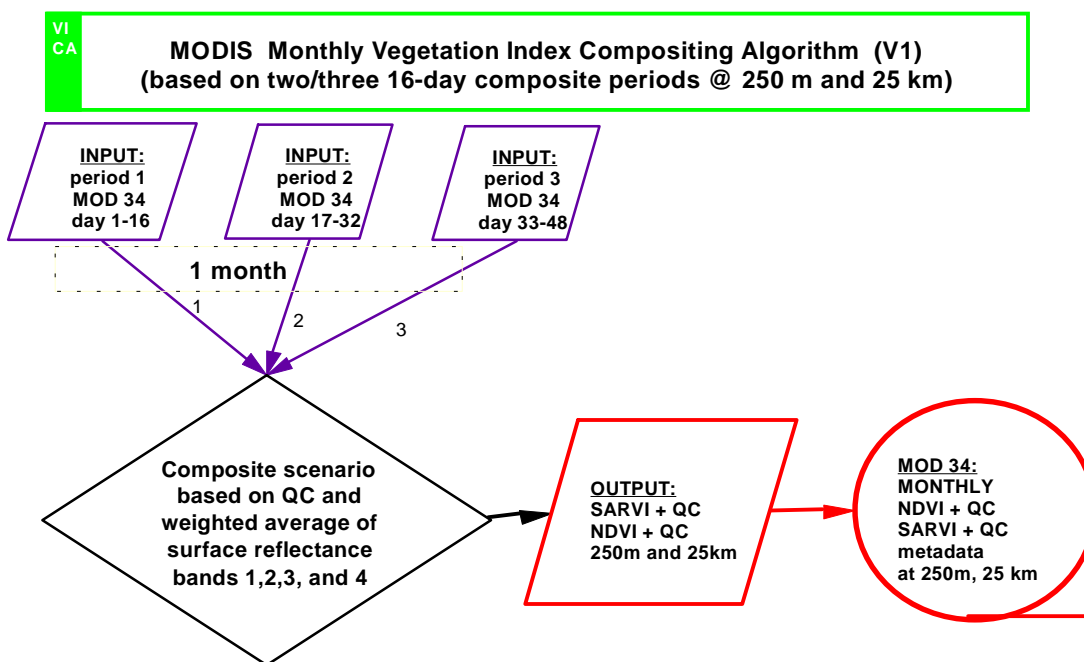


Figure 3.16: Version 1 monthly VI composite algorithm for 250m and climate modeling grid.

3.1.6.2 Continuity vegetation index: NDVI compositing scenario

$$\text{NDVI} = f(\rho_{\text{nir}}, \rho_{\text{red}}, \theta_v, \theta_s, \phi_s, \phi_v, \text{QC})$$

Input for each day of composite period (8, 16 days, and monthly):

- atmospherically corrected reflectances ($\rho_{\text{nir}}, \rho_{\text{red}}$)
- QC (data integrity, cloud and land mask, atmosphere correction flag)
- view, sun, azimuth/zenith angle,
- geolocation (position, Day of year)

Algorithm:

1. Reflectance data preprocessing based on QC.
2. BRDF model application and inversion to retrieve standardized, nadir surface reflectances.
3. If the nadir reflectance retrieval from the BRDF model is not possible, a view angle constrained maximum NDVI approach is applied.
4. If all observations within the composite time interval did not meet the cloud-free quality criteria (cloud flag indicated cloudy pixels), a maximum NDVI criterion will be applied to all observations with a 'good' data integrity flag.
5. Composited reflectance data corresponding to the composited VIs @ 250m will be used to aggregate to the climate modeling grid.

Output for each composite period:

- NDVI
- Quality control flags
- Sun angle and geolocation metadata

3.1.6.3 BRDF algorithm

The BRDF is important for the interpretation and comparison of the reflectance data collected at off-nadir and nadir view angles and variable sun angles. Since both sun and view geometry affect the VIs, the input to the VI should be standardized. The BRDF parameters can be used to normalize the surface reflectance to nadir view angles. The sun angle variability will be minimally incorporated in the BRDF correction, since the data necessary to standardize to a certain sun angle on a 16 day basis is very limited and thus would be inaccurate outside of the observed sun angle range. More research is needed as to how far the sun angle can be extrapolated to a standard sun angle throughout a year.

Numerous canopy bidirectional reflectance distribution function (BRDF) models have been developed to account for the anisotropy in land reflectances as a function of view and solar zenith angles. However, a BRDF model must be robust and operational on a global scale. Our approach is to use the simple Walthall model (Walthall et al., 1985) to standardize the reflectance data to nadir and compute nadir-based VIs. This has been shown to be far superior than a maximum NDVI (MVC) approach (Leeuwen, 1996). The BRDF approach estimated nadir-equivalent VIs better than the MVC, which overestimated the nadir-equivalent NDVI. The BRDF approach is also thought to represent changes during a composite period best. The Walthall model was found to work equally well as Roujean's BRDF model. Experience with ASAS and AVHRR data showed the Walthall model to be more robust than any of the other linear models. The Walthall model also requires the least number of floating operations per pixel. Privette et al. (1996b) compared most linear models and found that nadir interpolation with the Ross-thick/Li-sparse worked best for many vegetation types (Parabola data sets).

The empirical Walthall BRDF model:

$$\rho(\theta_v, \phi_s, \phi_v) = a \theta_v^2 + b \theta_v \cos(\phi_v - \phi_s) + c, \quad (22)$$

where the reflectance ρ is a function of the view zenith angle, θ_v , and the sun and view azimuth angles, ϕ_s, ϕ_v ; a, b and c are coefficients obtained using a least squares curve fitting procedure. c is equal to the nadir reflectance.

The semi-empirical Roujean model and the Ross-thick/Li-sparse models have the same linear equation:

$$\rho(\theta_s, \phi_s, \theta_v, \phi_v) = k_{iso} + k_{geo} f_{geo} + k_{vol} f_{vol}, \quad (23)$$

where f_{geo} , and f_{vol} are functions related to geometric and volume scattering components which cause the difference between the Roujean, Ross-thick/Li-sparse and Ross-thin/Li-sparse; k_{iso} represents the isotropic bidirectional reflectance (for $\theta_s = \theta_v = 0$), k_{geo} and k_{vol} are parameters related to several canopy geometric and optical properties (Wanner et al., 1995).

3.1.6.4 MODIS BRDF Product (MOD09B)

The MODIS BRDF product will produce BRDF parameters every sixteen days with a 1 km spatial resolution, which will be derived from MODIS and MISR data. The MODIS BRDF database is incompatible with the needs of the gridded NDVI due to the coarser spatial and temporal resolutions of the BRDF product:

- The BRDF product is produced at 1 km resolution and the VI product at 250 m resolution. The application of the BRDF product (1 km) to finer resolutions (250 m) (sharpening mode of the BRDF product) has to be investigated further.

- The MODIS-BRDF product will be produced every 16 days and needs a minimum of 10 cloud-free observations to be reliable (Strahler et al., 1995). A 16 day product would also have to be sharpened to an 8 day temporal resolution. Since the VI compositing has only the objective to get the nadir equivalent reflectance, and not the complete BRDF, 5 observations are considered sufficient to interpolate the reflectance to nadir.

3.1.7 Vegetation Index Composite Scenarios

Several vegetation index composite scenarios can be designed with the goal of achieving cloud-free, near-nadir, atmospherically clean imagery. In the following sections, results from research related to the composite scenarios are presented to evaluate the best possible and consistent solution on a global scale as well as to show the accuracy of the different composites in selecting near-nadir, cloudless pixels. Each composite scenario starts with a method which has the best solution followed by an alternative or 'backup' solution for less ideal data. The advantages and disadvantages of each scenario have been evaluated with ground, aircraft and satellite data to approximate MODIS data.

NOAA-AVHRR, ASAS and PARABOLA sensor data were used to test the different composite scenarios on a global scale. Seven different composite scenarios for the 8 and 16 day NDVI composites, summarized below, were evaluated.

3.1.7.1 Maximum value composite scenario (MVC)

The advantages and disadvantages of the MVC scenario are described in section 3.1.5.2.

3.1.7.2 Minimum view angle composite scenario (MV-MVC)

The VI may be selected based on the minimum view angle (pixel closest to nadir) with a data quality flag check included in order to exclude cloudy and bad data. This will select a single, near-nadir pixel from the 8 or 16 day composite period, however if a quality flag is not set or set inaccurately, the results may not be reliable, although the finest spatial resolution will be selected. Tests with global AVHRR data demonstrated the lower NDVI values selected using minimum view angles for all continents (results in 3.1.7.13).

3.1.7.3 View angle threshold composite scenario (TV-MVC)

A VI selection approach may be based on a maximum NDVI value within a view angle threshold ($\leq 15^\circ$) with data quality flag checks (cloudy and bad data excluded). If none of the reflectance data falls within this threshold, the maximum VI value composite (MVC) approach could be implemented. Pixels with fine spatial resolutions will tend to be selected, but if observations fall out of the view angle threshold, larger errors in the NDVI may occur due to anisotropic effects and increased pixel size. Tests with AVHRR data demonstrated artifacts related to the view angle effects on the VI causing some striping in the VI images when displayed. In particular, the continent of Australia was affected with striping artifacts due to the preferential selection of the VI.

3.1.7.4 Constraint view angle composite scenario (CV-MVC)

The VI may be selected based on the two observations with the lowest view angle (constraint view angle maximum VI value) with data quality check. This would preferentially select pixels with view angles close to nadir and filter out the pixel with cloud contamination. This approach is similar to the view angle threshold approach but more flexible and accurate for a larger range of view angles. Tests with the AVHRR data showed minimal artifacts.

3.1.7.5 Three method composite scenario (TV-MVC/BRDF/MVC)

This scenario starts with a VI selection based on a view angle threshold. If no pixels are selected from this first approach a BRDF model is applied to derive nadir-view reflectances. Finally, the MVC + QC check approach is used if the previous two yield no VI values. Results from using this scenario indicated the view angle threshold caused visible artifacts in the regions of the world with frequent observations and thus minimal cloud cover. The BRDF approach was also found to be rarely invoked.

3.1.7.6 BRDF based and MVC composite scenario (BRDF/MVC)

This is a direct BRDF model approach for nadir-view compositing, followed by the MVC criterion if there are insufficient points to invoke the model. The preferential selection of observations within a certain view angle threshold was implemented in scenarios 3 and 5 (Table 4), but has been shown not to improve upon a direct BRDF approach. The three-way compositing approach (section 3.1.7.5) has the disadvantage in causing some discontinuities if the view angle threshold is applied. Instead of applying the view angle threshold, research results suggested to apply the BRDF directly and skip the first composite approach.

3.1.7.7 Version 1 MODIS composite scenario (BRDF/CV-MVC/MVC)

This is also a direct BRDF model approach followed by the constraint view angle approach. This is named version 1 in that it is the current composite code delivered to the SDST. This 8 or 16-day composite scenario consists of:

- a. NDVI based on nadir-equivalent reflectance values estimated by modeling the observations with a BRDF model.
- b. NDVI selected based on the two observations with the lowest view angle (constraint view angle maximum NDVI value).
- c. MVC for all values because of bad QC flags.

Table 4. Overview of the evaluated composite scenarios

#	composite scenario	successive methods per scenario and time period (for 8 and 16 day time intervals)
1	Maximum value composite (MVC)	maximum NDVI value based on all observations (no quality control (QC) check)
2	minimum view angle - MVC (MV-MVC) beta 1 version	a. NDVI selection based on minimum view angle (closest to nadir) including a data quality control flag check (cloudy and bad data were rejected) b. MVC + QC check
3	view angle threshold - MVC (TV-MVC) beta 2 version	a. NDVI selected on a view angle threshold $ 15^\circ $ and data quality check. b. MVC + QC check
4	Constraint view angle MVC (CV-MVC) beta 3 version	a. MVC based on the two observations with the view angles closest to nadir (constraint view angle maximum NDVI value) and data quality check b. MVC + QC check
5	Threshold / BRDF/ MVC beta 4 version	a. NDVI selected on a view angle threshold $ 15^\circ $ and data quality check b. NDVI based on nadir-equivalent reflectance values estimated by modeling the observations with a BRDF model c. MVC + QC check
6	BRDF / MVC beta 5 version	a. NDVI based on nadir-equivalent reflectance values estimated by modeling the observations with a BRDF model b. MVC + QC check
7	BRDF/CV-MVC/ MVC Version 1	a. NDVI based on nadir-equivalent reflectance values estimated by modeling the observations with a BRDF model b. NDVI selected based on the two observations with the lowest view angle (CV-MVC) c. MVC

A straight BRDF approach without view angle thresholds will have several advantages:

- all 16 days will be more representative of vegetation changes over this period,
- the BRDF model automatically extrapolates to finer pixel resolution when the reflectance data are standardized to nadir, and
- the BRDF approach will better prevent discontinuities observed for the "view angle threshold approach".

These compositing scenarios are summarized in Table 4.

3.1.7.8 Alternative composite approaches

A moving average has been suggested since this would smooth out some irregularities and make use of the BRDF product when possible. However, this moving average was considered to have few advantages over a straightforward compositing period at the current stage of research. The incorporation of the BRDF product and a moving average would be difficult to implement, but may be done post launch. The use of the middle infra-red in the composite scenario could aid in the detection of clouds and aerosols. The use of albedo as input to the VIs could be another solution to the anisotropic behavior of VIs. Some results for albedo-based VIs are presented in section 3.1.7.10.

There are other alternatives to simply choosing the highest NDVI value over a compositing cycle. One may integrate or average all cloud-free pixels over the period. Myer et al. (1995) demonstrated the importance of the effect of surface anisotropy and sun/sensor geometry on the NDVI from AVHRR, and suggested that averaging the NDVI was superior to the MVC approach. The Best Index Slope Extraction (BISE; Viovy et al., 1992) method reduces noise in NDVI time series by selecting against spurious high values and through a sliding compositing cycle. Use of the thermal channel has also been shown to be helpful. Knowledge of the ecological evolution of a land cover with respect to a VI temporal response might also be of use for the improvement of compositing techniques (Viovy et al., 1992; Qi et al., 1993; Moody and Strahler, 1994). This will not be used for the initial MODIS compositing algorithm due to the advance knowledge required of the dynamics of landcover growth patterns, seasonality, and response to climate change (precipitation, temperature). The use of land cover specific composite scenarios would also introduce discontinuities, but might perform better on a regional scale.

Current investigations are considering a (1) BRDF approach followed by (2) a previous (historic) BRDF results if the current is either not good or impossible to derive due to limited observations.

Standardization of VI to nadir view and a certain sun angle is being investigated for a monthly climate modeling grid VI product. Monthly compositing would ensure sufficient input data for BRDF determination using inversion of a simple BRDF model (Rahman's; Rahman et al., 1993). The VI would be globally normalized to a constant solar-view geometry (possibly determined by the angle most sensitive to canopy biomass) at 0.25° spatial resolution (25 km). At the lower temporal resolution, this product would be catered towards modelers and those doing interannual comparisons. Local/regional work demanding more frequent data would probably rely on the 16 day level 3 VI as planned. A flow diagram of this approach is presented in Figure 3.17.

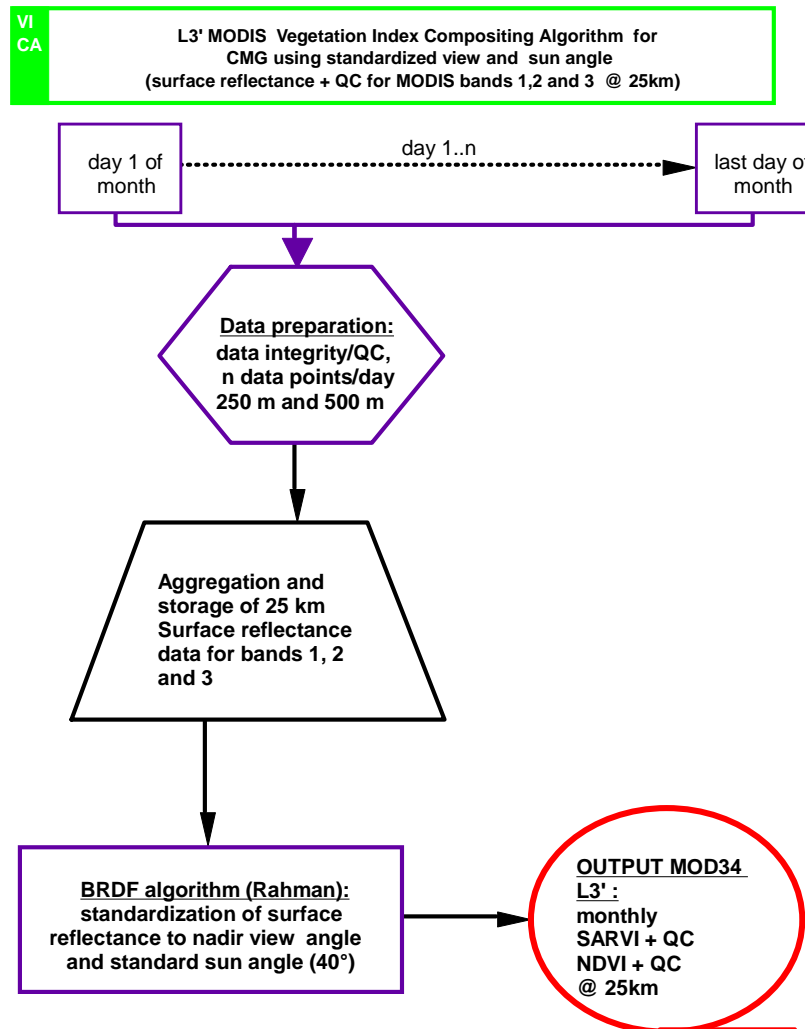


Figure 3.17: Diagram of the coarse grid monthly composite scenario that would standardize view and solar zenith angles

3.1.7.9 Accuracy of BRDF models to estimate reflectance values (PARABOLA)

Privette et al. (1996b) studied the overall accuracy of 10 simple BRDF models in estimating the nadir reflectance. The 10 models were inverted with subsets of ground-based PARABOLA (Deering and Leone, 1986) data (red and NIR) collected over nine land surface cover types. Land cover types included soil, grassland, cotton, shinnery Oak, Black Spruce, Spruce Hemlock, Aspen, Jack pine, and lava soil (Table 5). 50 randomly chosen data sets, with each set containing 5 to 15 unique data points, were created to invert each model with the red and NIR data. The subsets were defined by restricted view zenith and azimuth and solar zenith angle ranges representative of satellite sampling and cloud cover frequency. The retrieved model parameters were used to estimate the nadir reflectances at a limited range of solar zenith angles. The results were found to be strongly dependent on sampling distribution, especially the view azimuth angles of the inversion data (distribution of observations in the forward and backscatter view angle sectors as well as in the orthogonal and principal plane), and less dependent on the spectral bands and land cover types (Privette et al, 1996). The different BRDF models were ranked according to the accuracy of the estimated nadir reflectances as the solar zenith angle changed. The non-linear Rahman model and the Ross-Thick/Li-sparse models worked best.

Table 5 : Information on the PARABOLA data sets with Leaf area index (LAI) and Plant area index (PAI)

Land cover	Location	Date	No of solar zenith angles	range of solar zenith angles	LAI/ *PAI
soil (lava-based)	New Mexico	7/18/89	6	21°-73°	0
Grassland	Kansas (FIFE)	6/04/87	4	17°-66°	no data
Grassland	Kansas (FIFE)	8/08/89	5	43°-75°	2
Cotton	Maricopa (AZ)	9/07/91	7	37°-76°	no data
Shinnery Oak	Texas (west)	9/12/84	4	31°-71°	0.7
Spruce Hemlock	Howland Maine	8/25/91	6	36°-76°	3.9*
Aspen	Sakatchewan (BOREAS)	7/21/94	7	41°-72°	3.3
Black Spruce	Sakatchewan (BOREAS)	6/07/94	8	35°-70°	6.3
Jack pine	Sakatchewan (BOREAS)	5/31/94	8	34°-69°	1.2

In a separate experiment, the accuracy of the BRDF models to estimate nadir reflectances at one solar zenith angle was examined. The mean solar zenith angle for each of the 50 inversion data sets was determined. Then, linear interpolation was used to estimate the NDVI at this angle from the nadir PARABOLA reflectance values. Next, the NDVI was computed from model-estimated nadir reflectances at the two solar angles in the solar angle pair, then linearly interpolated to the NDVI at the mean solar

angle. The absolute difference between the two NDVIs: one from the measured nadir or closest to nadir data and one from the models (both estimated by linear interpolation from values at the solar angles around the mean value) was taken as the absolute difference. The performance of the BRDF models were evaluated by counting the number of sampling combinations/land cover cases in which the model was best. A model was counted as "best" if it was within 0.005 of the lowest mean absolute error for a given land cover type, solar zenith angle and azimuth sector. Table 6 reports the best models per azimuth sector and Table 7 the best models per land cover type. In contrast to the previous results, the Rahman model performed best, closely followed by Ross-thin/Li-sparse and Roujean's and then the modified Rahman and Ross-thick/Li-sparse models.

Table 6: Number of landcover types for which the mean absolute error in the resulting VI, computed from the nadir reflectances, was within 0.005 of the lowest mean absolute error for a given land cover, solar zenith angle and sampling sector combination. Results are given a function of view azimuth sector (1 VI and 9 covers = 9 possible per sector) and NDVI. Model codes are: Dksn= Dickenson, Jacq=Jacquesmoud, MRPVMISR= modified Rahman-Pinty-Verstraete-MISR, Rahm=Rahman, ThnS=Ross-thin-Li-sparse, ThnD= Ross-thin-Li-dense , ThkS=Ross-thick-Li-sparse , ThkD=Ross-thick-Li-dense , Wlth= Walthall, MWlth=modified Walthall, Rouj= Roujean

BRDF	Backward	Orthogonal	Forward	Principal	NDVI total #
Dksn	1	5	1	2	9
Jacq	0	6	0	4	10
MRPVMISR	2	5	3	7	17
Rahm	5	7	3	5	20
ThnS	4	5	5	5	19
ThnD	1	3	6	3	13
ThkS	3	5	5	5	18
ThkD	2	2	2	1	7
Wlth	2	4	1	2	9
MWlth	0	2	0	4	6
Rouj	3	5	5	5	18

Table 7: Number of landcover types for which the the mean relative error in the resulting VI, computed from the nadir reflectances, was the lowest or was within 0.01 of the lowest. Results are given as a function of land cover.

Land cover	soil	grassl.	grassl.	cotton	shin. oak	Spruce Heml.	Black Spruce	Aspen	Jack pine
Dick	0	0	1	0	4	1	1	0	2
Jacq	2	2	2	0	0	1	1	2	0
MISR	2	2	0	2	1	1	3	4	2
Rahm	4	3	2	1	1	1	2	3	2
ThnS	2	4	1	4	0	2	2	2	2
ThnD	2	0	1	3	0	0	2	2	2
ThkS	2	3	1	3	0	2	2	2	2
ThkD	2	1	0	0	0	0	2	2	0
Wlth	3	0	0	0	3	0	1	2	0
MWlth	2	1	0	0	0	1	0	2	0
Rouj	3	2	1	4	1	2	2	2	1

3.1.7.10 Solar Zenith Angle effects on VI (PARABOLA)

The potential errors due to the variable solar zenith angle between different days and swaths (20° max) can be estimated by using ground (Parabola) data for different vegetation cover types (see Table 5 for the description of the data set; Parabola data does not include a blue band). The nadir reflectance values, and NDVI and SAVI were plotted as function of solar zenith angle in Fig 3.18. For most land cover types the NDVI increased with solar zenith angle and had a flatter response at high NDVI values. The SAVI generally increased with solar zenith angle, except for Black Spruce, which decreased with higher solar zenith angles. For a solar zenith angle range of about 40° (Table 5), the mean relative difference in the VI is about 18% for the NDVI and about 31% for the SAVI (Table 8). It is estimated that the differences within a swath are about half off these relative difference values. Considering the large solar zenith angle changes in the mid- and high latitudes (Table 3), seasonal changes easily can cause relative differences of 20 % in the NDVI.

Results in Table 8 showed that the albedo derived VIs were less sensitive to solar zenith angle changes as indicated by the lower coefficients of variation and mean relative difference. However, Table 9 shows the difference between the reflectance derived VI and the albedo derived VI, indicating that each VI would need to be interpreted differently and that separate biophysical translations would be required.

Table 8. Average coefficient of variation (CV) and relative difference (RD) in the red and NIR reflectance and albedo value and the associated NDVI and SAVI values as a function of solar zenith angle for the 9 vegetation types as measured by the Parabola instrument (where CV = 100 std/mean and RD=100 (max-min)/mean; computed for each vegetation cover type)

	reflectance		albedo		vegetation indices			
	red	NIR	red	NIR	NDVI % (refl.)	NDVI % (alb.)	SAVI % (refl.)	SAVI % (alb.)
mean CV	19.06	12.64	8.77	8.37	6.00	2.76	10.37	6.50
mean RD	52.72	36.92	25.37	24.00	17.61	8.00	31.15	18.79

Table 9: Mean and standard deviation (std) of the difference between VIs derived from nadir reflectances and from albedo's for all sun angles and vegetation cover types

	NDVI	SAVI
mean(VIrefl-VIalb)	-0.0135	-0.0632
std(VIrefl-VIalb)	0.0405	0.0485

The orbital mechanics of EOS-AM1 create an advantage in the NDVI in that the solar zenith angle effect per swath would cause a higher NDVI in the backscatter direction than in the forward scatter direction. Thus, the sun angle effect tends to counteract the view angle effect, reducing the combined influence from each.

The solar zenith angle effects on the surface reflectance values can only be quantified based on the limited variation of the sun angles during the 8-day, 16-day and monthly composite periods. However, extrapolation of the observations to a nadir sun angle was shown to be very inaccurate for a set of ASAS data. The isotropic (nadir view and sun angles) reflectance data resulting from extrapolating the ASAS observations with Roujean's BRDF model was shown to cause unrealistic results (negative reflectances and VIs that were very low) for nadir sun-angles and limited (7) observations, (Leeuwen et al., 1996). This was likely due to the lack of variable solar zenith angles in the data sets. Therefore, extrapolation to solar zenith angles outside of the range observed in the composite period requires multiple observations for a range of solar and view zenith angles and likely a more physically based BRDF model (Rahman's). Currently, standardization of VIs to nadir view angle and a certain sun angle is being investigated for the climate modeling grid VI product at monthly time intervals. At the moment, the normalization of the 8-day and 16-day level 3 vegetation index products for sun angle effects is mostly left as a post-launch effort.

The solar zenith angle information from the metadata will be used to evaluate the VI, and carried through in the metadata of each tile. This information is also useful for a FASIR (Sellers et al., 1994) like algorithm that would normalize the sun angle variability to make annual comparisons of the NDVI. Annual evaluations of the influence of the variability in solar zenith angle on the inter-comparison of vegetative covers at different latitudes and in different seasons will be made with post-launch MODIS data.

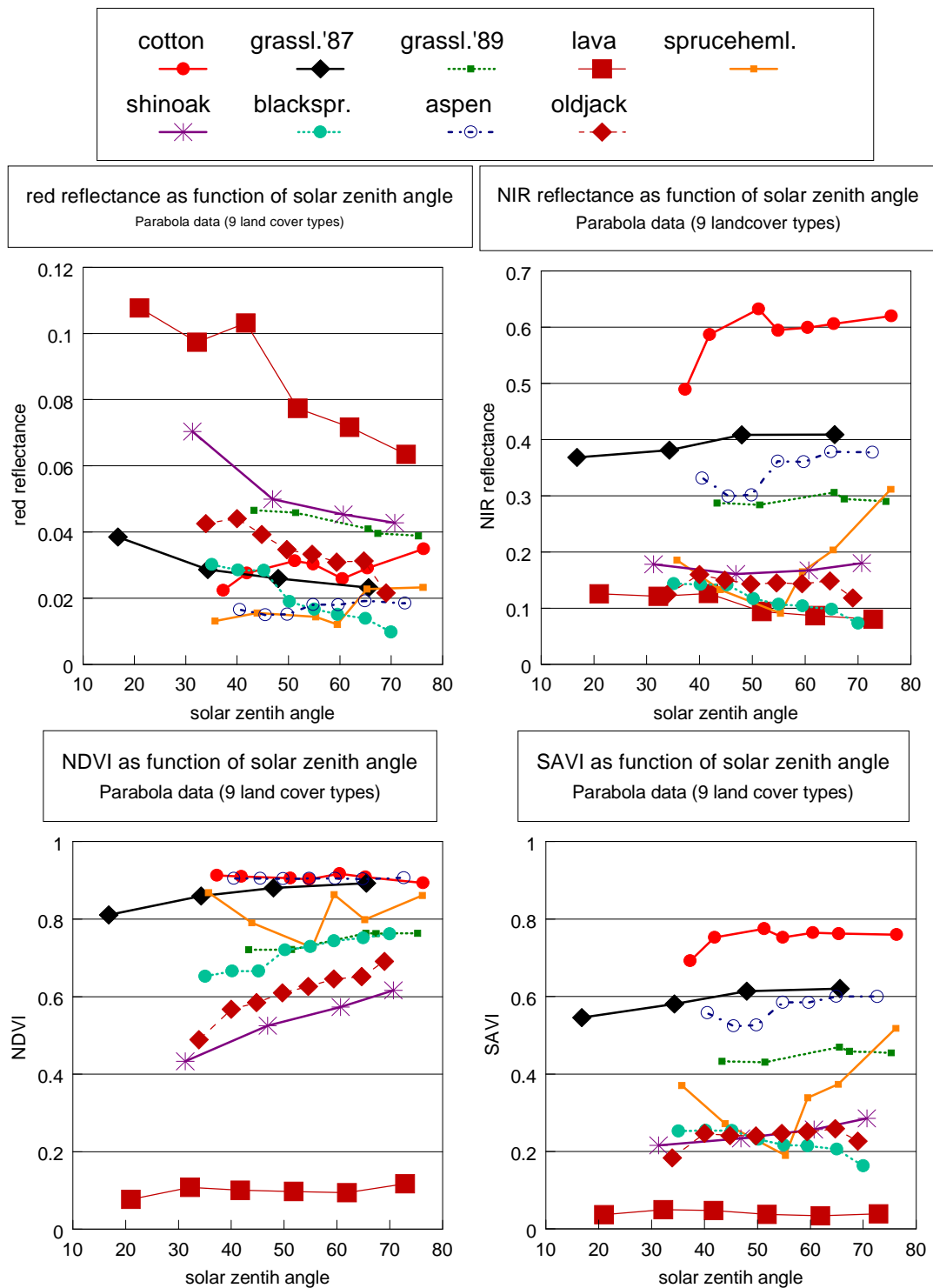


Figure 3.18: Nadir Red and NIR reflectance and NDVI and SAVI as a function of solar zenith angle for a range of vegetation types (PARABOLA data).

3.1.7.11 BRDF models and VI compositing scenarios (ASAS)

High spectral resolution bidirectional reflectance factor (BRF) measurements from the Advanced Solid State Array Spectroradiometer (ASAS) instrument flown at ~5000m altitude over various field campaigns were used to:

- ▶ simulate the MODIS sensor
- ▶ determine anisotropic effects on VIs
- ▶ evaluate the accuracy of simple linear BRDF models in estimating nadir-equivalent VI values
- ▶ compare nadir-equivalent VI estimates with results from the MVC approach
- ▶ evaluate the effect of view angle distribution on the performance of the BRDF models.

The ASAS reflectance data were convolved into the first three MODIS bands (ρ_{red} , ρ_{nir} , ρ_{blue} ; 620-670 nm, 841-876 nm, 459-479 nm) and corrected for atmosphere effects using aircraft and ground sunphotometer optical depth measurements with "6S" (Vermote et al., 1996). Major land cover types included in this study are deciduous and coniferous forest (Oregon Transect Ecosystem Research Project - OTTER, Boreal Ecosystem Atmosphere study- BOREAS), grassland (First ISLSCP Field Experiment - FIFE) and shrub savanna sites (Hydrologic, Atmospheric pilot Experiment in the Sahel - HAPEX-Sahel). The view zenith angles ranged between 0° and 60° in both the forward scatter and backscatter direction, along the principal and orthogonal planes. Surface reflectances of the major canopies were extracted over areas of 1-2 km² following co-registration of all view angles.

Examples of ASAS red and NIR Bidirectional reflectances are given in Fig. 3.19 for "Grassland", "Tigerbush", and "Black Spruce". Backscatter view angles are assigned a negative sign. For most vegetation types, the backscatter direction had the highest reflectance response and generally the lowest NDVI response (Fig. 3.20). The NDVI response about nadir showed significant variability and was different for each vegetation type (Fig. 3.20).

Leeuwen et al. (1996) compared vegetation index composite scenarios involving BRDF and maximum value vegetation index approaches for 14 sets of bidirectional ASAS images. The utility of the different BRDF models to correct off-nadir measurements to nadir-equivalent values was evaluated and different vegetation index compositing scenarios compared. Nadir-equivalent VI accuracy and predictability were evaluated for the MVC and BRDF compositing scenarios using the measured nadir observations as a 'true' reference. Extrapolation of the BRDF models to nadir sun angles was found to be highly inaccurate. VI composite scenarios based on the standardization of reflectances to nadir view angles (at a representative sun angle) was more accurate than the MVC approach.

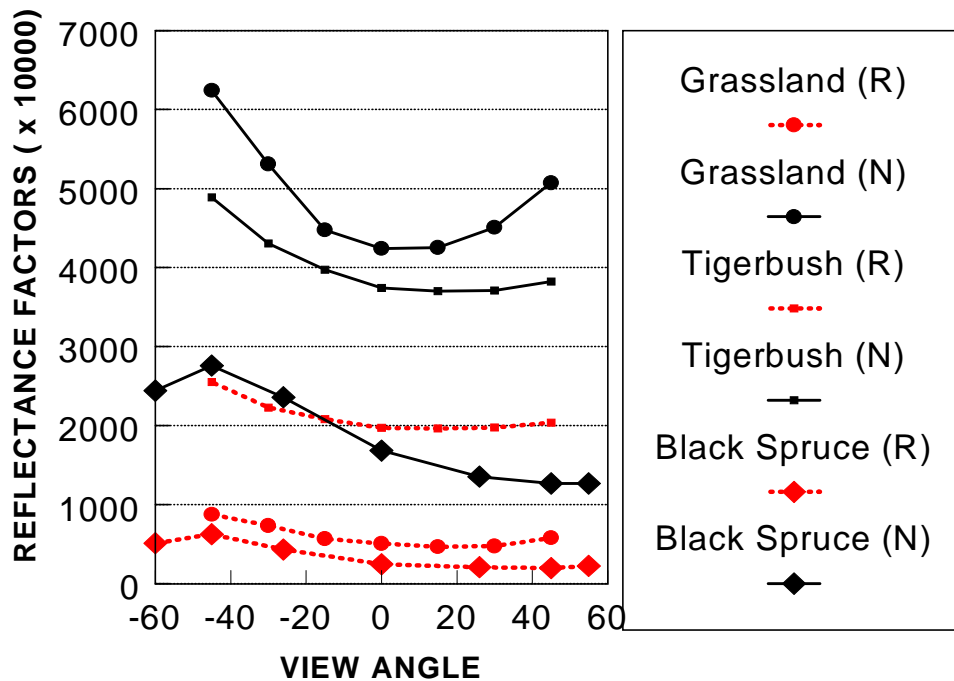


Fig. 3.19: Bidirectional red (R) and near-infrared (N) reflectance factors for the ASAS results [FIFE Grassland, HAPEX Tigerbush site and BOREAS Black Spruce site; ASAS data in solar principal plane]

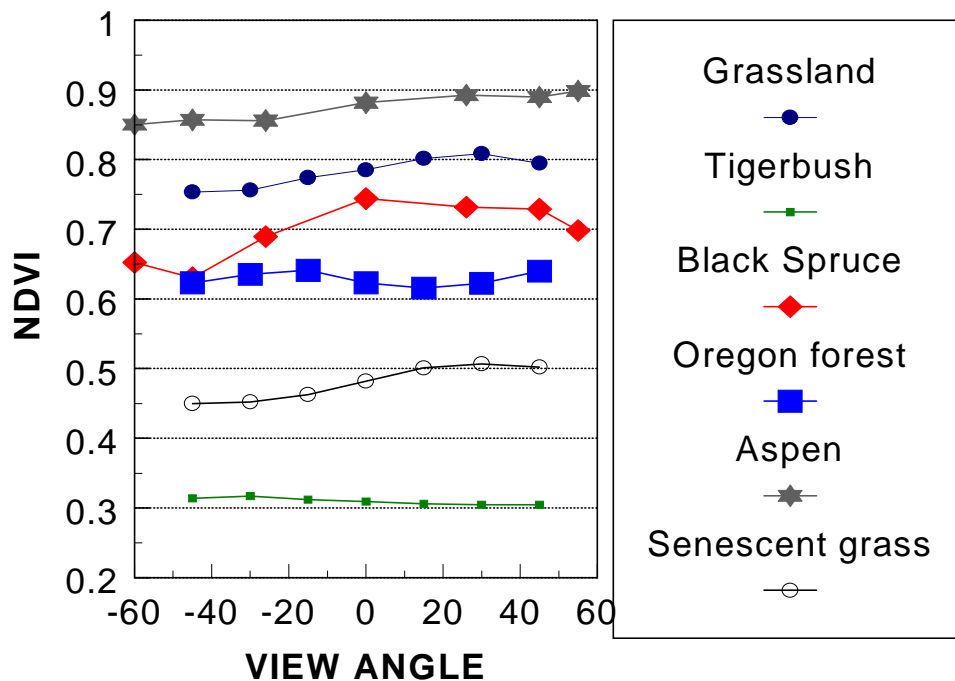


Fig. 3.20: Effect of surface anisotropy on NDVI for a range of vegetation types. [Grassland (FIFE), Tigerbush (HAPEX), Black Spruce (BOREAS), Oregon forest (OTTER), Aspen (BOREAS), and Senescent Grassland (FIFE); ASAS data collected in the solar principal plane; not all NDVI data was plotted to avoid clumping].

A bidirectional vegetation index function (BVIF) composite scenario, in which the bidirectional distribution of VI values are modeled (rather than reflectances) was successful with only slightly higher errors than the BRDF composite scenario. The main disadvantage of the BVIF, however is the loss of the actual (nadir) surface reflectances which could be used to compute other VIs, for instance. The BRDF models (Walthall's and Roujean's) performed equally well for most vegetation types. A simple BRDF model (Walthall's) seemed adequate to model the BRDF for a range of global vegetation types and produced nadir-equivalent VIs with a mean absolute error of about 0.005 from the 'true' nadir NDVI, (standard deviation was 0.01; Table 10). The MVC approach resulted in NDVI values which deviated from the 'true' nadir NDVI values of 0.011, or with three times more error than the Walthall derived NDVI values. The results of the analysis emphasize the importance of standardizing BRDF for vegetation index compositing schemes and retrieval of biophysical parameters.

A second experiment with the same ASAS data was performed to evaluate the effect of the distribution of view angles on the accuracy of several BRDF models to derive nadir equivalent reflectances and NDVI. Based on the findings of the PARABOLA experiment and the previous ASAS research, the four best BRDF models were included in the evaluation: Walthall, Roujean, Ross-thin/Li-sparse and Ross-thick/Li sparse. The non-linear Rahman model was excluded because of its computation intensive fitting procedure, which is operationally not practical. The accuracy was computed by comparing the 'true' measured nadir reflectances with the predicted nadir reflectances. A final evaluation was made by using the vegetation index as a qualifier for the uncertainty that is introduced by standardizing the reflectance values. The BRDF models were parameterized for the following five different view angle distributions which were created with a minimum of 4 data points:

1. all reflectance observations were used (most vegetation types covered by ASAS included -45°, -30°, -15°, 0°, 15°, 30°, 45°; backscatter, nadir and forward scatter observations)
2. all reflectance observations were used excluding nadir
3. all reflectance observations greater than |15°| were used
4. all reflectance observations were used except forward scatter and nadir; to keep 4 points one backscatter observation with the highest view angle was included.
5. all reflectance observations were used except backscatter and nadir; to keep 4 points one forward scatter observation with the highest view angle was included.

Forward modeling of the BRDF models resulted in estimates of the nadir reflectance values for the red and NIR wavebands.

The NDVI was computed to compare its sensitivity to the standardization of reflectance values to nadir. The summary of the results for the BRDF and MVC composite scenarios are presented for the red and NIR reflectance values and NDVI in Figure 3.21 and Table 10. The mean difference between the measured nadir reflectance values and the modeled reflectance values for the 14 vegetation

cover/ASAS sites (for red and NIR reflectance bands, 5 view angle distributions and four BRDF models) is presented in Figure 3.21a . The mean difference (error) in reflectance values is generally lower than 0.006 for the red (R) waveband for the Walthall, Roujean and the Ross_thin/Li_sparse models. The error of the predicted nadir reflectance values in the NIR (N) was generally lower than 0.0075 for the Walthall, Roujean and the Ross_thin/Li_sparse models. The error in the predicted nadir reflectance values for the Ross_thick/Li_sparse was generally higher than the other three models for both bands. The error in the predicted reflectance values is generally the largest for view angle distributions that lack forward scatter observations.

The mean difference between the measured NDVI values and the modeled NDVI values for the 14 vegetation cover/ASAS sites (5 view angle distributions, and for the four BRDF models) is presented in Figure 3.21b. The mean difference (error) in VI is generally between 0.002 and 0.02 for the NDVI for the Walthall, Roujean and the Ross_thin/Li_sparse models. The error in the predicted nadir VI values for the Ross_thick/Li_sparse was generally higher than the other three models. The mean absolute difference between the measured nadir VIs and the VIs resulting from the different composite scenarios were computed for all vegetation types and view angle distribution combination as shown in Table 10. The errors due to the MVC approach ($MVC-NDVI_{nadir}$) and the maximum error due to non standardization (or range) of the NDVI ($NDVI_{max} - NDVI_{min}$) are presented as a reference. The absolute error due to the BRDF approach is three times smaller than the error in the MVC approach and about 10 times smaller than the error using an NDVI without standardization (full NDVI range) (Table 10).

The error in the predicted VI values is generally the largest for view angle distributions that lack forward scatter observations. The Ross_thin/Li_sparse model in particular showed some large errors for the old black spruce vegetation type, where it predicted negative reflectance values. NDVI values derived from the BRDF model are underestimated with respect to the measured nadir NDVI.

The BRDF models can be ranked according to the least number of times the error in the VI was more than 0.01 (Table 11). Going from best to less good: Walthall, Roujean, Ross_thick/Li_sparse, Ross_thin/Li_sparse. This ranking is in agreement with the results in Table 10. For these data sets, the Roujean and Walthall BRDF models were more accurate than the Ross_thick and Ross_thin models. Ross_thin had several outliers. The overall performance of the Ross_thick model was the least accurate in terms of the prediction of nadir VI. The results do show that all models perform best for low and medium density vegetation covers. Differences in relative azimuthal plane can cause significant differences in the performance for each model e.g. Grassland, Old Aspen and Old Black Spruce.

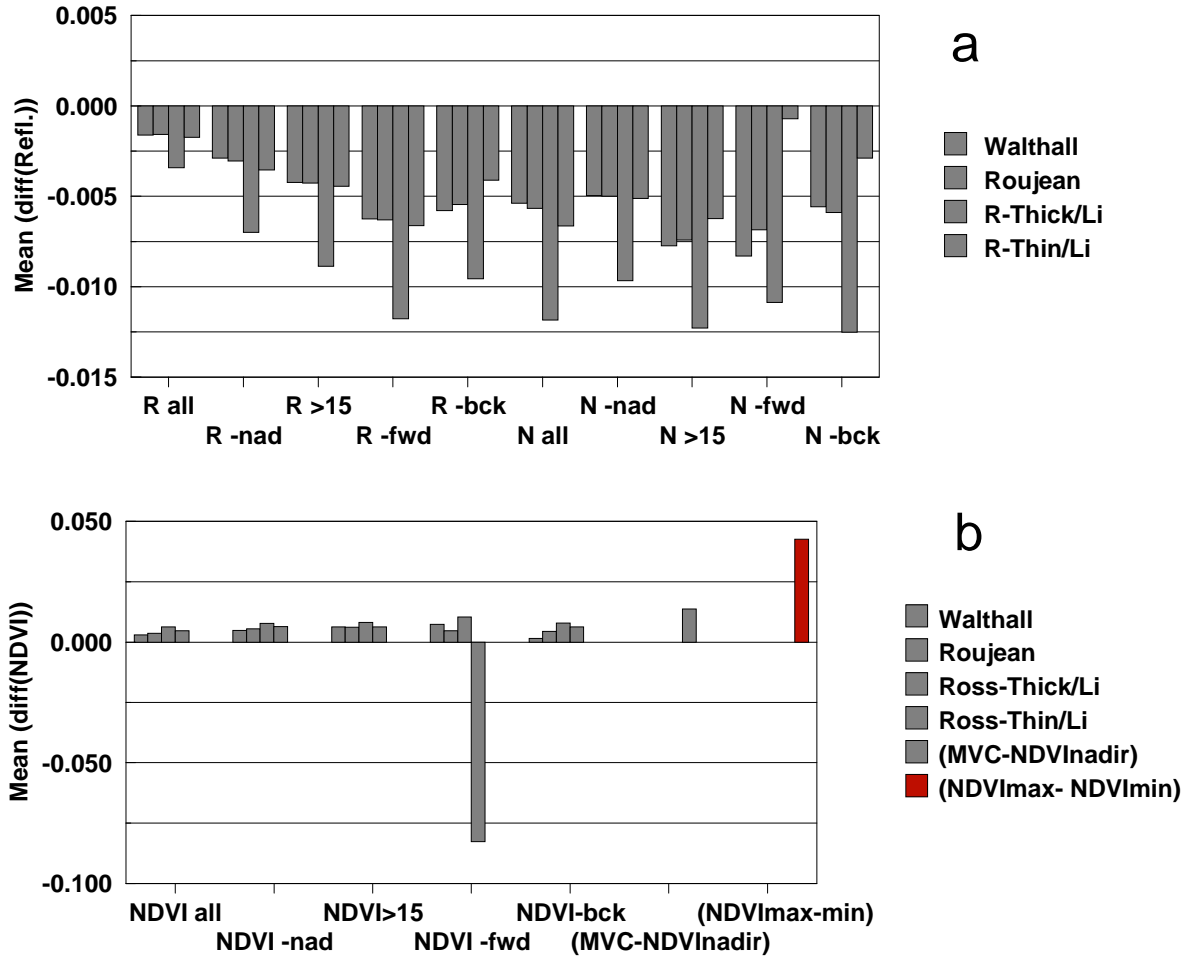


Fig. 3.21 : a) Mean difference between measured and modeled nadir red and NIR reflectance factors for four BRDF models and 5 different view angle distributions of 14 vegetation cover sites.

b) mean error in the predicted nadir vegetation index values of 14 vegetation covers, for five different view angle distributions and 4 different BRDF models using the measured nadir VI value as a reference; the error due to the MVC approach ($MVC-NDVI_{nadir}$) and the maximum error due to non standardization or range of the NDVI ($NDVI_{max}-NDVI_{min}$) is plotted as well.

"all"- all observations used for modeling the BRDF (n=7), "-nad" - all observation but the nadir view angle(n=6), ">15" - all observations with view angles larger then 15° (n=4), "-bck" - all observations in the forward scatter direction used, but the highest view angle in the backscatter direction included (n=4), "-fwd" - all observations in the backscatter direction used, but the highest view angle in the forward scatter direction included (n=4).

Table 10: Overview of errors in the NDVI due to BRDF and MVC composite scenarios (ASAS data)

	Walthall	Roujean	Ross-Thick/ Li Sparse	Ross-Thin/ Li sparse	(MVC-NDVI _{nadir})	(NDVI _{max} - NDVI _{min})
NDVI absolute error	0.005	0.005	0.008	-0.012	0.014	0.043
standard deviation	0.011	0.013	0.020	0.066	0.098	0.026

Table 11: The number of times the error in the NDVI was larger then |0.01|, for 5 view angle distributions of the reflectance data for each vegetation type and BRDF model; H-HAPEX, F-FIFE, B-BOREAS, O-OTTER, pp-principal plane, op-orthogonal azimuthal plane).

vegetation type	Walthall	Roujean	Ross_thick/ Li_sparse	Ross_thin/ Li_sparse
Fallow, pp (H)	0	0	1	2
Tigerbush, pp (H)	0	0	0	0
Grassland, pp (F)	1	0	0	2
Grassland, op (F)	1	1	1	0
Grassland, pp (F)	2	2	1	2
Grassland, op (F)	0	0	0	0
Old Aspen, pp (B)	3	3	4	2
Old Aspen, op (B)	0	0	0	1
Old Black Spruce, pp (B)	5	5	5	5
Old Black Spruce, op (B)	1	3	3	5
Alder, pp (O)	3	3	5	5
old growth forest, pp (O)	3	3	5	5
Waring woods, pp (O)	2	2	1	1
Fir, pp (O)	0	1	5	4
total # (error VI > 0.01)	21	23	31	34

3.1.7.12 Anisotropy of the enhanced VIs (ASAS)

As was shown in figure 3.20, bidirectional reflectance factors affect the anisotropic behavior of the NDVI significantly. The enhanced VIs are also affected in different ways by the BRDF. Fig 3.22 shows examples of the anisotropic effects on the SARVI, SAVI, WdVI, and SR. It is evident that the accuracy of the composited product is best when the reflectance data can be standardized to nadir. The availability of cloud-free data will mostly determine what part of the globe can be standardized over 8 and 16 day periods. As mentioned in section 3.1.7.8, we are investigating the use of historic BRDF data and larger spatial and temporal resolution data sets to accomplish better view angle standardized VIs. Fig 3.22 show the enhanced VIs (SARVI, SAVI, and WdVI) to be more sensitive to view angle effects than was the case with the NDVI (Fig. 3.20). This would indicate that these VIs are more dependent on the accurate derivation of nadir-equivalent surface reflectance from BRDF models. These results would also suggest that in cases where nadir standardization cannot be achieved, the NDVI-MVC could still be used for pixel selection from which the SARVI could be computed. Thus,

the entire level 3 compositing algorithm would remain the same in the derivation of an enhanced level 3 VI product,

Our results have shown that most VIs have a backscatter (or sunlit) bias for higher VI values, opposite that of the NDVI, which favors the darker (shaded) view direction (Fig. 3.20 and 3.22). These results also show the simple ratio (NIR/red) to be very sensitive to view angle effects. This is a very important finding because this states that ratios do not alleviate bidirectional view angle effects and it is not the ratioing properties of the NDVI that render this index less sensitive to view angle effects. Thus, the non-linear transform equation of the NDVI (functionally equivalent to the NIR/red ratio, Fig. 3.4) has stabilized the Aspen and grass view angle profiles (Fig. 3.20, 3.22) through compression of the NDVI signal, making the NDVI invariant to not only noise influences but also useful vegetation information as well. This is corroborated in Fig. 2.5, where large variations in solar and view angles resulted in the same “saturated” NDVI value while the NIR/ red ratios remained very sensitive to these angular variations. As discussed in section 3.14, both the signal and noise must be considered in evaluation of the performance of a VI equation. If NDVI angular behavior at higher levels of vegetation is invariant due to signal compression, then the use of the maximum NDVI value as a ‘backup’ criterion will have to be re-assessed.

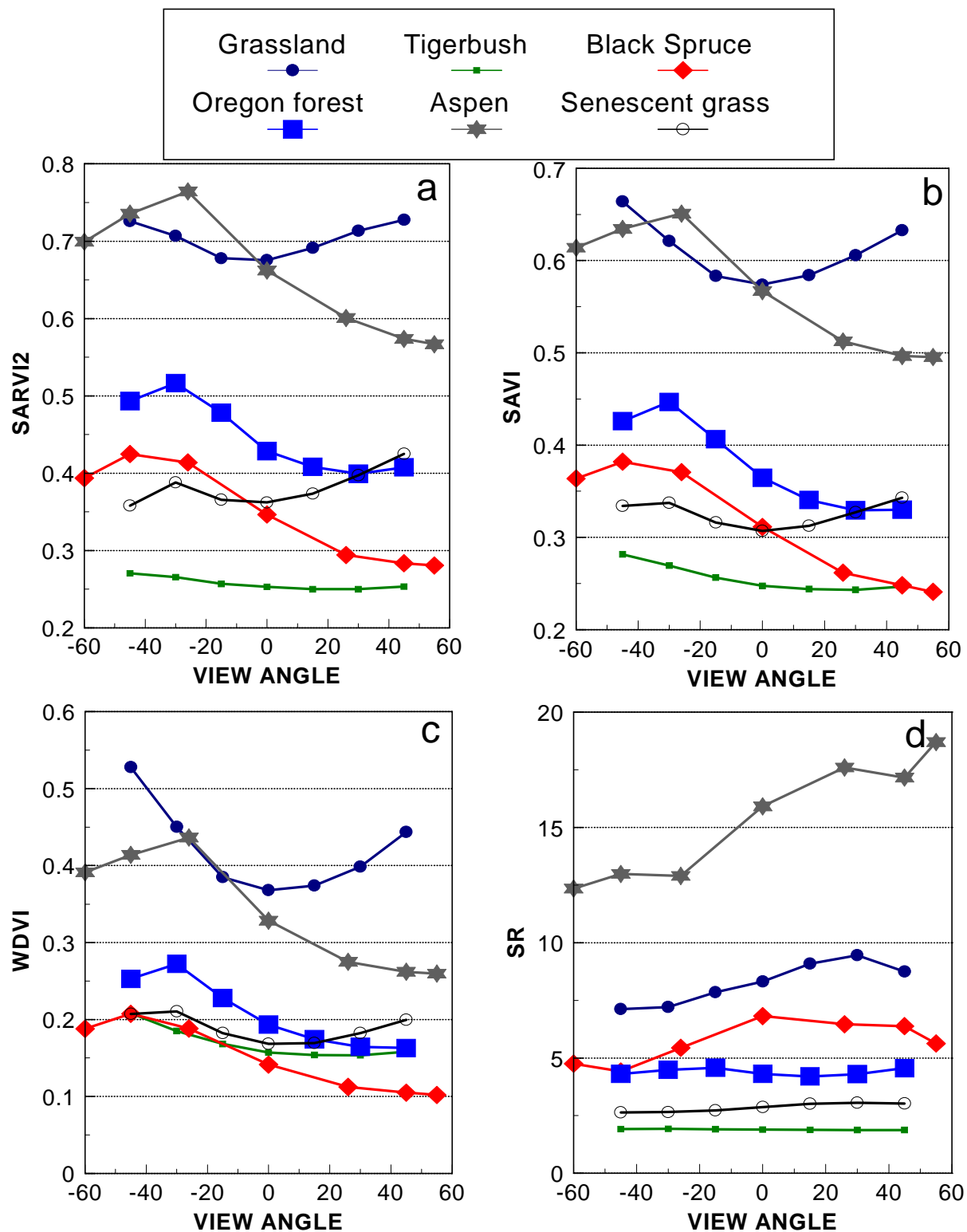


Fig 3.22 Examples of the anisotropic effects on the SARVI2 (a), SAVI (b), WDVl (c), and SR (d) for a range of vegetation types. (Derived from ASAS data collected in the principal plane)

3.1.7.13 Multitemporal AVHRR Data, results for different composite scenarios

Global, NOAA-AVHRR 8km-Pathfinder data were used to demonstrate the advantages and disadvantages and nadir-view accuracy of each composite methodology. The composite results are presented for a 16-day composite period (August 2-August 17 1988), using daily AVHRR red and NIR normalized reflectance data at 8 km resolution. The data were atmospherically corrected for Rayleigh and ozone only and came with a cloudmask. Seven different vegetation index composite scenarios (see Table 4) were applied and analyzed with their corresponding QC images.

For each pixel, the QC flags included information about data integrity, clouds and the composite technique selected for each scenario. Table 12 gives an overview of the NDVI composite results and Table 13 the relative difference between the MVC and other VI composite scenarios. Both tables are graphically represented by Fig. 3.23a and 3.23b. The MVC approach excluded the clouds very well, but largely overestimated the NDVI relative to nadir values. The NDVI-MVC scenario overestimated the NDVI between 4 and 18 % depending on the continent and composite scenario it was compared to.

The minimum view angle VI composite (MV-MVC) showed view angle discontinuities and problems with clouds, despite the use of the QC flags. The latter caused lower NDVI values for each continent because days with cloudy pixels were included in the NDVI composite. It selected cloudy pixels in cases where the cloud mask was not working well. The view angle threshold TV-MVC approach by itself caused some discontinuities in the NDVI images related to view angle effects, especially over desert areas and areas with low cloud cover during the 16 day composite period. The constraint view angle CV-MVC approach was the best approach of the MVC related approaches. It had few artifacts and had better cloud screening capabilities. The NDVI results from the composite scenario 5 was very similar to the composite scenario 6 and 7. However the main disadvantage of this three-way composite scenario was the discontinuities that are caused by the view angle threshold.

The two BRDF based scenarios had few discontinuities, although some speckle was observed which was caused by cloud contamination and possible misregistration of pixels. It has the advantage in averaging the 16 days of observations. The BRDF also tends to extrapolate the spatial resolution from the larger pixel sizes to the finer pixel resolution. The current version 1 MODIS algorithm, BRDF/CV-MVC scenario, was considered to represent a composite period best. The NDVI was 6 to 18 % lower for this composite scenario compared to the MVC. It should be noted that for scenarios 6 and 7, large portions (about 40 %) of the continents were BRDF corrected, but lack of cloud free data always caused the secondary solution to take into effect, which is close to the MVC. If more pixels would be standardized to nadir the difference between MVC and BRDF based scenarios would be even larger.

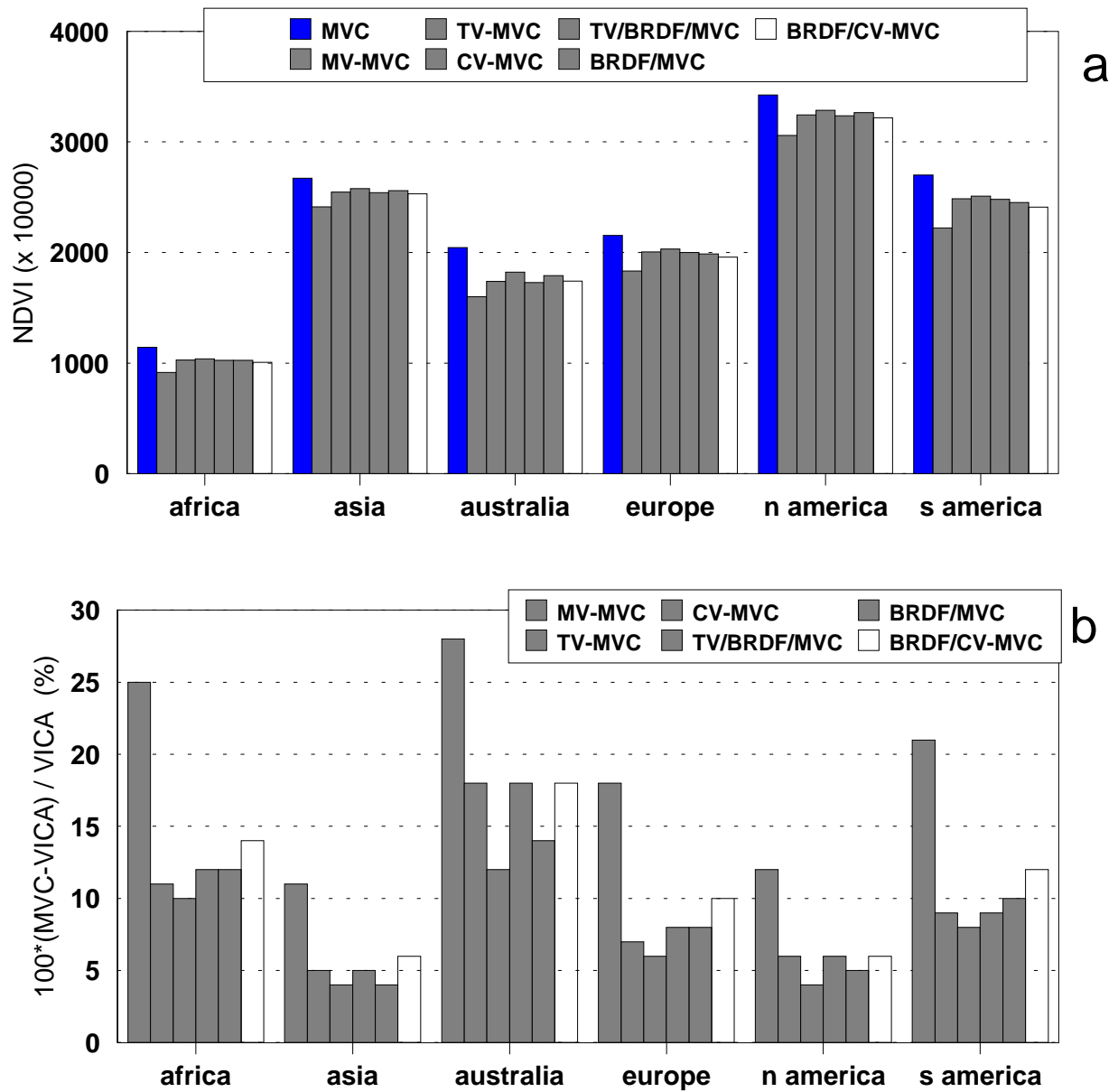


Figure 3.23: a) Mean NDVI response per continent for 7 different composite scenarios using 16 days of AVHRR data; b) Relative difference between the MVC and the other 6 composite scenarios (Table 4) for each continent.

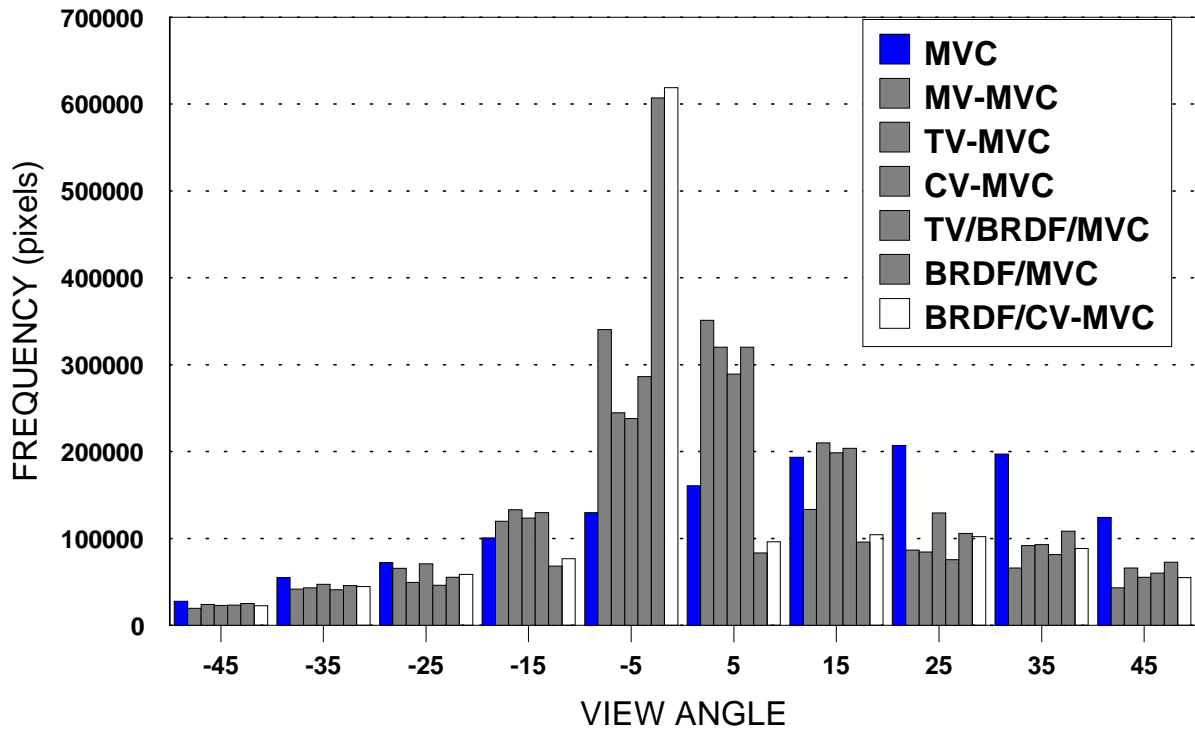


Figure 3.24: Global frequency distribution for 10° view angle intervals and seven composite scenarios (see Table 4 for explanation of the legend)

Fig. 3.24 shows the global view angle distribution of the different composite scenarios. The BRDF scenario showed to have the best view angle distribution close to nadir and thus the least pixels with larger view angles. For most composite scenarios the view angle distributions (outside the view angle threshold or about nadir) are skewed towards the forward scatter view angles. Different continents have preferential selection of forward view angles e.g. around 23° for Africa, Asia and Europe, 38° for Australia and North America and both 13° and 48° for South America. An example of the results of the proposed V1 MODIS composite scenario is presented for the global NDVI in Fig. 3.25a. The quality control flags are displayed in Fig 3.25b.

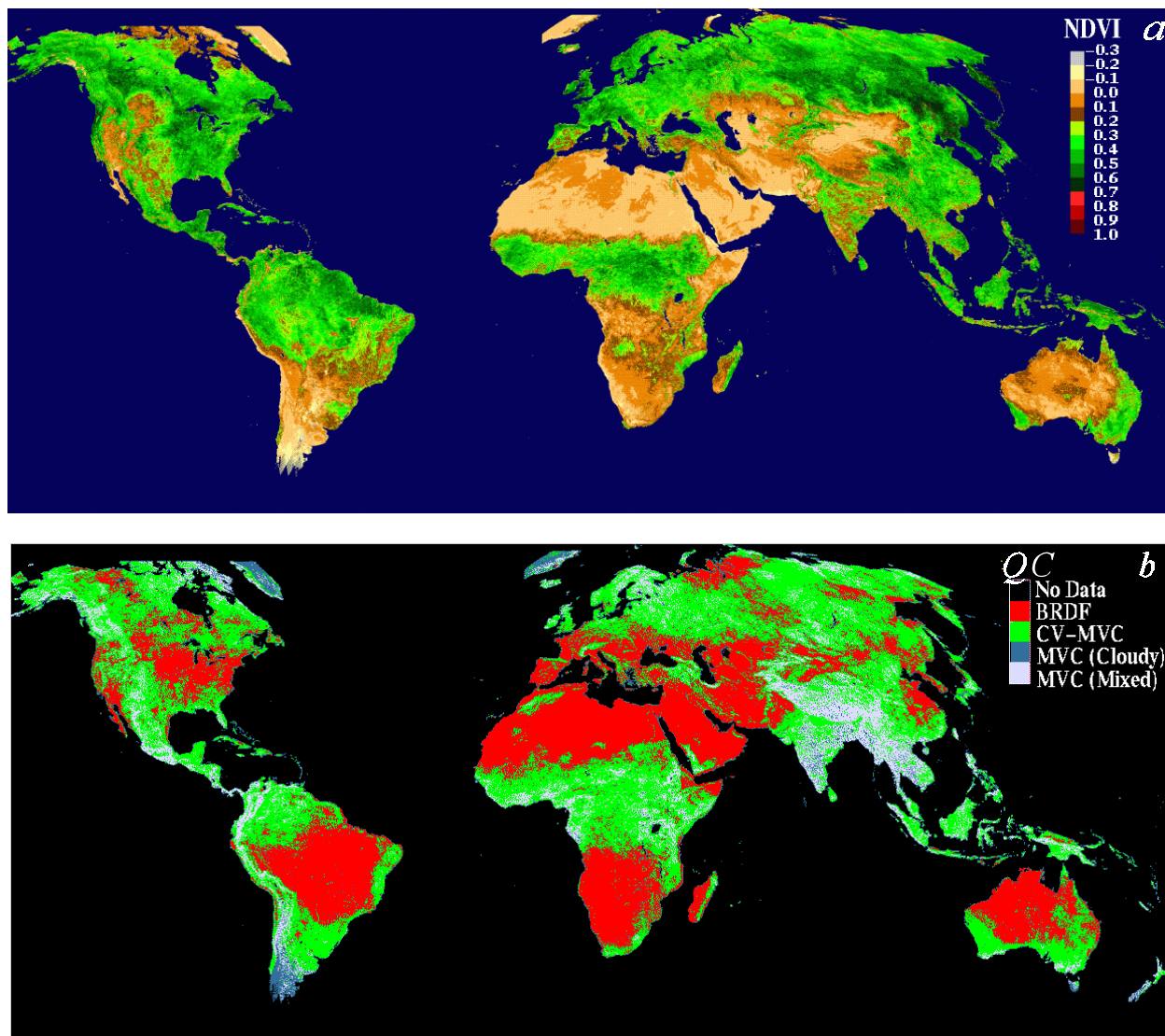


Figure 3.25: a) Pseudo color NDVI image produced with the version 1 composite scenario (BRDF/CV-MVC/MVC); b) Global distribution of quality control flags including information on the applied composite method and clouds (input data: 16 days of AVHRR red and NIR reflectance and QC; 8 km, August 2-17, 1988).

Table 12. Average NDVI value (x10000) per continent and composite method

	MVC	Min. view angle (MV-NDVI)	TV-MVC	CV-MVC	Threshold / BRDF/ MVC	BRDF/ MVC	BRDF/ CV-MVC/ MVC	land pixel frequency (8km)
Africa	1144	915	1028	1038	1025	1025	1007	572285
Asia	2672	2414	2547	2580	2543	2560	2531	810373
Australia	2046	1600	1740	1822	1729	1793	1741	176330
Europe	2155	1832	2006	2031	2000	1989	1958	347430
N. America	3426	3059	3246	3287	3236	3265	3218	356482
S. America	2700	2222	2487	1028	2482	2453	2411	272483

Table 13. Relative difference (%) between MVC and other vegetation index composite approaches (VICA) [$100 * (MVC - VICA) / VICA$]

	Min. view angle MV-NDVI	TV-MVC	CV-MVC	Threshold / BRDF/ MVC	BRDF/ MVC	BRDF/ CV-MVC/ MVC
Africa	25	11	10	12	12	14
Asia	11	5	4	5	4	6
Australia	28	18	12	18	14	18
Europe	18	7	6	8	8	10
N. America	12	6	4	6	5	6
S. America	21	9	8	9	10	12

3.1.7.14 Continuity with AVHRR

Data from six different AVIRIS scenes were processed to MODIS and AVHRR bands in order to conduct a preliminary analysis of continuity issues. The images used were from the SCAR-B project, specifically from the areas of Campo Grande, Ji-Parana, North Brasilia, and Porto Velho (Brazil). Our goal was to outline a relationship between MODIS-NDVI and AVHRR-NDVI over target sites which included Soils, Forest, Agricultural, Burned, and mixed sites. The extraction window size was approximately 50x50 pixels (each pixel ~ 20x 20 m).

The NDVI response was then computed from reflectances for (1) '6S' atmospheric correction, (2) Rayleigh atmospheric correction and (3) No atmospheric correction. The procedure consisted of plotting AVHRR-NDVI against MODIS-NDVI when 6S, Rayleigh and no correction were applied. In a fourth scenario MODIS-NDVI with '6S' correction and Rayleigh corrected AVHRR-NDVI were plotted. The MODIS-NDVI and AVHRR-NDVI data sets were highly linear. That led us to investigate this relationship by means of linear regression through the different data sets. The results of

the linear regression equations that relate NDVI, NIR, and Red between AVHRR and MODIS are summarized in Table 14 and Figs. 3.26, 3.27, 3.28.

Table 14. Linear regression equations that relate NDVI, NIR, and Red between AVHRR and MODIS.

		MODIS		
	NDVI	6S	Rayleigh	No Correction
AVHRR	6S	$0.9824x+0.0469$ $R^2 = 0.9426$		
	Rayleigh	$1.0135x-0.0715$ $R^2 = 0.9253$	$1.0729x-0.0679$ $R^2 = 0.9414$	
	No Correction			$0.9399x-0.0784$ $R^2 = 0.9235$
		MODIS		
	Red	6S	Rayleigh	No Correction
AVHRR	6S	$1.0085x-44.632$ $R^2 = 0.9913$		
	Rayleigh	$0.8911x+66.585$ $R^2 = 0.9826$	$0.9945x-30.184$ $R^2 = 0.9926$	
	No Correction			$0.9926x-8.5276$ $R^2 = 0.9925$
		MODIS		
	NIR	6S	Rayleigh	No Correction
AVHRR	6S	$1.0055x+145.95$ $R^2 = 0.941$		
	Rayleigh	$0.6656x+370.59$ $R^2 = 0.8561$	$0.8188x+129.56$ $R^2 = 0.9015$	
	No Correction			$0.8159x+145.43$ $R^2 = 0.9025$

All relations were linear when data from the different sensors and for different atmospheric corrections are plotted, i.e., a linear equation can easily be used to translate between the two sensors. Some deviations were obvious and were related to the differences in the target spectral characteristics (e.g. Vegetation and soils), and differences associated with the sensor band width and the atmosphere absorption windows for water vapor. The AVHRR has much wider NIR and Red bands than MODIS.

When the data are partially atmospherically corrected (Rayleigh), the MODIS-NDVI is higher than the corresponding AVHRR-NDVI (Fig. 3.26). This is due to the higher NIR signals from MODIS, presumably from a narrower bandwidth which avoids secondary water absorption. When the data is atmospherically corrected, there is less deviation in values, a stronger linear relationship, and the AVHRR-NDVI yields slightly higher values (Fig 3.27). However, if we are to compare atmosphere corrected MODIS with only Rayleigh corrected AVHRR-NDVI data series (True meaning of ‘continuity’), then we see (Fig. 3.28) very large differences in the resulting NDVI values with MODIS-

NDVI values much higher than its predecessor AVHRR. The potential implications to 'saturation' will be further analyzed. We plan to conduct a much more thorough analysis of all factors influencing continuity relationships.

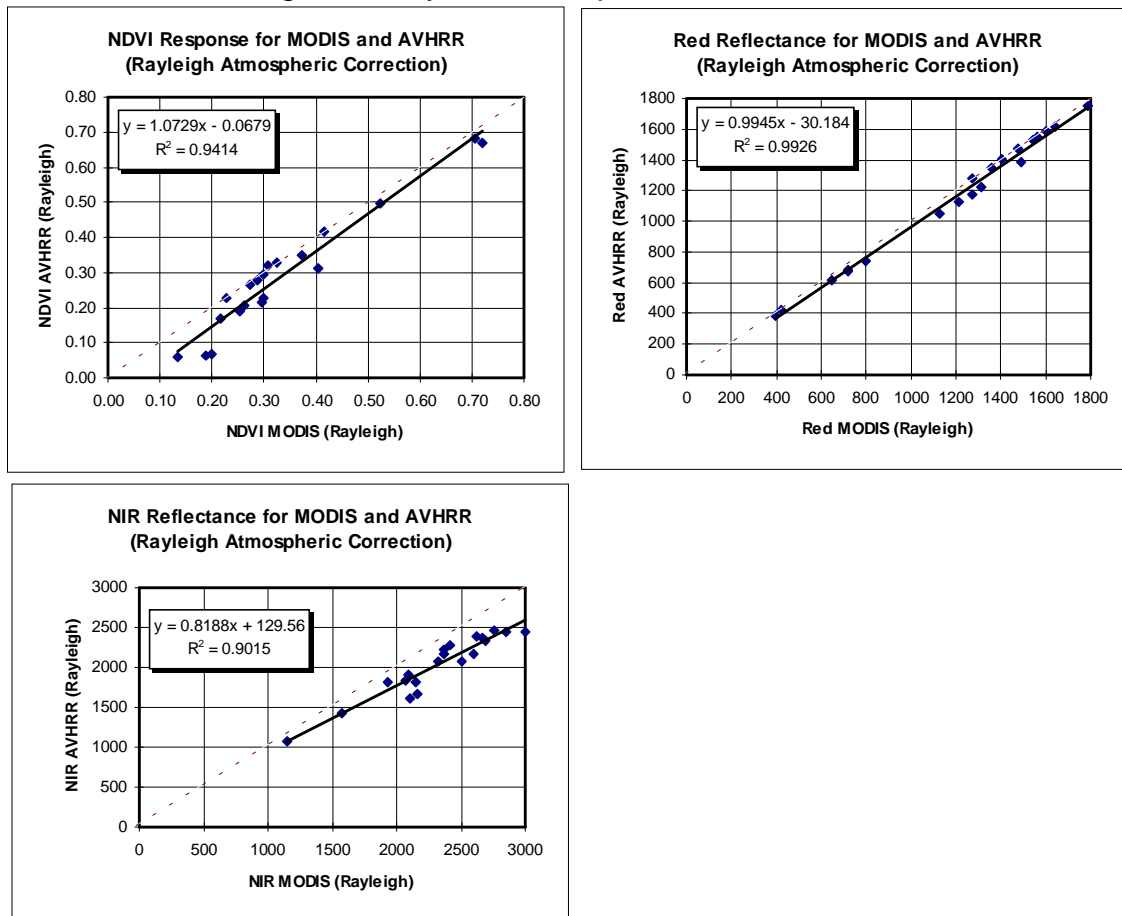


Figure 3.26 Relationships between AVHRR and MODIS for NDVI, NIR, and Red using Rayleigh corrected data.

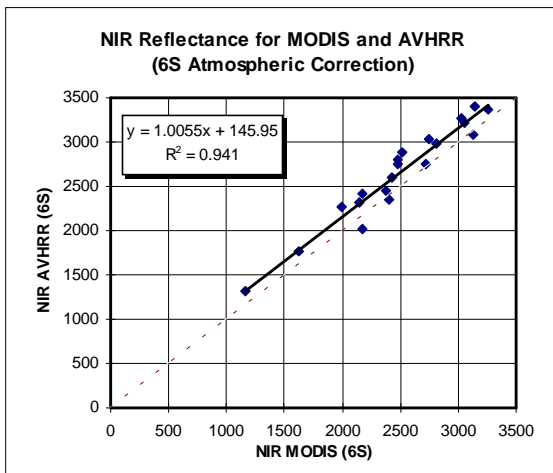
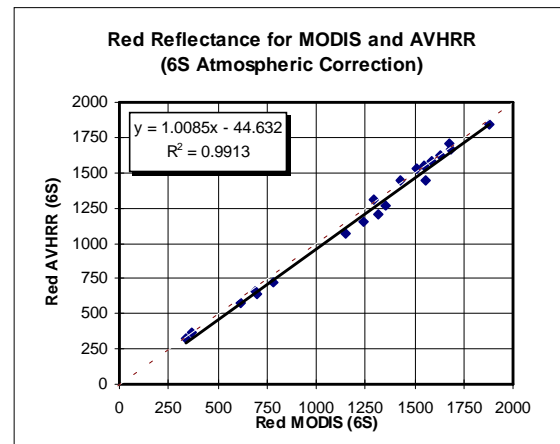
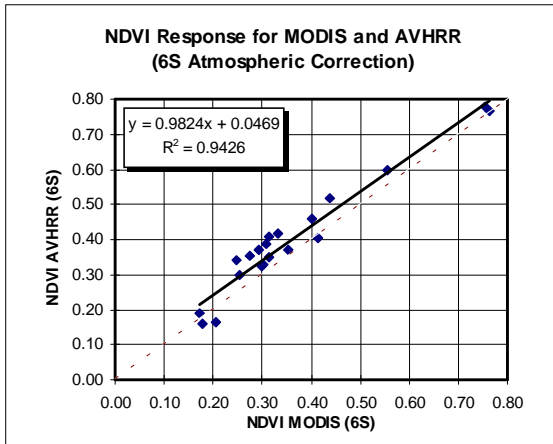


Figure 3.27 Relationships between AVHRR and MODIS for NDVI, NIR, and Red using '6S' corrected data.

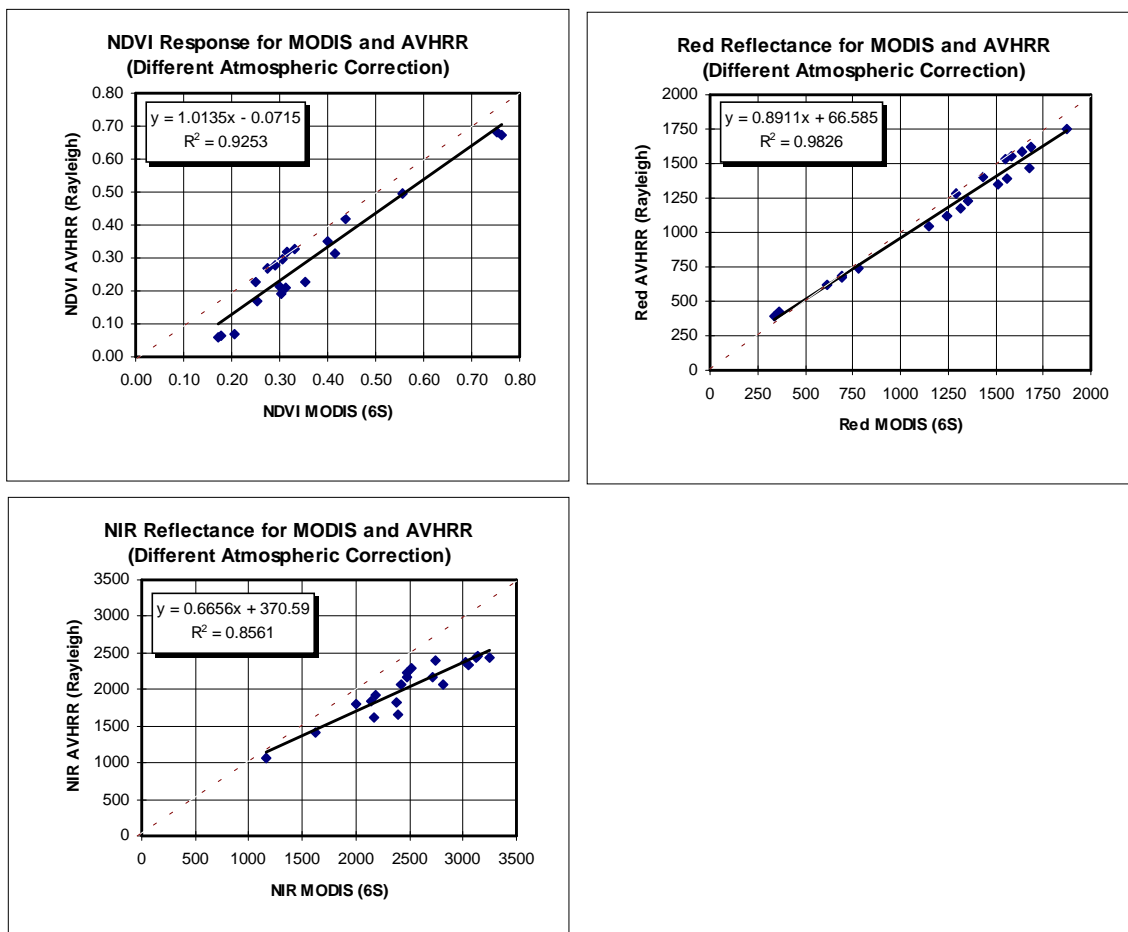


Figure 3.28 Relationships between AVHRR and MODIS for NDVI, NIR, and Red using '6S' corrected MODIS data and Rayleigh corrected AVHRR data.

3.2 Practical considerations

3.2.1 Numerical computation considerations

Practically all floating point computation will take place within the BRDF compositing algorithm. For the BRDF models under consideration, a least-squares solution for model parameters requires that a 3 variable system of linear equations is solved. In the current version, this is achieved through a partial-pivoting matrix inversion, performed by a standard LU decomposition/back-substitution procedure. In the case of the Walthall BRDF model, where the final kernel "c" is defined as the nadir reflectance value, the first two kernels do not necessarily need to be explicitly solved. The nadir approximation can then be directly determined through forward Gaussian elimination rather than a complete matrix inversion at a substantial savings in floating point operations.

3.2.2 Programming /Procedural considerations

The floating point efficiency of the compositing algorithm was tested using the Walthall BRDF model for 8 and 16 day composite periods. Addition, subtraction, multiplication, and division were equally ranked as one FPO (Floating Point Operation), and comparisons, typecasts, and assignments were not recorded.

Accumulating the coefficients of the Walthall least squares matrix required 24 FPOs per data point per channel at a minimum of 5 data points and a maximum of 8 or 16. Solving explicitly for Wathall's 3 kernels using matrix inversion required a fixed cost of approximately 116 FPOs per channel. The total cost of a Walthall BRDF derived pixel therefore lies between 700 and 1500 FPOs when matrix inversion is used. In calculating only the Walthall "c" (nadir) kernel by Gaussian elimination, the fixed cost of solving the linear system is reduced to an estimated 30 FPOs, reducing the overall cost of a BRDF corrected pixel to between 450 and 1250 FPOs.

According to trials on global 8km AVHRR Pathfinder data, BRDF modeling comprised approximately 18% of pixels for 8 day composites and 40% of pixels for 16 day composites. The average number of data points contributing to the BRDF modeled pixels was found to be roughly 5 points for the 8 day composite and 8 points for the 16 day composite. This adjusts the average number of FPOs per pixel to about 90 FPOs for the 8 day composite and 270 FPOs for the 16 day composite as the standard case.

Given a complete tile of 4800 x 4800 land pixels, this gives an average requirement of 2.1 billion FPOs per channel per tile for 8 day composites and 6.2 billion FPOs per channel per tile for a 16 day composite. As a worst case scenario, where the entire composite tile is composed of BRDF derived pixels over the entire composite period, 15.3 billion FPOs are required to produce an 8 day composite tile and 28.6 billion FPOs for 16 days.

3.2.3 Calibration and Validation

3.2.3.1 Introduction

Validation of the vegetation index requires both a radiometric as well as geophysical component. Validation of VI performance in discriminating spatial and temporal vegetation differences is accomplished through independent means which include surface biophysical measurements, theoretical canopy modeling, bioclimatic model outputs, and precursor airborne and satellite data sets. Post-launch validation with the MODIS sensor includes correlative measurements and emphasizes the long term performance and quality of the VI product. The validation of the VI products are highly dependent on coupling of the VI values with ground-based "real" variations in photosynthetic and/ or canopy structural activity.

The validation approach and measurements required are related to the science objectives and planned uses of the algorithm. In this section, we outline a validation strategy for the VI equations over a wide range of vegetation conditions. The reliability, sensitivity, limitations, assumptions, and spatial/temporal error fields associated with the algorithm will be determined, clearly stated, as will the conditions/ situations where the algorithm becomes weak or invalid.

Measurement and science objectives:

Spectral vegetation indices (VIs) are widely used in remote sensing as precise radiometric measures of the spatial and temporal patterns of vegetation photosynthetic activity, and the derivation of biophysical vegetation parameters such as leaf area index (LAI), fraction of absorbed photosynthetic active radiation (fPAR), net primary production (NPP), biomass, and percent green cover (see Justice et al., 1985; Sellers et al., 1994; Townshend et al., 1991). The ubiquitous nature of a global-based VI mandates that it be robust and applicable over all biomes of the earth.

The primary science objectives of the VIs include:

- Spatial and temporal discrimination of vegetation differences (precision);
- Seasonal vegetation profiles of the growing season (phenological);
- Coupling and translation of VIs to biophysical parameters.

Thus, the vegetation indices have both radiometric and biophysical components. The VI units themselves are useful for change detection and analysis of inter- and intra-annual variability patterns in vegetation growth. The goal is to be able to detect vegetation 'changes' at such a resolution as to evaluate the impacts of both climatic and

human processes on terrestrial systems/ processes. Derivation of biophysical parameters is a much more sophisticated use of the vegetation index and thus requires a more complex validation strategy. However, in both cases (radiometric and biophysical), it needs to be made clear, that the validation of the VI algorithm concerns the outputs, and not inputs, of the VI product. Having well calibrated and validated red and NIR reflectances does not constitute validation of the VI, as validation is concerned with the performance of the output results, which is the ability of VI values to depict spatial/temporal variations as well as phenology and biophysical parameters.

3.2.3.2 Validation criteria

Validation of the VI algorithm involves testing and confirmation that the VI is performing as designed in meeting its primary science objectives, or intended uses. Pre-launch validation efforts are aimed at testing the robustness of the algorithm with simulation (MODIS-like) data sets. Post-launch validation efforts incorporate actual instrument performance, product interdependence and long term performance and stability.

There are six general components to the VI validation plan:

1. Comparisons with output from canopy radiant transfer models:

these are utilized to provide a theoretical and physical basis to the VI equations to ensure that the performance and behavior of the VI agrees with that of radiant transfer theory. Radiant transfer modeling is used to vary sensor specifications, vegetation structure and amounts, canopy backgrounds, atmosphere conditions, and sun-target-view geometries. The vegetation indices are tested with simulated data sets generated from simplified 2-stream models, SAIL, and Myneni 3-d canopy models. The 3-d models of Myneni will be conducted over six major, structurally variant, land cover types.

2. Field-based correlative measurements: radiant transfer models can only give a preliminary and restrictive indication of algorithm performance. We are constrained to those surfaces which are readily modeled and in which the models themselves have been validated. A more realistic sampling of the spatial, radiometric, and temporal characteristics of the land surface are obtained with experimental, field measurement campaigns. Field-based radiometry enable data collection under very controlled conditions (sun, view angles, soil, etc.) with negligible atmospheric concerns. Field-based correlative data sets will be used in both pre- and post-launch validation activities and will involve both radiometric and biophysical measurements over a distributed series of test sites. These generally involve point-based measurements which can be coupled with intensive biophysical measurements and destructive vegetation sampling.

3. Experimental aircraft data: these are valuable in generating correlative data over larger 'footprints' or pixel sizes. These data sets are also generally accompanied with ground biophysical measurements as part of larger field campaigns. AVIRIS, ASAS, AirMISR, and MAS data collected over various land cover types are particularly beneficial in validation of the MODIS VIs in that they allow for approximate simulation of MODIS spectral bandwidths, viewing angles, and can be degraded to MODIS pixel sizes (250 & 500 m). Airborne data sets are being amassed over major biome types and processed into simulated MODIS VI data sets.
4. Existing satellite data sets: these primarily include the Landsat Thematic Mapper (TM) and the NOAA-Advanced Very High Resolution Radiometer (AVHRR). The Landsat TM possess the spectral bands useful in simulation nadir-based, VI imagery at 250 m and 500 m pixel sizes. The AVHRR data, with daily acquisitions, are useful in simulation and testing of the Level 3 compositing algorithm. Both Landsat TM and AVHRR data sets are being collected and processed over the major biome types.
5. Future satellite data sets: in the post-launch phase, the MODIS VI product itself will be validated with correlative ground-based measurements and cross-referenced with future satellite data sets from SeaWiifs, SPOT-VEGETATION, ADEOS-GLI, ASTER, MISR, and Landsat 7.
6. Comparisons with output from bioclimatic models: this involves a similar approach as the first component. Bioclimatic models follow current meteorological events and give indications as to "dry" or "wet" years with consequent changes in vegetation activity.

Sampling requirements and tradeoffs:

As no sensor can simulate the spatial, spectral, temporal, and radiometric resolutions of the MODIS sensor, we must use, in the pre-launch phase, a limited quantity of data derived from a suite of satellite sensors. The sampling requirements are constrained by both the availability of global (spatial and temporal) image data sets and by the amount of biophysical ground sampling that can be accomplished.

Spatial and temporal global coverage is best accomplished with a combination of Landsat TM and AVHRR sampling over the major land cover types. We will use 50-60 'test sites', in accordance with the MODIS-EOS test site program, for a thorough documentation of VI spatial and temporal performance over major land cover types. TM imagery can potentially simulate the 16-day composited MODIS- VI product since TM is readily degraded into the 250m and 500m MODIS channels and is at near-nadir view. The daily, temporal data from the AVHRR are suited to evaluate the ability of the level 3 composited VI to construct 'growing season' and phenological curves throughout the year amidst the angular problems and distortions in the AVHRR data. Furthermore, over the major land cover types, we plan to construct Landsat TM & AVHRR growing

season profiles to validate the VI compositing algorithm and determine their performance and accuracy in depicting 'changes' associated with seasonal phenomena.

Measures of success:

The accuracy and performance of the VI will be assessed for each of its intended uses/objectives. In field-measured experimental data sets, Landsat TM data, and canopy model output, changes in biophysical parameters (LAI, fPAR, biomass, green cover) should result in corresponding changes in the VI values for a wide range of vegetation canopies, densities, and structural conditions. The VI should be able to discriminate differences in vegetation within and between the major land cover types and allow for true intercomparisons of spatial and temporal vegetation variations on a global basis.

In the temporal domain, we are concerned with atmospheric residual contamination and angular view angle effects on the VI compositing algorithm which may give false indications of 'change' as well as modify the true nature of a temporal profile. In situ measures of BRDF over some of the test sites as well as ASAS overflights at numerous sites provide for 'true' bidirectional correction of the data and an assessment as to how well the compositing routine is minimizing angular noise. Similarly, seasonal measures of biophysical vegetation parameters, like LAI, provide a "true" seasonal profile of a vegetation growing season.

The 'continuity' role of the NDVI requires appropriate translation coefficients between the AVHRR-NDVI product and the MODIS-NDVI product. These will be obtained on a regular basis over the 'test' sites via co-registration of the AVHRR and MODIS data, post-launch. In the pre-launch period, AVIRIS data are convoluted to simulate both sensors over different land cover types.

The true measure of success of the VI product will be its performance in discriminating spatial/temporal vegetation patterns. This will mean coupling the VI values with ground biophysical measures that can be independently confirmed (measured) to vary or to have changed. The VI algorithms will be evaluated with field-measured biophysical variables, including LAI, fPAR, ground cover, and structure. We will periodically check on a set of translation coefficients to go from VI to biophysical parameters, over many of the land cover types.

In the case of the enhanced VIs such as SARVI, there should also be minimal changes in VI values due to canopy background differences (dry/wet soil, snow, litter, soil color, etc.) and the capability of the SARVI in removing atmospheric residual contamination (e.g., smoke plumes) will be determined with in situ data sets and sun photometer measures. Over limited periods, the sun photometer network will be used to manually correct for atmosphere and assess the performance of the atmospheric resistance component of the SARVI equation. The accuracy of the 'operational'

atmospheric correction algorithm, based on dark object subtraction, and its impact on the VI product, will also be evaluated.

Examples of tests to be conducted as measures of success for the NDVI and enhanced VI include:

- **Baseline test:** VI values will be extracted over a global set of hyperarid sites (no vegetation) for spatial and temporal (long term) invariance of the VI values. Some of these tests will be conducted jointly with MCST level 1b calibration sites over uniform areas devoid of vegetation.
- **Saturation test:** VI values will be extracted over a global set of densely forested, grassland, and agricultural sites to check and monitor the upper sensitivity range of the VIs, including 'saturation' problems.
- **Threshold test:** this involves a performance analysis of VI values in arid & semiarid regions to determine lower vegetation detection limits of the vegetation indices.
- **Correlative measurements:** biophysical measurements will be collected and monitored (long term) over the major land cover test sites to ensure linearity and sensitivity of the VI equations over a wide range (desert to forests) of vegetation conditions.
- **Seasonal profiles:** detailed correlative field data and meteorological data will be collected to assess the accuracy of the level 3 composited product in depicting growing season (phenologic) profiles for the major land cover types.
- **Transition zones:** gradients in climatic variation (precipitation, temperature, and topography) which are known to produce corresponding differences in vegetation are ideal and will be used to test VI sensitivities.
- **In-situ nadir-based reflectances:** these will be measured, in conjunction with sun photometer measures, to assess the accuracy of nadir-generated output from the level 3 compositing algorithm. This will include a sensitivity analysis of the atmospheric correction product on VI performance.

3.2.3.3 Pre-launch algorithm test/development activities

In the pre-launch period, a combination of sensors and data sets are used to simulate MODIS data for the anticipated range of terrestrial surfaces with atmospheric, topographic, and angular variations. Initial validation of the VI equations themselves is accomplished with canopy radiative transfer models such as the Myneni 6 biome canopy code, the SAIL model, and two-stream canopy model. Field experimental data sets are also widely used including radiometric measures (e.g., PARABOLA) and aircraft sensor data. Aircraft and helicopter field measured BRDF data sets are very valuable in simulating MODIS view, angular relationships. Atmospheric radiative transfer codes are also utilized to superimpose varying degrees of atmospheric contamination onto the experimental and canopy model data sets. In this manner, the sensitivity of the VI equations to the atmosphere as well as angular variations can be assessed. Finally, precursor satellite data from the Landsat TM and AVHRR are extremely important in VI validation on a global basis. Pre-launch activities are summarized in Table 15.

Field experiments:

Several airborne sensors provide partial simulation data sets for MODIS algorithm validation. These airborne sensors are normally flown over intensive field campaigns with fairly large ground measurement components. Combinations of the MAS, ASAS, AVIRIS, TMS, and Polder provide data sets for algorithm tests. For these field campaigns, calibrated ground instrumentation provide useful and accurate information, including calibrated sun photometers, ceptometers, fPAR measurements, and field radiometers. The atmospheric measurements gathered over these sites are crucial in effective analysis of the performance of the algorithm over a range of atmospheric conditions.

Table 15 Summary of pre-launch validation activities

Campaign/Data Set	Dates	Sensors	Purpose
Chile - GLCTS (Test Sites)	September, 1996	Cimel, Exotech, (Ground and Light Aircraft)	<ul style="list-style-type: none"> • VI-saturation test (rainforest) • VI-baseline test (hyper-arid) • VI-threshold test (arid/semiarid) • VI-biophysical (all)
LTER Sites, U.S.A. (Long-Term Ecological Research)	Ongoing, 1992 - (Annual and Seasonal)	TM, AVHRR, ASAS, MAS	<ul style="list-style-type: none"> • VI-seasonality, compositing • Field correlative measures <ul style="list-style-type: none"> - biophysical - phenologic
SCAR-B (Brasil)	August to September, 1995	MAS, AVIRIS, Exotech, Cimel	<ul style="list-style-type: none"> • VI-smoke analysis • VI-saturation (bandwidths) • VI-biophysical • Continuity analysis (AVHRR, MODIS) (Tropical forest/cerrado)
HAPEX-Sahel (Niger, Africa)	August to October, 1992	ASAS, TM, Exotech, Cimel	<ul style="list-style-type: none"> • VI-biophysical, angular compositing threshold (Semiarid)
OTTER Transect (Oregon)	1992	ASAS, TM	<ul style="list-style-type: none"> • VI-biophysical, angular, compositing saturation (Forests)
Monsoon '90	August to September, 1990 September, 1991 Seasonal, 1992	ASAS, AVIRIS, TM, Exotech, (Air, Ground), Spectron	<ul style="list-style-type: none"> • VI-angular, compositing threshold • VI-seasonality, biophysical (semiarid)
FIFE (Kansas, USA)	May to September, 1987 and July to August, 1989	ASAS, TM	<ul style="list-style-type: none"> • VI-biophysical, angular, compositing (grassland)
BOREAS (Canada)	August to September, 1995	ASAS, TM	<ul style="list-style-type: none"> • VI-biophysical, angular, smoke, compositing (boreal forest)
Global- TM/AVHRR GLCTS Pathfinder	1985 to Present	TM, AVHRR	<ul style="list-style-type: none"> • VI intercomparisons (global) • VI-compositing
MAC (Maricopa Agricultural Center, Arizona)	1986 to Present	TM, Exotech, Sun Photometer, BRDF	<ul style="list-style-type: none"> • VI-seasonal; biophysical, angular • Dry-wet backgrounds

Some of the field experiments already incorporated into the VI validation effort include:

- SCAR-B experiment in the primary and secondary (regrowth) tropical forests of the Amazon. We have AVIRIS and MAS imagery for the 1995 campaign under clear and very smoky (burning season) conditions. In addition, we collected ground radiometric and biophysical data such as canopy transmittance, ceptometer readings for LAI and fPAR, and sun photometer measurements. Historical and recent values of LAI are also available from various INPE scientists for many of the sites.

- BOREAS experiment in the boreal forests of Canada. This includes MAS (1994) and AVIRIS (1996) overflights over boreal forests in the growing and snow covered seasons. An intensive ground measurement campaign was conducted, including biophysical, and radiometric (Parabola-SE-590) measurements, including sun photometers.
- OTTER experiment in the coniferous forests of the Oregon coastal range as well as Cascade Mountains. We have ASAS and TM data as well as LAI transects and sun photometers.
- FIFE experiment in the tall-grass prairie, Konza Prairie, Kansas. There is ASAS, TM, and ground-based biophysical and radiometric measurements as well as sun photometers.
- HAPEX-Sahel experiment in the semiarid zones of Niger, West Africa. This also includes airborne (ASAS) and satellite data (TM) as well as ground measurements of vegetation and soil biophysical and radiometric properties, and sun photometers.
- Walnut Gulch MONSOON-90 experiment in the arid/semiarid watershed of southeastern Arizona. There is ASAS and AVIRIS data, a multitemporal series of seven Landsat TM scenes covering the 1992 growing season, and a large amount of ground biophysical and radiometric data, including sun photometers.
- Agricultural, uniform crop canopy areas near the Konza Prairie and Maricopa Agriculture Center (MAC), Arizona. These well- controlled, precision grown broadleaf and cereal crops represent homogeneous areas for VI validation. The advantage of these areas are their wide temporal and canopy structural range of vegetation conditions ('zero' vegetation prior to planting and densely vegetated conditions just prior to harvest). The broadleaf and cereal crops present a good set of architectural canopy differences.

Existing satellite data:

In 1992, approximately 20 Landsat 4 & 5, TM scenes were made available to the MODIS team over some of the GLCTS candidate test sites, including broadleaf deciduous and evergreen forests, grasslands, savanna, and deserts. These TM scenes have been processed to simulate MODIS nadir-looking imagery at 250 and 500 m pixel resolutions. The data have been processed into reflectances with a new set of calibration (vicarious) coefficients, exo-atmosphere irradiances, and atmospheric correction algorithms. The atmospheric corrections include corrections based on in-situ measurements of optical depth; and automated dark object subtraction (DOS) procedures. The derived MODIS-like reflectances are then used as input into the VI algorithms. This data set has been useful in assessing the performance of the VI

equations over a global range of vegetation conditions from sparse desert vegetation to very dense temperate and tropical forests (see, for example, Figs. 3.3, 3.4, and 3.6).

A Landsat TM multitemporal data set of seven images during the 1992 growing season at the Walnut Gulch Experimental Watershed in southeastern Arizona has also been processed into MODIS simulated VI imagery. These Landsat scenes include the U.S. - Mexican border where differences in land-use yield contrasting differences in pixel responses on both sides of the border. The data set is thus quite useful in analyzing spatial vegetation patterns associated with land use differences and temporal phenological patterns associated with the monsoon and growing seasons. This is useful as a threshold test in both the spatial and temporal domains.

Daily 1 km AVHRR data sets over HAPEX-Sahel, Konza Prairie, H.J. Andrews, and Coweeta sites are being initially used for development and validation of the compositing algorithm. We plan on using daily AVHRR from other GLCTS sites as the data become available. The 8 km Pathfinder data is also useful in evaluating temporal seasonal VI profiles over major global land cover types.

3.2.3.4 *Post-launch activities*

In the post-launch period, the primary focus will be on the validation of the global data product. This includes an assessment as to how the products will be evaluated through the operational life of the sensor (or product). In the post-launch period, correlative measurement activities will continue over the test sites and the performance of the algorithm over time will be carefully evaluated from which quality controls will be presented.

Correlative measurement activities in support of VI product validation will occur over a global-based distributed network of test sites currently under development. These include the EOS Tier 1, 2, and 3 integrated test site classifications (intensive field, fully instrumented, and biome tower sites). In coordination with the broader scientific community, we expect to participate in several intensive field and airborne campaigns, summarized in Table 16. This includes the instrument calibration sites where vicarious calibration activities are planned. In addition, with MODLAND participation, we plan to conduct a broader list of mini-campaigns summarized in Table 17. The resulting timeline of VI-validation activities is presented in Table 18. For all of these sites we plan on conducting field correlative activities which are summarized as a set of basic "measurement packages" (see below).

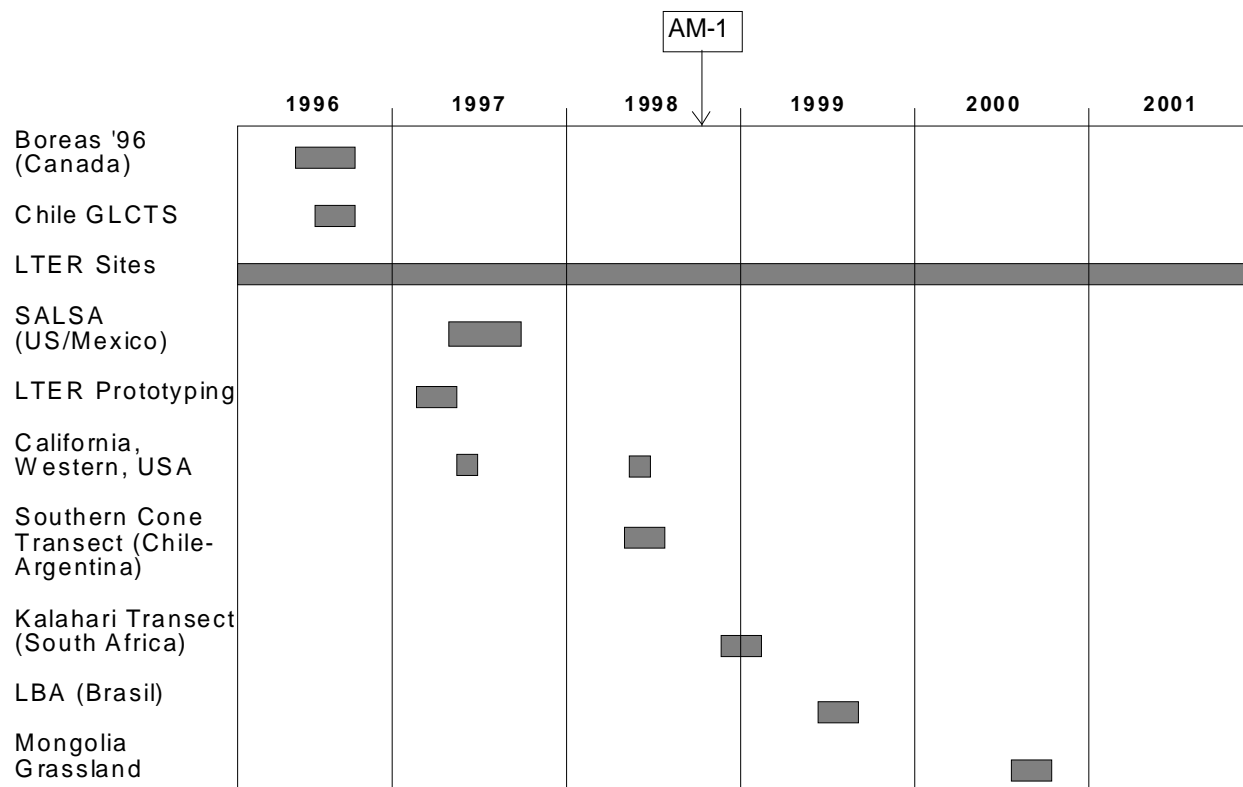
Table 16 Intensive Field and Airborne Campaigns

Mission	Dates	Sensors	Purpose
BOREAS (Canada)	August to September, 1996	MAS, AVIRIS	<ul style="list-style-type: none"> • Boreal forest biophysical - VI • Snow background
SALSA (US - Mexico)	August to September, 1997	AVIRIS, TM	<ul style="list-style-type: none"> • Semiarid biophysical - VI • VI-Threshold
LBA (Brasil)	September, 1999	MAS and AVIRIS	<ul style="list-style-type: none"> • Tropical forest/cerrado biophysical - VI • VI-saturation
Railroad Valley, Lunar Lake (Nevada)	TBD (1998)	Cimel, Ground Radiometers	<ul style="list-style-type: none"> • MCST Level 1B vicarious calibration sites • VI-baseline tests and calibration

Table 17 Proposed EOS/MODIS Field Mini-Campaigns

Mission	Dates	Sensors	Purpose
California, Western, USA	June, 1997	MAS	<ul style="list-style-type: none"> • VI-threshold test (arid/semiarid)
LTER site (La Jornada)	August, 1997	MAS, (Tower network), (BRDF, Sun photometer)	<ul style="list-style-type: none"> • Validation prototyping • VI-aerosols • VI-angular
Southern Cone transect (Chile-Argentina)	October, 1998	Tower Site, Cimel, BRDF, Light aircraft (Exotech) Spectron, MAS (?)	<ul style="list-style-type: none"> • Climatic gradients (Hyperarid—>Rainforest) • Biophysical <ul style="list-style-type: none"> – Temperate rainforest – Pampas • Desertification, Snow background
Kalahari transect (South Africa)	February, 1999	MAS, Landsat 7, BRDF, Cimel, Exotech	<ul style="list-style-type: none"> • Climatic gradient (Arid, semiarid, subhumid) • Biophysical <ul style="list-style-type: none"> – savannah – grassland
Mongolia grasslands (GLI-MODLAND)	TBD (2000)	TBD (Tower, BRDF, Light aircraft)	<ul style="list-style-type: none"> • Grassland monitoring and Biophysical

Table 18 Time line for vegetation index validation activities.



Basic Vegetation Measurement Package:

Intensive measurements are limited to the basic land cover types, and over fairly homogeneous (uniform) areas representative of the land cover type. Here we are interested in VI behavior and ranges in output values over the major land cover types, spatially and seasonally. Representative VI values and performance will be analyzed for various land cover types including:

- Tundra
- Forests
 - temperate needleleaf
 - temperate broadleaf, evergreen
 - temperate broadleaf, deciduous
 - boreal
 - tropical broadleaf
- Grasslands
 - temperate humid
 - temperate dry
 - tropical dry
 - tropical wet
- Shrub
 - desert
 - cerrado
 - montane
- Wetlands
- Hyperarid (no vegetation)
- Agricultural
 - broadleaf crops
 - cereal crops
 - rice paddies

More complicated heterogeneous and mixed biomes are in the realm of experimental research and cannot be thoroughly validated within the resources of this project. If an algorithm performs well over forest and grass, the user would understand that mixed grass-forest areas may behave unlike either component. The measurement schemes for these 'test' sites involve:

1. Uniform and representative sites for the basic land cover types will be chosen. Ideally we would have two-three replicates for each land cover type (e.g., for hyperarid - Gobi, Sahara, and Atacama), and validation conducted during the wet and dry growing seasons.
2. Locate sites with GPS and set up a 2 km x 2 km square grid composed of 4 x 4 (or 16), 250 m pixels in the center and 4 x 4 (or 16) 500 m pixels around it.

3. Sampling may now be conducted with linear (1-d) transects or with the spatial (2-d) grid, depending on the statistical rigor required for that land cover type.

4. Vegetation Characterization

- d. *Basic Optics*; for dominant vegetation species, measure leaf reflectance and transmittance. Similarly, soil, litter, woody material, and other significant non-photosynthetic material would be optically characterized. These measures are to aid in the coupling of the vegetation index with LAI and fPAR parameters.
- e. *Vegetation Biophysical*; these measures include percent cover by components (green, senesced, soil, litter, etc.), LAI (green and total), biomass (in the case of grasslands and herbaceous types), fPAR, and basic vegetation structure and morphology, on a qualitative or semi-quantitative basis.

It is recognized that not all measures can be conducted in a similar manner over all vegetation types. In some cases, a limited amount of destructive sampling may be performed, while in the majority of cases, allometric techniques may be employed over indirect methods such as ceptomtry. The best measure of vegetation characteristics will normally already be provided by the local "expert" or institute with previous experience over specific land cover types. The specific method employed will have to be well documented and referenced to previous studies in that area. Allometric and other indirect methods will have relationships already established and traceable to "destructive sampling" methods, thus having its own validation and calibration history.

- f. *Meteorological/Environmental*; a basic set of climatic and meteorological parameters, including weekly precipitation, air temperature, incoming or net radiation, vapor pressure deficit, and possibly soil moisture deficit.
- g. *Radiometric*; this is included in the MODLAND radiometric package. Fundamentally, for a uniform and intensive validation site, we would like to measure canopy reflectance and transmittance, BRDF, atmosphere condition and canopy background reflectance. A "biome tower" network is envisaged, instrumented with nadir-based and BRDF radiometers, and sun photometer.

Long-Term Validation Performance (Temporal Sampling):

Long term VI calibration is built into the validation test sites. For example, the zero-baseline (hyperarid) sites will be used to monitor long term stability and integrity of the MODIS-VI data record (sensor and filter stability). Humid region, protected forests with dense vegetation covers, will be used to monitor the

upper limits of vegetation. Extensive grasslands are being considered as an intermediate calibration point.

Here we are interested in less intensive measures and instead wish to obtain simple and precise measures indicative of "change" in the vegetation canopy. Here is where many indirect methods of vegetation sampling, such as ceptometry, will prove useful. In addition, we would like to employ these rapid measures over a larger set of test sites, which no longer are to be uniform. In fact, here we are interested in test sites or transects which are located in "transition areas" (e.g., the hyperarid to arid transition zones or arid - semiarid transition zones). We would like these sites to be situated in areas where we may most likely expect to encounter "long term" changes and we would like to validate that the VI algorithms will be able to detect such changes. We will also determine the performance of the algorithms by verifying its sensitivity to such changes. Results of field experiments and validation exercises will be coordinated with and made available to the scientific community via EOSDIS.

Intercomparisons (multi-instrument):

Cross-calibration and validation activities are planned with the following sensors:

ADEOS -GLI (250 m channels)
MISR (Angular)
ASTER (Zoom, biophysical)
AVHRR (Compositing)
Landsat TM 7 (Zoom, biophysical)
SeaWifs (Compositing)

3.2.4 Quality control and diagnostics

3.2.4.1 Level 2 vegetation indices

Two Level 2 vegetation indices will be produced at 250 m resolution, the Normalized Difference Vegetation Index (NDVI) and the Soil and Atmospheric Resistant Vegetation Index (SARVI). These products will come with QA flags taken partially from MOD09 (surface reflectance product). The standard QA will be used as proposed by Roy (1996), with some minor changes. Data integrity and a run time QA test will be performed on the input data and the output data, resulting in a bit that will tell if the NDVI and SARVI are usable or not. One bit is for the NDVI and another bit for the SARVI. Table 19 gives an overview of the proposed Level 2 QA flags. Since the input to the NDVI is based on two bands, the least good QC flag from the reflectance product will be representative for the VI QC flag. The SARVI will have 3 input QC flags from the reflectance product, and thus the least good QC flag will be chosen to represent the VI QC.

3.2.4.2 Level 3 vegetation index compositing

Two level 3 gridded vegetation indices will be produced, the Normalized Difference Vegetation Index (NDVI) and the Soil and Atmospheric Resistant Vegetation Index (SARVI). The gridded VIS are 8-day, 16-day and monthly spatial and temporal resampled products designed to provide cloud free vegetation maps at nominal resolutions from 250 m to 0.25° (CMG-climate modeling grid). The output for the composited NDVI and SARVI for the different spatial and temporal resolutions will be two bytes for the VIS and 1 byte for quality (QC) control which will contain information on data integrity, composite method used and cloud cover.

The algorithms use the information in the reflectance-QC, partially derived from the MODIS cloud mask product, to pre-process the atmospherically corrected reflectance data of MODIS bands 1, 2, and 3 (red, NIR, blue). Land pixels with clouds, shadow, and bad data integrity will initially be excluded from the VI composite. The composite algorithm consists of 3 criteria which will be tracked with the QC flags (Table 20). Sun angle information for each tile will be stored in the metadata.

The monthly 250 m VI products are created by a weighted average of the 250 m, 16-day composite reflectance files resulting from the 16-day composite approach. Within a particular month 2-3 files will be combined to get the monthly composite. The QC will indicate which composite periods were used in the monthly products (Table 21). The aggregated 0.25° NDVI and SARVI composites are calculated from atmospherically corrected, gridded surface reflectances which were used to produce the VIS at 250 m resolution (level 3). The number of cloudy and/or bad pixels are counted for each CMG pixel to compute the percentage cloud cover (Table 22).

3.2.4.3 Run time data quality assurance (QA) evaluation

Before the VI can be composited, the surface reflectance data and their quality control flags must be analyzed and pre-processed to evaluate whether the surface reflectance data meets the composite threshold conditions and can be used in the VI composite algorithm. These threshold conditions have different levels of accuracy and applicability.

- ▶ Pixels observed at view zenith angles larger than $\sim 50^\circ$ will be ignored
- ▶ Pixels observed at very low sun angles will not be processed (terminator effect)
- ▶ Pixel reflectance data with bad data integrity will be discarded.
- ▶ Pixels with clouds and shadow will be discarded unless there are no good pixels
- ▶ Reflectance values below zero or above 1 will be discarded.
- ▶ VI values below -0.3 and above 1 will be discarded.
- ▶ Fill value will be -1.0

After the input and output are 'screened' the run time QA will provide information on accuracy of the compositing algorithm. For the CMG (25 km) the cloud statistics are provided per pixel based on the 250 m input data.

All run time QA procedures result in storage of the mandatory QA plane. For level 2 the composition of the surface and cloud state bits and the 'good to bad QA bits' is slightly different from the proposed composition. For Level 3 the composition of the mandatory plane is different from the proposed Level 2 composition due to differences in functionality. Currently no optional QA plane is planned. The location of the run time QA procedures is at the DAAC

The following is an overview of the QC definitions as they are produced for each pixel as a result of the input QC and run time algorithm. Currently the NDVI and SARVI are produced at the same resolution and the QC flags could be combined into one byte to minimize storage requirements. However if the NDVI and SARVI were produced at different spatial or temporal resolutions, the flags must remain separated.

3.2.4.4 Run time Quality Control (QC) for daily and composited NDVI and SARVI (Level 2 and 3)

Based on the QA-plan (D. Roy, 1996), the Level 2 cloud state bits (0-2) and the summary QA bit (3) are mandatory QA bits. There are some slight deviations to be discussed with the larger MODIS community.

Table 19 Definition of quality control bits per pixel and daily vegetation indices (250 m) (level 2)

bit	Long name	Key
00	bits 1-2 determined/ undetermined	0 determined 1 undetermined
01-02	atmosphere status	00 atmospherically clear 01 cloudy 10 mixed 11 shadow
3	usefulness of product	0 product useful 1 product not useful
04	data integrity NDVI	0 usable NDVI 1 unusable NDVI
05	data integrity SARVI	0 usable SARVI 1 unusable SARVI
06	land mask	00 land 01 water
07	undetermined	

Table 20. Definition of quality control bits per pixel for 8 and 16 day composite (level 3)

bit	Long name	Key
00	NDVI data integrity	0 usable NDVI data 1 unusable NDVI data
01	cloud mask for NDVI	0 clear (NDVI) 1 cloudy/ mixed/ shadow
02-03	composite method NDVI	NDVI 00 BRDF model based 01 CV-MVC (constraint view angle) 10 MVC (last resort)
04	SARVI data integrity	0 usable SARVI data 1 unusable SARVI data
05	cloud mask for SARVI	0 clear (SARVI) 1 cloudy/mixed/shadow (SARVI)
06-07	composite method SARVI	SARVI 00 BRDF model based 01 CV-MVC (constraint view angle) 10 MVC (last resort)

The standard QA state bits are not useful for Level 3. QC flags 00 and 04 (Table 20) indicating whether the NDVI and SARVI are usable are based on reflectance and VI-threshold tests and the land-water mask. If the land mask bit indicates water, the flag is set to unusable.

Table 21. Definition of quality control bits per pixel for a monthly composite @ 250 m resolution (level 3)

bit	Long name	Key
00	data integrity	0 usable VI 1 unusable VI
01	cloud mask	00 clear 01 cloudy/ mixed/ shadow
02-04	composite periods 1,2 and/or 3	000 periods 1,2,3 100 periods 2,3 010 periods 1,3 001 periods 1,2 011 period 1 101 period 2 110 period 3 111 period none
05-07	composite methods 1- BRDF 2- CV-MVC 3- MVC (cloudy)	000 method 1,2,3 100 method 2,3 010 method 1,3 001 method 1,2 011 method 1 101 method 2 110 method 3 111 none

Both NDVI and SARVI will have separate QA flags in the monthly composites (Table 21 and 22).

Table 22. Definition of quality control bits per pixel for 25 km monthly composite (level 3)

bit	Long name	Key
00	data integrity	0 usable VI 1 unusable data (bad, cloudy or water)
01-07	cloud cover over land for 25 km pixels 0 - 100% of pixels are cloudy, but not used to compute the VI	0000000 0% cloud cover 0000001 1% 0000010 2% 0000011 3% 0000100 4% etc..... till 1100100 100%

3.2.4.5 Run time product metadata QA considerations for Level 2 and Level 3

The proposed (QA document; Roy, 1996) product metadata will summarize some of the mandatory QA plane results numerically and text-based on the granule or tile level.

Numerically based flags which indicate the % of pixels in processed granule or tile:

- ▶ % land;
- ▶ % water;
- ▶ % atmospherically clear;
- ▶ % clouds;
- ▶ % mixed clouds;
- ▶ % usable; %unusable;
- ▶ % pixels derived from BRDF model;
- ▶ % pixels derived from MVC with constrained view angle;
- ▶ % pixels derived from MVC where pixels are mixed cloudy and cloudy;
- ▶ % pixels where $MVC > (MODIS \text{ algorithm result})$; % pixels where $MVC < (MODIS \text{ algorithm result})$;
- ▶ Average difference per tile between MVC and MODIS composite algorithm.

Text based flags are not yet determined, but a list of product specific category meanings will be considered.

3.2.4.6 Post run time QA

All in depth QA analysis will require the data analysis of MOD09 and MOD13. A parallel algorithm will run at the science computing facility (SCF) reading in the original MOD09 output data and compute the VIS at different spatial and temporal resolutions. The code at the SCF will have extra code that will enable in depth evaluation of all steps involved to get the composited VI product.

Tiles will be regularly extracted on a global basis. Special attention will be given to validation test sites and data windows extracted for temporal analysis. Difference images between different composite scenarios will be evaluated for artefacts. Some post run time QA will involve the correlation of biophysical parameters and VI values for certain test sites. These results will be useful to evaluate the sensitivity of the VI to biophysical parameters.

3.2.4.7 DATA and Tools to be used

MODIS data to be used: MOD09 MOD13 monthly data for certain tiles that coincide with validation sites. Several ancillary data sets will be used to do cross validation of the input data (MOD09) and output data (MOD13). These ancillary data sets will be reflectance data of MISR, ASTER, GLI, LANDSAT7 as long as these are calibrated. Other ancillary data will include calibrated aircraft reflectance data from MAS and

additional biophysical measurements collected at LTER, GLCTS and MODIS field campaign sites (SALSA, LBA).

Several application programs and tools will be used and written in c-code to extract, process and analyze data in a timely fashion. Xspace and Khoros software will be used to display MODIS tiles (reflectance and VI input). IDL (Interactive Data Language) will be used for autoregressive modeling and forecasting [temporal analysis], differencing, multivariate analysis, correlation analysis, statistical fitting of data, signal processing and image processing, visualization, 2-D plotting of satellite data and other miscellaneous software, where needed.

The expected QA results will be presented in reports containing pseudo color imagery representing QA planes, 2-D plots, and written quality evaluations and uncertainties based on time series analysis of the input reflectance data and output vegetation index data.

3.2.5 Exception Handling

Exceptions will be handled under three possible scenarios:

- i. Tile is unavailable, incomplete, or corrupted.
- ii. Tile is determined not usable by information contained within metadata files. This includes problems with tiles at high latitudes associated with low illumination conditions. These are sometimes referred to as the terminator effect (Holben, 1986).
- iii. Tile is determined not usable after unsuccessfully attempting to process it. Conditions include unfavorable atmospheric correction procedures, heavy cloud cover, missing data, unfavorable image geometry, and unusable reflectance values.

Under all three scenarios, daily products cannot be produced. No binary files are written and the output metadata is flagged appropriately. Composite products are capable of recovering from the above conditions, provided there is at least one usable tile available. Otherwise, as with the daily product, no binary files are written and output metadata is thus flagged.

4.0 Constraints, Limitations, and Assumptions

Only day time, cloud free data should be processed to the VI. We assume that the data is cloud-free and that sub-pixel clouds will be filtered with a compositing cycle. We are assuming fairly good geolocation and registration of multi-temporal data (within MODIS specifications) and we will need a careful assessment of geometric performance post-launch. We are assuming that a first order topographic correction

will be made post-launch in the derivation of surface reflectances. We envisage that 16 days of data will be stored and kept on-line in order to look for anomalies.

ACKNOWLEDGMENTS

The BRDF model analysis, using the Parabola data sets collected by Dr. D. Deering et al., was contributed by Dr. Jeff Privette and is greatly appreciated. Thanks to Trevor Laing who contributed to the coding and computation related topics. We are grateful to Lindy Fletcher and many others who helped in preparing this document.

REFERENCES

- Ackerman et al., 1994. Discriminating clear sky from cloud with MODIS. Algorithm Theoretical Basis Document V2.
- Asrar, G., Myneni, R.B., and Choudhury, B.J., 1992, "Spatial heterogeneity in vegetation canopies and remote sensing of absorbed photosynthetically absorbed radiation: a modeling study", *Remote Sens. Environ.* 41:85-101.
- Asrar, G., Fuchs, M., Kanemasu, E.T. and Hatfield, J.L., 1984, Estimating absorbed photosynthetic radiation and leaf area index from spectral reflectance in wheat, *Agron. J.*, 76:300—306.
- Baret, F. and Guyot, G., 1991, Potentials and limits of vegetation indices for LAI and APAR assessment, *Remote Sens. Environ.*, 35:161-173.
- Baret, F., Guyot, G. and Major, D., 1989, TSAVI: a vegetation index which minimizes soil brightness effects on LAI and APAR estimation, in 12th Canadian Symp. on Remote Sensing and IGARSS'90, Vancouver Canada, 10-14 July 1989.
- Barker, J.L., Brown, K.S. and Harnden, J.M.K., 1993, MODIS: Calibration & Characterization Algorithm Theoretical Basis Document (Cal ATBD), Version 0, 1 July, 1993.
- Bartlett, D.S., Hardisky, M.A., Johnson, R.W., Gross, M.F., Klemas, V., and Hartman, J.M., 1988, "Continental scale variability in vegetation reflectance and its relationship to canopy morphology", *Int. J. Remote Sens.* 9:1223-1241.
- Bausch, W., 1993, Soil background effects on reflectance-based crop coefficients for corn, *Remote Sens. Environ.* 46:1-10
- Begué, A., 1993, Leaf area index, intercepted photosynthetically active radiation, and spectral vegetation indices: a sensitivity analysis for regular-clumped canopies, *Remote Sens. Environ.* 46:45-59.
- Buschmann, C., and Nagel, E., 1993, In vivo spectroscopy and internal optics of leaves as basis for remote sensing of vegetation, *Int. J. Remote Sens.* 14:711-722.
- Choudhury, B.J., 1987, Relationships between vegetation indices, radiation absorption, and net photosynthesis evaluated by a sensitivity analysis, *Remote Sens. Environ.* 22:209-233.
- Cihlar, J., Manak, D., and Voisin, N., 1994a. AVHRR Bidirectional Reflectance Effects and Compositing. *Remote Sens. Environ.*, 48:77-88

Cihlar, J., Manak, D., and D'Iorio, M., 1994b. Evaluation of Compositing Algorithms for AVHRR Data over Land. *IEEE Trans. Geosc. Remote Sens.*, 32:427-437.

Clevers, J.G.P.W., and Verhoef, W., 1993, LAI estimation by means of the WdVI: a sensitivity analysis with a combined PROSPECT-SAIL model, *Remote Sens. Reviews*, 7:43-64.

Clevers, J.G.P.W., 1989, The application of a weighted infrared-red vegetation index for estimating leaf area index by correcting soil moisture, *Remote Sens. Environ.* 29:25-37.

Colwell, J.E., 1974, Vegetation canopy reflectance, *Remote Sens. Environ.* 3:175-183.

Curran, P.J., 1982, "Multispectral remote sensing for estimating biomass and productivity", in: *Plants and the Daylight Spectrum*, edited by H. Smith (London: Academic Press).

Curran, P.J., 1980, Relative reflectance data from preprocessed multispectral photography, *International Journal of Remote Sensing*, 1:77-83.

Daughtry, C.S.T., Gallo, K.P., Goward, S.N., Prince, S.D., Kustas, W.P., 1992, Spectral estimates of absorbed radiation and phytomass production in corn and soybean canopies, *Remote Sens. Environ.* 39:141-152.

Deering, D.W. and Eck, T.E., 1987. Atmospheric optical depth effects on angular anisotropy of plant canopy reflectance. *Int. J. Remote Sensing*, 8(6), 893-916.

Deering, D.W. and Leone, 1986. A sphere-scanning radiometer for rapid directional measurements of sky and ground radiance, *Remote Sens. Environ.*, 19:1-24.

Deering, D.W., 1978, Rangeland reflectance characteristics measured by aircraft and spacecraft sensors. Ph.D. Dissertation, Texas A & M University, College Station, TX, 338 pp.

Demetriades-Shah, T.H., Steven, M.D., and Clark, J.A., 1990, High resolution derivative spectra in remote sensing, *Remote Sens. Environ.* 33:55-64.

Eidenshink, J.C. and Faundeen, J.L., 1994, "The 1km AVHRR global land data set: first stages in implementation," *Int. J. Remote Sensing*, 15(17), pp. 3443-3462.

Eidenshink, J.C., Steinwand, D.R., Wivell, C.E., Hollaren, D.M., and Meyer, D.J., 1993. PECORA 11, Symposium on land information systems, Sioux Falls August 1993. p. 214-221.

Elvidge, C.D., and Chen, Z., 1995, Comparison of broad-band and narrow-band red and near-infrared vegetation indices, *Remote Sens. Environ.* 54:38-48.

Elvidge, C.D., and Lyon, R.J.P. (1985), Influence of rock-soil spectral variation on the assessment of green biomass, *Remote Sens. Environ.* 17:265-279.

Flittner, D.E. and Slater, P.N. 1991, Stability of narrow-band filter radiometers solar-reflective range, *Photogramm. Eng. Remote Sens.* 57:165-171.

Franklin, J.F., Bledsoe, C.S. and Callahan, J.T., 1990, Contributions of the long-term ecological research program, *BioScience*, 40:509-523.

Gallo, K.P., Daughtry, C.S.T. and Bauer, M.E., 1985, Spectral estimation of absorbed photosynthetically active radiation in corn canopies, *Remote Sens. Environ.* 17:221-232.

Gitelson, A.A., Kaufman, Y.J., and Merzlyak, 1996, "An atmospherically resistant "green" vegetation index (ARGI) for EOS-MODIS", *Remote Sens. Environ.*, (in press).

Goward, D.G., Turner, S., Dye, D.G., and Liang, J., 1994. University of Maryland improved Global Vegetation Index. *Int. J. Remote Sensing*, 15(17), 3365-3395.

Goward, S.N. Dye, D.G., Turner, S., and Yang, J., 1993. Objective assessment of the NOAA global vegetation index data product. *Int. J. Remote Sensing*, 14, 3365-3394.

Goward, S.N., and Huemmrich, K.F., 1992, Vegetation canopy PAR absorptance and the normalized difference vegetation index: an assessment using the SAIL model, *Remote Sens. Environ.* 39:119-140.

Goward, S.N., B. Markham, D.G. Dye, W. Dulaney, J. Yang, 1991, "Normalized difference vegetation index measurements from the Advanced Very High Resolution Radiometer", *Remote Sens. Environ.*, 35:257-277.

Goward, S.N., Tucker, C.J., and Dye, D.G., 1985, "North American vegetation patterns observed with the NOAA-7 advanced very high resolution radiometer", *Vegetatio*, 64:3-14.

Gutman, G.G., 1991, Vegetation indices from AVHRR: an update and future prospect, *Remote Sens. Environ.*, 35:121-136.

Gutman, G., 1989. On the relationship between monthly mean and maximum-value composite normalized vegetation indices. *Int. J. Remote Sensing*, 10(8), 1317-1325.

Hall, F.G., Huemmrich, K.F., and Goward, S.N., 1990, Use of narrow-band spectra to estimate the fraction of absorbed photosynthetically active radiation, *Remote Sens. Environ.* 32:47-54.

- Heilmen, J.L. and Kress, M.R., 1987, Effects of vegetation on spectral irradiance at the soil surfaces, *Agron. J.* 79:765-768.
- Holben, B., Kimes, D., and Fraser, R.S., 1986. Directional reflectance Response in AVHRR Red and Near-IR Bands for Three Cover Types and Varying Atmospheric Conditions. *Remote Sens. Environ.*, 19:213-236.
- Holben, B.N. 1986. Characterization of maximum value composites from temporal AVHRR data. *Int. J. Remote Sensing*, 7:1417-1434.
- Holben, B., Fraser, R.S., 1984. Red and Near-infrared sensor response to off-nadir viewing. *Int. J. Remote Sensing*, 5(1), 145-160.
- Huete, A.R., Liu, H.Q., Batchily, K., and van Leeuwen, W., 1996, A comparison of vegetation indices over a global set of TM images for EOS-MODIS, *Remote Sens. Environ.*, (in press).
- Huete, A.R., and Liu, H., 1994, An error and sensitivity analysis of the atmospheric and soil correcting variants of the NDVI for MODIS-EOS, *IEEE Trans. Geosc. Remote Sens.*, 32:897-905.
- Huete, A., Justice, C. and Liu, H., 1994, "Development of vegetation and soil indices for MODIS-EOS", *Remote Sens. Environ.*, 49:224-234.
- Huete, A.R., Hua, G., Qi, J., Chehbouni, A. and van Leeuwen, W.J.D., 1992, Normalization of multidirectional red and NIR reflectances with the SAVI, *Remote Sens. Environ.*, 40:1-20.
- Huete, A.R. and Tucker, C.J., 1991, Investigation of soil influences in AVHRR red and near-infrared vegetation index imagery, *International Journal of Remote Sensing*, 12:1223-1242.
- Huete, A.R. and Warrick, A.W., 1990, Assessment of vegetation and soil water regimes in partial canopies with optical remotely sensed data, *Remote Sens. Environ.* 32:155-167.
- Huete, A.R. ,1988, A soil adjusted vegetation index (SAVI), *Remote Sens. Environ.* 25:295-309.
- Huete, A.R., Jackson, R.D. and Post, D.F., 1985, Spectral response of a plant canopy with different soil backgrounds, *Remote Sens. Environ.* 17:37-53.
- Hutchinson, C.F., 1991, Use of satellite data for Famine Early Warning in sub-Saharan Africa. *International Journal of Remote Sensing*, 12(6):1405-1421.

IGBP, 1992, The International Geosphere-Biosphere Programme: A Study of Global Change, Improved Global Data for Land Applications, IGBP Report No. 20, Stockholm, Sweden: IGBP Secretariat.

Irons, J.R., Ranson, K.J., Williams, D.L., Irish, R.R. and Huegel, F.G., 1991, An off-nadir imaging spectroradiometer for terrestrial ecosystem studies, *IEEE Trans. Geosci. and Remote Sens.*, 29:66-74.

Jackson, R.D. and Huete, A.R., 1991, Interpreting vegetation indices, *Prev. Vet. Med.* 11:185-200.

Jackson, R.D. and Pinter, Jr., P.J., 1986, Spectral response of architecturally different wheat canopies, *Remote Sens. Environ.*, 20:43-56.

Jackson, R.D., Teillet, P.M., Slater, P.N., Fedosejevs, G., Jasinski, M.F., Aase, J.K., and Moran, M.S., 1990. Bidirectional measurements of surface reflectance for view angle correction of oblique imagery. *Remote Sens. Environ.*, 32,189-202.

James, M.D., and Kalluri, S.N.V. (1994), The Pathfinder AVHRR land data set: An improved coarse resolution data set for terrestrial monitoring, *Int. J. Remote Sensing*, 15(17):3347-3363.

Jordan, C.F., 1969, Derivation of leaf area index from quality of light on the forest floor. *Ecology* 50:663-666.

Justice, C.O., Townshend, J.R.G., Holben, B.N. and Tucker, C.J., 1985, "Analysis of the phenology of global vegetation using meteorological satellite data", *Int. J. Remote Sensing*, 6:1271-1318.

Kaufman, Y.J., and Tanré, D., 1996, Strategy for direct and indirect methods for correcting the aerosol effect on remote sensing: from AVHRR to EOS-MODIS, *Remote Sens. Environ.* 55:65-79.

Kaufman, Y.J. and Tanré, D., 1992, Atmospherically resistant vegetation index (ARVI) for EOS-MODIS, *IEEE Trans. Geosci. Remote Sensing*, 30:261-270.

Kauth, R.J., and Thomas, G.S. (1976), The tasseled cap - A graphic description of the spectral-temporal development of agricultural crops as seen by Landsat in *Proceedings of the Symposium on Machine Processing of Remotely Sensed Data*, LARS, Purdue University, West Lafayette, Indiana, pp. 41-51.

Kimes, D.S., Holben, B.N., Tucker, C.J., and Newcomb, W.W., 1984. Optimal directional view angles for remote-sensing missions. *Int. J. Remote Sensing* 5(6), 887-908.

- King, M.D., Kaufman, Y.J., Menzel, W.P. and Tanré, D., 1992, "Remote sensing of cloud, aerosol, and water vapor properties from the Moderate Resolution Imaging Spectrometer (MODIS)", IEEE Trans. Geosci. Remote Sensing, 30:2-27.
- Kneizys, F.X., Shettle, E.P., Abreu, L.W., Chetwynd, J.H., Anderson, G.P., Gallery, W.O., Selby, J.E.A. and Clough, S.A., 1988, Users Guide to LOWTRAN 7, Report AFGL-TR-88-0177, AFRCL, Bedford, Mass., August, 137 pp.
- Leeuwen van, W.J.D. A.R. Huete, S. Jia, C.L Walthall, 1996. Comparison of Vegetation Index Compositing Scenarios: BRDF Versus Maximum VI Approaches. IEEE-IGARSS'96, Lincoln Nebraska, Vol.3, 1423-1425.
- Leeuwen van, W.J.D., A.R. Huete, J. Duncan, J. Franklin, 1994. Radiative transfer in shrub savanna sites in Niger -- preliminary results from HAPEX-II-Sahel: 3. Optical dynamics and vegetation index sensitivity to biomass and plant cover. Agricultural and Forest Meteorology 69, 267-288.
- Liu, H.Q., and Huete, A.R., 1995, "A feedback based modification of the NDVI to minimize canopy background and atmospheric noise", IEEE Trans. Geosci. Remote Sensing, 33:457-465.
- Major, D.J., Baret, F. and Guyot, G., 1990. A ratio vegetation index adjusted for soil brightness. International Journal of Remote Sensing, 11:727-740.
- Meyer, D., Verstraete, M. and Pinty, B., 1995. The effect of surface anisotropy and viewing geometry on the estimation of NDVI from AVHRR. Remote Sensing Reviews, 12:3-27.
- Middleton, E.M., 1991, Solar zenith angle effects on vegetation indices in tallgrass prairie, Remote Sens. Environ. 38:45-62.
- Moreau, L. and Li, Z., 1996, A new approach for remote sensing of canopy absorbed photosynthetically active radiation. II: Proportion of canopy absorption. Remote Sens. Environ. 55:192-204.
- Moody, A. and Strahler, A.H., 1994, Characteristics of composited AVHRR data and problems in their classification. Int. J. Remote Sensing, 15(17), 3473-3491.
- Myneni, R.B., Hall, F.G., Sellers, P.J., and Marshak, A.L., 1995, "The interpretation of spectral vegetation indices", IEEE Trans. Geosci. Remote Sens.
- Myneni, R.B. and Asrar, G., 1993, Atmospheric effects and spectral vegetation indices, Remote Sens. Environ.

Perry, C.R., Jr. and Lautenschlager, L.F., 1984, "Functional equivalence of spectral vegetation indices", *Remote Sens. Environ.*, 14:169-182.

Pinter, P.J., Jr., 1993, Solar angle independence in the relationship between absorbed PAR and remotely sensed data for alfalfa, *Remote Sens. Environ.* 46:19-25.

Pinty, B. and Verstraete, M.M., 1992, GEMI: A non-linear index to monitor global vegetation from satellites, *Vegetatio* 101:15-20.

Price, J.C., 1992, Estimating vegetation amounts from visible and near infrared reflectance measurements, *Remote Sens. Environ.*, 41:29-34.

Price, J.C., 1991. Timing of NOAA afternoon passes. *Int. J. Remote Sensing*. 12(1), 193-198.

Price, J.C., 1987. Calibration of Satellite Radiometers and the Comparison of Vegetation Indices. *Rem. Sensing Environ.*, 21:419-422.

Prince, S.D., Kerr, Y.H., Goutorbe, J.P., Lebel, T., Tinga, A., Bessemoulin, P., Brouwer, J., Dolman, A.J., Engman, E.T., Gash, J.H.C., Hoepffner, M., Kabat, P., Monteny, B., Said, F., Sellers, P., and Wallace, J., 1995, "Geographical, biological and remote sensing aspects of the Hydrologic Atmospheric Pilot Experiment in the Sahel (HAPEX-Sahel)", *Remote Sens. Environ.*, 51:215-234.

Prince, S.D., Justice, C.O., and Moore, B., 1994, Remote Sensing of NPP. IGBP DIS Working Paper #10, IGBP-DIS, Paris.

Prince, S.D., 1991, A model of regional primary production for use with coarse resolution satellite data. *International Journal of Remote Sensing*, 12(6):1313-1330.

Prince, S.D. and Justice, C.O., 1991, (Editorial) Special issue on Coarse Resolution Remote Sensing of the Sahelian Environment. *International Journal of Remote Sensing*, 12(6):1137-1146.

Privette, Myneni, R.B., Emery, W.J. and Hall, F.G., 1996a. Optimal sampling conditions for estimating grassland parameters via reflectance model inversions. *IEEE Trans. Geosci. Remote Sens.* Vol. 34(1):272-284.

Privette, J.L., Deering, D.W., and Eck, T.E., 1996b. Estimating albedo and nadir reflectance through inversion of simple BRDF models with AVHRR/MODIS-like data. *J. Geoph. Res.* BOREAS special issue, submitted.

Qi, J., Chehbouni, A., Huete, A.R., Kerr, Y.H. and Sorooshian, S., 1994a, A modified soil adjusted vegetation index, *Remote Sens. Environ.*, 48:119-126.

- Qi, J., Huete, A.R., Cabot, F., and Chehbouni, A., 1994b. Bidirectional properties and utilizations of high spectral resolution spectra from a semi-arid watershed. *Water Resour. Res.*, 30 1271-1279.
- Qi, J., Huete, A.R., Hood, J., and Kerr, Y., 1994c. Compositing Multi-temporal remote sensing data sets. *PECORA 11, Symposium on land information systems*, Sioux Falls August 1993. p. 206-213.
- Qi, J., Huete, A.R., Moran, M.S., Chehbouni, A., and Jackson, R.D., 1993. Interpretation of vegetation indices derived from Multi-temporal SPOT images. *Remote Sens. Environ.* 44:89-101.
- Rahman, H., Pinty, B. and Verstraete, M.M., 1993. Coupled surface-atmosphere reflectance (CSAR) model 2. Semiempirical surface model usable with NOAA AVHRR. *J. Geophys. Res.* 89(D11):20791-20801.
- Richardson, A.J. and Wiegand, C.L., 1977, Distinguishing vegetation from soil background information, *Photogramm. Eng. Remote Sens.* 43:1541-1552.
- Roujean, J.L., Leroy, M., Podaire, A., and Deschamps, P.Y., 1992. Evidence of surface reflectance bidirectional effects from a NOAA/AVHRR multi-temporal data set. *Int. J. Remote Sensing* 13(4), 685-698.
- Roy, D.P., 1996. The MODIS Land (MODLAND) quality assurance plan (draft)
- Running, S.W., Justice, C., Salomonson, V., Hall, D., Barker, J., Kaufmann, Y., Strahler, A., Huete, A., Muller, J.P., VanderBilt, V., Wan, Z.M., Teillet, P. and Carneggie, D., 1994. Terrestrial Remote Sensing Science and Algorithms planned for EOS/MODIS. *Int. J. Remote Sensing*, Vol. 15, 17:3587-3620.
- Running, S.W., 1990, Estimating terrestrial primary productivity by combining remote sensing and ecosystem simulation, IN: *Ecological Studies Vol "Remote Sensing of Biosphere Functioning"*. H. Mooney and R. Hobbs., eds. Springer-Verlag, pp. 65-86.
- Running, S.W., Nemani, R.R., Peterson, D.L., Band, L.E., Potts, D.F., Pierce, L.L. and Spanner, M.A., 1989, Mapping regional forest evapotranspiration and photosynthesis by coupling satellite data with ecosystem simulation, *Ecology* 70:1090-1101.
- Runyon, J., Waring, R.H., Goward, S.N., and Welles, J.M., 1994, "Environmental limits on net primary production and light-use efficiency across the Oregon transect", *Ecological Applications*, 4:226-237.
- Salomonson, V.V., Barnes, W.L., Maymon, P.W., Montgomery, H.E. and Ostrow, H., 1989, MODIS: advanced facility instrument for studies of the earth as a system, *IEEE Trans. Geosci. Remote Sens.* 27:145-153.

Sellers, P.J., Tucker, C.J., Collatz, G.J., Los S., Justice, C.O., Dazlich, D.A., and Randall, D.A., 1994, "A global 1° * 1° NDVI data set for climate studies. Part 2 - The adjustment of the NDVI and generation of global fields of terrestrial biophysical parameters", *Int. J. Remote Sensing*, 15:3519-3545.

Sellers, P.J., 1985, Canopy reflectance, photosynthesis and transpiration, *International Journal of Remote Sensing*, 6:1335-1372.

Singh, S.M., 1988, Simulation of solar zenith angle effect on global vegetation index (GVI) data, *Int. J. Remote Sensing*, 9:237-248.

Slater, P.N., and Jackson, R.D., 1982, Atmospheric effect on radiation reflected from soil and vegetation as measured by orbiting sensors using various scanning directions, *Appl. Opt.* 21:3923-3931.

Strahler, A, et al., 1995. MODIS BRDF/Albedo Product : ATBD version 3.2.

Teillet, P.M., and Fedosejevs, G., 1995, "On the dark target approach to atmospheric correction of remotely sensed data", *Canadian J. Remote Sens.* (in press).

Teillet P.M. and Staentz, K., and Williams, D.J., 1994. Effects of spectral and spatial resolutions on NDVI. In: *Proceedings of the International Symposium on Spectral Remote Sensing Research*, 10-15 July, 1994, San Diego, I-365-374.

Teillet P.M. and Staentz, K., 1992. Atmospheric effects due to topography on MODIS vegetation index data simulated from AVIRIS imagery over mountainous terrain. *Can. J. Remote Sensing* 18(4), 283-291.

Teillet, P.M. (1989), Surface reflectance retrieval using atmospheric correction algorithms, *Proceedings 1989 International Geoscience and Remote Sensing Symposium (IGARSS '89)*, (Vancouver, British Columbia: IGARSS) pp. 864-867.

Townshend, J.R.G., 1994, Global data sets for land applications from the AVHRR: an introduction. *Int. J. Remote Sensing*, 15:3319-3332.

Townshend, J.R.G., Justice, C.O., Skole, D., Malingreau, J.P., Cihlar, J., Teillet, P., Sadowski, F., and Ruttenberg, S., 1994, "The 1 km resolution global data set: needs of the International Geosphere Biosphere Programme", *Int. J. Remote Sensing*, 15:3417-3441.

Townshend, J.R.G., Justice, C.O., Gurney, C. and McManus, J., 1992, The impact of misregistration on the detection of changes in land cover, *IEEE Trans. Geosci. Remote Sens.*, 30(5):1054-1060.

Townshend, J.R.G., C. Justice, W. Li, C. Gurney, and J. McManus, 1991, "Global land cover classification by remote sensing: present capabilities and future possibilities", *Remote Sens. Environ.*, 35:243-256.

Tucker, C.J. and Sellers, P.J., 1986, Satellite remote sensing of primary productivity, *International Journal of Remote Sensing*, 7:1395-1416.

Tucker, C.J. Holben, B.N., Elgin, J.H. and McMurtrey, 1981, Remote sensing of total dry matter accumulation in winter wheat. *Remote Sens. Environ.* 11:171.

Tucker, C.J., 1979, Red and photographic infrared linear combinations for monitoring vegetation, *Remote Sens. Environ.* 8:127-150.

Verhoef, W., 1984, Light scattering by leaf layers with application to canopy reflectance modeling: the SAIL Model, *Remote Sens. Environ.* 16:125-141.

Vermote, E., Tanré, D., Deuzé, J.L., Herman, M., and Mockette, J.J., 1996, Second Simulation of the Satellite Signal in the Solar Spectrum: an overview. *IEEE Trans. Geosc. Remote Sens.*, (in press)

Vermote, E., Remer, L.A., Justice, C.O., Kaufman, Y.J., and Tanré, 1995, ATBD Atmosphere correction algorithm: Spectral reflectances (MOD09), Version 2.

Viovy, N., Arino, O. and Belward, A.S., 1992. The best index slope extraction (BISE): A method for reducing noise in NDVI time series. *Int. J. Rem. Sensing*, Vol:13, 8:1585-1590.

Vogelmann, T.C., Rock, B.N., and Moss, D.M., 1993, Red edge spectral measurements from sugar maple leaves, *Int. J. Remote Sens.* 14:1563-1575.

Walter-Shea, E.A., Privette, J., Cornell, D., Mesarch, M.A., Hays, C.J., 1996, Relationship between directional spectral vegetation indices and leaf area and absorbed radiation in alfalfa. *Remote Sens. Environ.* (In press)

Walthall, C.L., Norman, J.M., Welles, J.M., Campbell, G., and Blad, B.L., 1985, Simple equation to approximate the bi-directional reflectance from vegetative canopies and bare soil surfaces," *Applied Optics*, 24(3), pp. 383-387.

Wanner W., X.Li, A.H. Strahler, 1995. On the Derivation of kernel-driven models of bidirectional reflectance. *J. Geoph. Res.*, 100, D10, 21077-21089.

Wickland, D.E., 1989, Future directions for remote sensing in terrestrial ecological research, In *Theory and Applications of Optical Remote Sensing* (G. Asrar, ed.), Wiley Series in Remote Sensing, Wiley, New York, pp. 691-724.

Wiegand, C.L., Richardson, A.J., Escobar, D.E., Gebermann, A.H., 1991, Vegetation indices in crop assessments, *Remote Sens. Environ.* 35:105-119.

Wu, A., Li, Z. and Cihlar, 1995, Effects of land cover type and greenness on advanced very high resolution radiometer bidirectional reflectances: Analysis and removal. *J. Geophys. Res.*, 100(D5), 9179-9192.

Yoder, B.J., and Waring, R.H., 1994, The normalized difference vegetation index of small Douglas-fir canopies with varying chlorophyll concentrations, *Remote Sens. Environ.* 49:81-91.

APPENDIX A VI ERROR ANALYSIS

Co-registration Error Analysis

δ - track shift

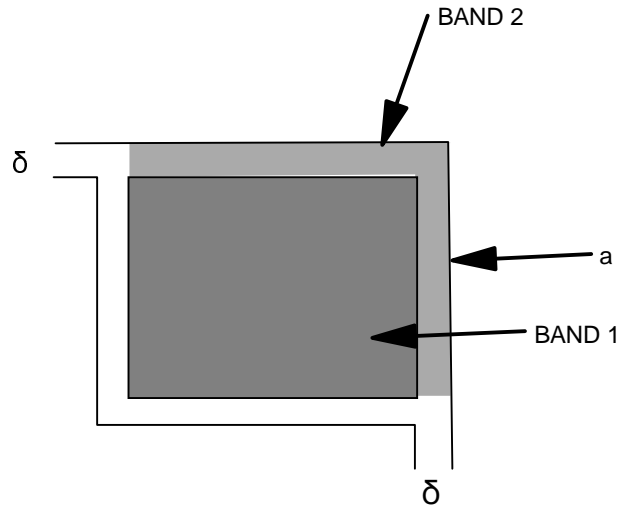
a - Common area of band 1 & band 2

Δ - VIs error because of track shift

n - NIR band

r - Red band

b - Blue band



1. NDVI

1) if NIR = true:

$$\Delta = \text{NDVI1} - [(n_1 - r_1') / (n_1 + r_1')]$$

$$\text{NDVI1} = [(n_1 - r_1) / (n_1 + r_1)]$$

$$r_1' = ar_1 + (1 - a) r_2$$

2) if Red = true:

$$\Delta = \text{NDVI1} - [(n_1' - r_1) / (n_1' + r_1)]$$

$$n_1' = an_1 + (1 - a) n_2$$

2. SAVI

1) if NIR = true:

$$\Delta = \text{SAVI1} - 1.5 [(n_1 - r_1') / (n_1 + r_1' + 0.5)]$$

$$\text{SAVI1} = 1.5 [(n_1 - r_1) / (n_1 + r_1 + 0.5)]$$

2) if Red = true:

$$\Delta = \text{SAVI1} - 1.5 [(n_1' - r_1) / (n_1' + r_1 + 0.5)]$$

3. ARVI

- 1) if NIR = true:

$$\Delta = \text{ARVI1} - [(n_1 - 2^*(r_1') + b_1') / (n_1 + 2^*(r_1') - b_1')]$$

$$\text{ARVI1} = [(n_1 - 2^*(r_1) + b_1) / (n_1 + 2^*(r_1) - b_1)]$$

$$b_1' = ab_1 + (1 - a) b_2$$

- 2) if Red = true:

$$\Delta = \text{ARVI1} - [(n_1' - 2^*(r_1) + b_1') / (n_1' + 2^*(r_1) - b_1')]$$

- 3) if Blue = true:

$$\Delta = \text{ARVI1} - [(n_1' - 2^*(r_1') + b_1) / (n_1' + 2^*(r_1') - b_1)]$$

4. SARVI

- 1) if NIR = true:

$$\Delta = \text{SARVI1} - 1.5 [(n_1 - 2^*(r_1') + b_1') / (n_1 + 2^*(r_1') - b_1' + 0.5)]$$

$$\text{SARVI1} = 1.5 [(n_1 - 2^*(r_1) + b_1) / (n_1 + 2^*(r_1) - b_1 + 0.5)]$$

- 2) if Red = true:

$$\Delta = \text{SARVI1} - 1.5 [(n_1' - 2^*(r_1) + b_1') / (n_1' + 2^*(r_1) - b_1' + 0.5)]$$

- 3) if Blue = true:

$$\Delta = \text{SARVI1} - [(n_1' - 2^*(r_1') + b_1) / (n_1' + 2^*(r_1') - b_1 + 0.5)]$$

Calibration Error & Band Shift Analysis

$\delta\%$ - Typical Calibration Required Accuracy (relative error)

Δ - Absolute error

1. Error Transform Equation

If $y = f(x_1, x_2, x_3, \dots, x_n)$, and $\Delta_1, \Delta_2, \Delta_3, \dots, \Delta_n$ are maximum absolute error of $x_1, x_2, x_3, \dots, x_n$, then,

Maximum Absolute error of y is:

$$\Delta_y = [|(\partial f)/(\partial x_1)| \Delta_1 + |(\partial f)/(\partial x_2)| \Delta_2 + |(\partial f)/(\partial x_3)| \Delta_3 + \dots + |(\partial f)/(\partial x_n)| \Delta_n]$$

Maximum Relative Error of y is:

$$\delta_y = [(\Delta_y)/(|y|)] = [|(\partial f)/(\partial x_1)| [(\Delta_1)/(|y|)] + |(\partial f)/(\partial x_2)| [(\Delta_2)/(|y|)] + \dots + |(\partial f)/(\partial x_n)| [(\Delta_n)/(|y|)]]$$

2. VI's Error Because of Calibration Error & Band Shift

1) NDVI

$$\Delta \text{NDVI} = |(\partial \text{NDVI})/(\partial n)| \Delta_n + |(\partial \text{NDVI})/(\partial r)| \Delta_r$$

$$= [|2r| \Delta_n + |2n| \Delta_r] / (n + r)^2$$

2) SAVI

$$\Delta_y = |(\partial \text{SAVI})/(\partial n)| \Delta_n + |(\partial \text{SAVI})/(\partial r)| \Delta_r$$

$$= 1.5 [|(2r + 0.5)| \Delta_n + |(-2n - 0.5)| \Delta_r] / (n + r + 0.5)^2$$

3) ARVI

$$\Delta_y = |(\partial \text{ARVI})/(\partial n)| \Delta_n + |(\partial \text{ARVI})/(\partial r)| \Delta_r + |(\partial \text{ARVI})/(\partial b)| \Delta_b$$

$$= [|(4r - 2b)| \Delta_n + |(-4n)| \Delta_r + |(2n)| \Delta_b] / (n + 2r - b)^2$$

4) SARVI

$$\begin{aligned}\Delta_y &= |(\partial(\text{SARVI})/(\partial n)| \Delta_n + |(\partial(\text{SARVI})/(\partial r)| \Delta_r + |(\partial(\text{SARVI})/(\partial b)| \Delta_b \\ &= 1.5 [(4r - 2b + 0.5) \Delta_n + (-4n - 0.5) \Delta_r + (2n + 0.5) \Delta_b] / (n + 2r - b + 0.5)^2\end{aligned}$$

APPENDIX C: SWAMP REVIEW May 1996

Panelists were invited to rate and provide comments on each of the EOS-AM 1 Land Data Products according to the following points:

EOS-AM 1 Data Product Review Criteria/Questions:

1. The data product

- (a*) technical/scientific soundness of the algorithm/approach described
- (b*) value of the data product to the Land science community
- (c*) soundness of the validation strategy
- (d*) extent to which 1994 ATBD review issues have been addressed
- (e) near-term recommendations for improvements to the data product
- (f) long-term recommendations for improvements or additions to the data product

2. Balance of Land Data Products as generated by EOS-AM 1 (i.e. ASTER, MISR, MODIS) to meet the needs of the broader Land science community

- (a*) extent to which the ATBD has addressed the compatibility of the role of this data product (and its accuracies) with the other instrument data products and the needs of the broader land science community
- (b*) assessment of plans for the comparison or enhancement of similar data products from the other instruments?
- (c) recommendations for changes to improve the balance of land data products

For each of the above review questions marked with an asterisk, the reviewers were asked to assign a numerical score according to the following guide:

- 9 - Excellent, strongly agree or high
- 5 - average, neutral, medium
- 1 - poor/needs work, disagree, or low
- 0 - insufficient information
- N/A - not applicable

7.2 Review Comments: Classification, Biophysics Products

7.2.1a Data Product: MOD13 - Gridded vegetation indices (NDVI_{max})

Huete et al.

(Review based on ATBD-MOD-14 dated November, 1994, and presentation at workshop, May 16, 1996)

(a) technical/scientific soundness of the algorithm/approach described (Rating: 4)
The document does not explain the product clearly and completely in any one section; thus the characteristics are listed first to lay out the basis for subsequent comments.

The Level 2 VI is a daily product. Four Level 2 VI products are proposed for generation, the combinations of resolution (250m, 500m) and atmospheric correction (Rayleigh and ozone only vs. Rayleigh, ozone, aerosols; refer to Fig. 10 of ATBD. Note that there have been a few changes to this scenario, based on the viewgraphs from the ATBD

review (atmospherically corrected products; 250m and 25 km pixel sizes only); however, the details are not clear and thus the present discussion relies more on the ATBD document). This product would be in the satellite projection, not resampled. The stated reason for using two versions of atmospheric corrections is that good aerosol data may not be available everywhere in the world. The reason for producing two versions of VI (NDVI, MVI/SARVI) is that NDVI suffers from background soil effects and presumably also atmospheric effects, for which the MVI/SARVI is compensated. Cloud masks (another MODIS product) would be used to eliminate cloudy or cloud shadow pixels. It is assumed that Level 2 product is intended for use by EOS data users, i.e. not only an intermediate product during processing to Level 3.

The production of several versions of the same parameter would be justified if each provides unique, new information. It is not evident that the four products do.

It is not evident that MVI/SARVI presents sufficient additional information to warrant its production. MVI/SARVI aims to compensate for atmospheric effects and soil effects. It does so using coefficients developed through modeling, using primarily the SAIL model. Atmospheric effects need not be compensated for if one uses atmospherically-corrected data. To compensate for soil effects, MVI/SARVI introduces four constants and a feedback correction loop. The constants are derived through modeling and presumably one set of these would be used for the globe. The assignment of constants for the global data set appears to be rather arbitrary, given the range of soil and atmospheric conditions around the world. The SAIL model does not represent the structure of a vegetation canopy, and will not provide a realistic representation of the forests and other woody cover types (most of which are clumped at several spatial scales). The MVI/SARVI approach loses the simple but powerful functional dependence of the simple ratio (or NDVI) which acts as a strong 'filter' of noise caused by heterogeneous pixels (e.g., forest with a rock outcrop; Chen, 1996; Canadian Journal of RS, in press). Other MVI/SARVI deficiencies were pointed out in the 1994 ATBD review.

From a practical perspective, four very similar products would present a bewildering choice to most users and would burden the processing and data management systems as well as increase costs.

The above arguments lead to a simple solution. EOS should ensure that MODIS channels are fully corrected for atmospheric and bi-directional effects and then produce one product, the NDVI, at 250m. This product could be in the satellite projection but should be fully navigated. If atmospheric aerosol information of varying quality is available around the world this could be handled through quality flags in the product. Alternatively one could have a three-channel product, red/NIR for NDVI and blue channel at 1 km to serve as a "quantitative flag" to assess smoke, aerosol, cloud screening, etc. It should be noted that the maximum pixel size used in the processing implies that other MODIS products, such as land cover, BRDF, cloud mask, land/water masks... be at a 'comparable' resolution.

Other comments about the current product:

- It is proposed that the full atmospheric corrections employ DEM data. Ideally, this is correct but it means that the MODIS data must be precisely navigated so that the geographic position of each pixel is accurately known for this operation.
- Should it be produced, the daily product will not be useful to most users if it is not georeferenced and resampled to a map projection. The resampling should thus have to be considered as part of Level 2 processing stream.
- The simulations in Fig. 7 to 9 of ATBD do not consider the noise caused by heterogeneous pixels that is critical for the derivation of biophysical variables for MODIS pixels.
- Corrections for bi-directional effects (all three angles, not just SZA or VZA) are important to compute surface NDVI. This means that the step now planned for Level 3 product (Fig. 10) needs to be brought to Level 2 processing.
- If fully atmospherically-corrected data are used, there is no need for atmospherically-compensated NDVI.

(b) value of the data product to the Land science community (Rating: 4)

In our opinion, the daily NDVI data will not be useful because the NDVI of the land surface does not change that rapidly and because much of the land will be obscured by clouds on any given day. Thus the product will have many gaps, endlessly frustrating to a user who needs the values for all pixels over an area of interest. Also, with 250m pixels it will be a high volume product with attendant demands on the user's processing capabilities.

As noted in the 1994 ATBD review, a VI map per se has limited value; its primary usefulness lies in the derivation of biophysical parameters on a global scale. We are not confident that the two VIs will allow the derivations of such parameters for all biomes. It appears that the optimal VI depends upon the biophysical parameter one wants to estimate and the biome one is studying. Thus two VIs are not likely to be sufficient. There is an argument for NDVI - continuity with previous data sets, one-to-one relation with simple ratio, linearity with FPAR, ...; beyond that, other VIs are likely to be optimum for various biomes.

(c) soundness of the validation strategy (Rating: 4)

The 1994 ATBD does not explain the validation plans in enough detail to assess their adequacy. On the other hand, it discusses validation beyond the VI itself (e.g., of LAI); this should be the responsibility of the team producing the LAI product. Although the ATBD discusses validation at three levels (Fig. 10), it is only Level 2 validation that should be the responsibility of the team (i.e. of the VI itself). For NDVI, no validation is needed once the correctness of the surface reflectances at a standard viewing geometry is ascertained (presumably, this is the responsibility of other teams/products). If MVI/SARVI or other VIs were to be used, a significant degree of validation would be required. The scope of such validation could be prohibitive if it is to encompass various combinations of atmosphere/soil/vegetation conditions. However, without such validation it cannot be known how well the MVI/SARVI represents the surface

conditions, both in absolute and relative (comparisons among areas) sense. The validation approach can be strengthened significantly through collaboration with one or more radiative transfer modelers and investigation/testing of other VIs for estimation of biophysical parameters for various biomes.

The error analysis used in the ATBD is inadequate as it is based on modeling and does not consider important effects, such as covariance of noise in spectral bands. The simulations appear biased to favor MVI/SARVI. An approach more accepted by other the community members should be followed. Error propagation has not been addressed.

(d) extent to which 1994 ATBD review issues have been addressed (Rating: 4)

The proposed MVI/SARVI was developed by the team members. The 1994 review recommended that the team would benefit either by broadening the team or by collaboration with others. This recommendation is reiterated by this panel.

The review recommended several kinds of sensitivity studies involving soil and leaf litter and the dependence of atmospheric correction on the surface properties. The team has addressed this to some extent (through semi-empirical work) but not adequately. In particular, the possible errors introduced by the MVI/SARVI in ecosystems with no bare soil have not been addressed.

The review recommended use of atmospherically-corrected reflectances and not TOA reflectances. The team has responded to this recommendation by investigating the use of such reflectances in the formulas for VIs.

The team has not responded to the critique of MVI/SARVI limitations (effect of ground cover other than bare soil, interference with canopy shadowing, ..).

(e) near-term recommendations for improvements to the data product

* The aim should be to produce NDVI from fully-corrected surface reflectances and composited over several days. In other words, do not make a 1-day VI a standard MODIS product. The VI product should be produced at the highest spatial resolution feasible, i.e. 250m as envisioned, because of the land surface heterogeneity. Coarser resolution versions would be derived from this basic product. The emphasis here is on a fully integrated approach from corrected surface reflectances to various vegetation indices, that can be used to generate biophysical parameters from quality data.

* The relationship between MODIS NDVI and NDVI computed from AVHRR Pathfinder data should be determined, to ensure continuity of the long-term data series.

* Beyond NDVI, the team should work with other teams to justify the need for a new index/indices based on their usefulness in estimating biophysical parameters in various biomes. The team should collaborate with one or more radiative transfer modelers and

field teams to determine optimal VIs. Candidate VIs should be tested and validated with actual data for various biomes and vegetation types.

(f) long-term recommendations for improvements or additions to the data product

* In the long-term the need for VI-type products should be assessed based on the state-of-the-art in the derivation of biophysical parameters. If the state-of-the-art in this area necessitates the use of indices they should be developed in a systematic way for various biomes through the involvement of field scientists and modelers in atmospheric scattering, radiative transfer from vegetation, and using data from carefully chosen biome sites. An algorithm for creating the data product can be changed fairly easily if the optimal VI is changed and provided the initial MODIS data processing was done appropriately.

7.2.1b. Balance of Land Data Products as generated by EOS-AM 1 (i.e. ASTER, MISR, MODIS) to meet the needs of the broader Land science community

(a) extent to which the data product (and its accuracies) is useful to the broader land science community and meshes with the other instrument data products (Rating: 4)

1-day product will not be useful to the broader community

(b) assessment of plans for the comparison or enhancement of similar data products from the other instruments? (Rating: 3)

MODIS-derived VIs will be used in conjunction with those from other sensors, e.g. ASTER and MISR, for more limited areas. Consistency in sensor calibration, atmospheric corrections and spectral bandwidths need to be ensured. This has not been fully accomplished.

(c) recommendations for changes to improve the balance of land data products
See above (reduce the number of product versions).

7.2.2a Data Product: MOD34 - Gridded VIs & integrated MVI
(Review based on ATBD-MOD-14 November, 1994 and presentation at workshop May 16, 1996)

(a) technical/scientific soundness of the algorithm/approach described
(Rating: 5)

The Level 3 product is understood to be (Fig. 10 of ATBD) four types of products that differ in the type of VI used (NDVI, MVI) and temporal resolution (10 days, 1 month). In addition, each is to be produced with different pixel sizes: a) NDVI (500 m input pixel size; outputs at resolutions 1 km, 10 km, 1 degree) and b)) MVI (1000 m input pixel

size; outputs at resolutions 10 km, 1 degree). Thus, a total of 12 different products are envisioned. In the presentation, two products were described (8-16 days, 250 m, 25 km)

The proposed algorithm assumes (Fig. 10) that Level 2 NDVI or MVI (based on Rayleigh + ozone OR Rayleigh + ozone + aerosols atmospheric corrections) will be geolocated with consideration of topographic effects, resampled, composited over the period of interest, corrected for BRDF effects, and then averaged over the specified pixel size. Fig. 10 seems to be the most specific description of the processing algorithm in the ATBD document; no more specific information could be found, and the table of contents was missing. A viewgraph in the presentation seemed consistent with this description. Based on this information the following comments are offered on the proposed product. It should be noted that an alternative proposal is made below, and it is not suggested that the problems listed below be fixed one-by-one:

- The rationale for keeping NDVI and MVI is insufficient, as discussed for the Level 2 product
- It is not clear how aerosol corrections can be made to the NDVI, based on the Rayleigh + ozone corrected product after all other corrections were made above to individual channels
- Same for BRDF corrections. Simple Walthall model was proposed in the presentation. Collaboration with BRDF teams (Strahler et al) should result in better BRDF corrections.
- The compositing algorithm description in the ATBD is vague and does not generate confidence in its realism. The candidate algorithm described in the presentation is plausible but should be tested in a range of biomes/environments before its adoption for global processing (Cihlar et al., 1994, IEEE Trans. GRS 32: 427).
- The rationale for offering composite products at a coarser resolution (500m for NDVI, 1000m for MVI) is not given. It is true that the composited product has a lower effective spatial resolution compared to 1-day images but on the other hand, the richness of the data set is much reduced by increasing the pixel size 4x. The importance of high spatial resolution has been demonstrated (Townshend et al., 1991, RSE 35: 243). A 250m product proposed in the presentation would eliminate this concern.
- How will the coarser resolution products be generated? If they are to be averaged from the smallest pixels this could be done by the user (to whatever pixel size he/she wishes), or in EOSDIS "on-the-fly" upon receiving data set requests. Producing these routinely and incurring the attendant costs of processing, storage and management seems unnecessary - at least no arguments are put forth to justify this.
- Level 3 product should be the composite NDVI product. The team's responsibility should not include higher level products derived from this (e.g., land cover, LAI etc.; Fig. 10).
- The rationale for a compositing period of 8 or 16 days is not given. Is this related to the 16 day repeat cycle for LANDSAT? Periods based on multiples of 5 are common (e.g. 10 days for Pathfinder AVHRR, 5 days for ISCCP data products). This may be a broader EOS issue as the various composite products should cover the same period. Are a nested hierarchy of time periods feasible?

(b) value of the data product to the Land science community (Rating: 9)

The composited NDVI products (mostly cloud-free) will be of great value to the community because they serve as the starting product for the derivation of biophysical parameters and provide an overview of the vegetation condition globally.

(c) soundness of the validation strategy (Rating: 3)

The validation strategy is not articulated in the ATBD. The important issues are: the soundness of the corrections going into the Level 2 product, the resampling algorithm chosen (should not be nearest neighbor because it degrades spatial resolution and radiometric precision is already ensured from Level 2), and the validation of the compositing algorithm (if different from maximum NDVI).

(d) extent to which 1994 ATBD review issues have been addressed (N/A) No serious issues were raised regarding the composite product.

(e) near-term recommendations for improvements to the data product
It is proposed that the Level 3 VI be simplified as follows:

- * Build on the proposed Level 2 product, i.e. (see more detail in Level 2 VI review): EOS should ensure that MODIS channels (especially 1,2) are fully corrected for atmospheric and bi-directional effects and then produce one product, the NDVI, at 250m. This product could be in the satellite projection but should be fully navigated. If atmospheric aerosol characterization of varying quality is available from around the world, this could be handled through quality flags in the product.

- * Resample the daily products, and composite over 5-8 (ideally) or 10-16 (backup) day periods. Explore possible compositing options but unless a new algorithm can be demonstrated to be superior in a range of environments, and to be consistent and generating a minimum of artifacts, use maximum NDVI (constrained by maximum view zenith etc.) as the compositing criterion. If cloud masks are of sufficient accuracy (especially for partial and thin clouds) consider using all clear-sky pixels in computing mean VI and statistics (stdev/range,...) for the compositing period (especially monthly time step). The desirability of retaining angular information for the initial composited products should be determined (it should not be necessary if the corrections are good but it would be required at least for quality control).

- * Produce lower resolution products (1 km, 1 degree) on-demand only.

- * Carefully consider the possible effects merging VI image products designed to be valid regionally onto the same "global" image product; flag algorithm assumptions.

- * See also comments above under Technical Soundness.

(f) long-term recommendations for improvements or additions to the data product
Better compositing algorithms should be developed, and cross-referenced with the maximum NDVI criterion to establish continuity.

See also recommendations for the Level 2 VI product.

7.2.2b. Balance of Land Data Products as generated by EOS-AM 1 (i.e. ASTER, MISR, MODIS) to meet the needs of the broader Land science community

(a) extent to which the data product (and its accuracies) is useful to the broader land science community and meshes with the other instrument data products (Rating: 6)

The prime users should be developers of biophysical data sets (including land cover,...). However, it is expected that NDVI will be used, especially in the initial period, by many other users because of its illustrative and intuitive value.

(b) assessment of plans for the comparison or enhancement of similar data products from the other instruments? (Rating: 5)

The collaboration with MISR team should be strengthened.

(c) recommendations for changes to improve the balance of land data products
See above.

APPENDIX D: Response to review of 1994 and 1996

Response to Review Panel #1 (June 1994).

1. Degree to which product meets EOS priorities: This was a given a high rating, however only in the context to which the vegetation indices can be used to reliably estimate biophysical parameters. VI maps in itself were deemed valueless. We disagree with this statement since the VI has been used in an operational mode for 16 years providing phenological growing season curves, inter-annual changes in vegetation distributions, famine early warning alerts, etc., all of which use the VI values outright without translation to biophysical parameters. It is also valuable to maintain a minimally altered data set (NDVI values) with no assumptions built into the algorithm, such as would be required in translation to biophysical parameters. Yes, we agree that derivation of biophysical parameters from the vegetation index data set is a high priority for EOS.

2. Appropriateness of input products: we plan to use calibrated surface reflectances, fully corrected for atmosphere in the computation of the NDVI and a second index, if applicable.

3. Error budgets: we agree that further work is needed here, especially in determining whether new sources of error and uncertainty are created in a second index. Additionally, error budgets are being prepared for the NDVI so that the user will have a clear idea on what can and can't be accomplished with the NDVI.

4. Validation strategy: a new validation plan has been included in the version 2 ATBD which presents a clearer strategy involving both radiometric, biophysical, and long term calibration and validation.

5. Broaden the team: the team has been broadened in that two new Post-doctorates have been hired. Dr. Wim van Leeuwen has joined the team as an associate MODIS team member. Dr. Leeuwen has taken primary responsibility for the level 3 vegetation index compositing algorithm. He has also has extensive field radiometry experience, participating in HAPEX-Sahel (2 summers), Walnut Gulch Monsoon 90, and SCAR-B in Brazil. This is very useful with the increased emphasis being placed on validation. Dr. Faizure Rahman has also been hired to work on the vegetation index - biophysical coupling. Dr. Rahman has useful experience in modeling and will work with theoretical and observational data sets to establish both land cover specific and global biophysical relations. This is also needed in the validation effort.

In addition, Chris Justice has extensive experience with the NOAA-AVHRR NDVI data record. He has hired Dr. Jeff Privette to work on the BRDF modeling of angular measurements to attain standard nadir views and constant sun angles for the vegetation index compositing effort. The vegetation index team also receives much support from Eric Vermote in atmospheric correction and derivation of surface reflectance data sets from satellite and aircraft platforms. Ranga Myneni has also participated in the VI program with his canopy radiative transfer models and with

atmosphere-surface radiative coupling. Finally Yoram Kaufman has contributed greatly with the empirical atmospheric resistance concept and development of atmospheric resistant vegetation indices.

6. MNDVI proposed index: there is a misconception that this index is only correcting for bare soils. Part of this reason concerns terminology. In soil science, the top organic layer of undecomposed plant material (litter) is defined as part of a soil profile and is labeled the 'O' horizon. The background adjustment is based upon Beer's Law and concerns the backscattering of canopy transmitted energy back toward the sensor. It is independent of the spectral (or color) properties of the "background" and is only concerned with the brightness of the surface (gray bodies), whether it is soil, litter, water, snow, rocks, etc... Since we believe most ecosystems, except the most dense forests, have a background reflected signal, a correction would be useful since the background reflected signal is not amenable to ratioing.

We disagree with the statement made that the NDVI primarily addresses illumination and canopy shadowing variations. ASAS imagery (3-5 m pixels) has clearly showed canopy shadows to be "brighter" in NDVI values. The shadowed edges of forest boundaries have very high NDVI values, higher than the forest itself, and despite the surface having none or slight amounts of vegetation. Canopy shadows are expected to have higher NIR/red ratios (and thus, NDVI) due to the very low red reflectances yet relative higher (transmitted and scattered) NIR values as long as the canopy is actively photosynthetic. The 'L' factor in the SAVI accounts for this differential red and NIR flux through a canopy. Since NDVI values are higher in canopy shadows, it is difficult to see structural variations in NDVI imagery and the image appears further saturated, with shadows contributing to the higher values. This is also the reason for the forward scattering bias of the NDVI in the 'shaded' view direction. The shadows result in higher NDVI values.

However, it is true that the NDVI will more effectively handle shadows due to irradiance differences caused by topography and cloud shadows since the signal variance is the same in both bands (red and NIR). We felt that the new generation of algorithms being developed for MODIS (atmosphere correction, cloud and cloud shadow masking, surface reflectance retrievals, and bidirectional/ topographic corrections, would reduce if not eliminate the dependence on "ratios" in data processing, noise removal, and information extraction.

We agree that the atmospheric resistance concept cannot do a better job than an atmospheric correction. However, the consistency and accuracy of an atmospheric correction remains to be seen. The atmospheric correction of aerosols will make many assumptions including an estimate of the surface reflectance of 'dark' objects. The aerosol correction grid is coarse and may be as high as 50km. Where there are no dark objects, climatology will be invoked at much coarser resolutions. This means that the high spatial variability of aerosols will not or cannot be corrected for and there will remain 'residual' aerosols in the vegetation index product. The current atmospheric aerosol correction algorithm will basically correct an "average" aerosol loading over much coarser grid cell sizes, relative to the 250 m NDVI product.

Thus, areas with smoke (burning season in the tropics), and particulate pollutants will leave residual aerosol contaminants in the VI product. Since the atmospheric resistant vegetation indices adjust for aerosols, indirectly, on a pixel by pixel basis, and since these VI values remain the same whether the data is corrected for atmosphere or not, we felt that the atmospheric resistance concept can only help the consistency of the final VI product.

However, the atmospheric resistance approach (and improvement) come at a cost, namely related to the 500m pixel size of the blue band which would degrade the final VI product to 500m unless an adequate 'blue sharpening' approach can be implemented. Further research has indicated that the blue band may also respond to shadows in manners not completely understood. We agree that the burden of proof should be on the developers and we continue to use TM images in search of problem areas and unwanted effects. Following this review, we placed much effort in simplifying the MNDVI equation and comparing its performance relative to the NDVI over a wide range of vegetation conditions.

7. Error and sensitivity analysis with fAPAR and LAI: Yes we are looking into VI relations with the biophysical parameters for sensitivity analysis. However, there are separate LAI and fAPAR products being developed and more community input is needed to very define the role of the VIs in the derivation of biophysical parameters in the EOS-era. Current thinking on our part is that the VI-biophysical relations work should continue and serve as a backup to the LAI and fAPAR products being derived from canopy models. The coupling to biophysical parameters is very important to the validation of the VI product, i.e., independent confirmations that the VI is responding to changes in 'real' vegetation parameters. We feel that it would be appropriate to investigate the range of NDVI values expected over various land cover types, canopy structures, and densities of vegetation.

Response to SWAMP Review of May 1996:

In general, there is much constructive criticism in the review report useful for the final implementation of the VI product(s) for the MODIS sensor. The main disappointment is that the review is almost entirely based upon the original, 1994 ATBD document with very little attention placed on the material presented in May 1996 and the accompanying view graph summaries. We would have liked to have seen a thorough critique and review of the material actually presented. Thus there are many comments which were already addressed following the 1994 review.

1. Daily, level 2 VI products:

"The daily VI product is not useful to the land community". This is an interesting and valid comment which needs careful attention and dialogue with the land community. The daily VI data could easily be made available 'on demand', or by request, and not be an operational product. Daily data may only be useful in very particular situations with more frequent land use activities (agriculture) or sudden perturbations such as fire, volcanic activity, and flooding.

2. Too many products at varying spatial resolutions:

The daily and composited VIs would only be made at 250 m and 25° in order to meet different user needs. The 250 m VI product is designed to achieve the best possible resolution consistent with sensor characteristics. The 25° VI product is primarily a climate modeling grid product.

3. Produce a 250m NDVI, with reflectances corrected for atmosphere and bidirectional effects:

Agree. This is the what we are doing already. The different atmospheric processing scenarios presented in the version 1- ATBD were already discarded as discussed in the presentation and only atmospheric corrected, surface reflectance inputs will be used. We also plan on correcting the reflectances for BRDF effects, a major component of the compositing algorithm presented in May 1996.

The review suggests improving upon the simplified Walthall model in BRDF correction with Strahler's BRDF product, not considering spatial resolution discrepancies. There is an inherent limitation of incorporating a 1km BRDF product into the 250m NDVI? Our Walthal testing has always resulted in nadir-value extractions as good as the more complex BRDF models. However, we continue to investigate the possibility of sharpening this 1 km BRDF product for use in 250 m data sets. Furthermore, as mentioned in the ATBD, if we are only interested in nadir-equivalent values rather than the entire BRDF distribution, a simplified model may be sufficient for our needs. The review suggests that the algorithm (compositing) needs to be tested in different environments. We agree, but feel that the global AVHRR data set being used is a step in the right direction.

Lastly, and confusing is the recommendation that the level 3 NDVI should be based upon the maximum value with view angle thresholds? If the data will be corrected for bidirectional and atmospheric effects then there is no longer a maximum value compositing scheme nor view angles to be concerned about. Furthermore, with AVHRR data we have shown the maximum NDVI approach to always yield values 5-15% higher than the nadir values. Our composite scenarios show the view angle threshold approaches to have several limitations and result in many 'discontinuities' in the resulting composited product.

4. NDVI - biophysical relationships:

The review report states that the primary use of an NDVI product is for estimation of biophysical parameters. This is an overly narrow view of the NDVI, ignoring the fact that the NDVI has been primarily used by the land community for the detection of spatial and temporal variations in vegetation or "change detection" (e.g. phenologic and seasonal variations, famine early warning detection, inter-annual drought monitoring, desertification, deforestation, etc.). The use of VIs for biophysical estimations is also a goal of the VI, however, biophysical products are also separate MODIS products (see comment 1, from responses to first review).

5. The VI group needs to be broadened:

Agree. See response comment 5 from first review.

6. 8 and 16 day composites:

Again, the rationale is not in the ATBD as these are very current developments involving dialogues with the broader land community, but the rationale was made in the presentation, namely the repeat cycle of the AM-platform, the distribution of view angles within a composite period, and the need to correct for BRDF.

7. Validation not thorough:

Agree. The validation plan was completed earlier this year and was not in the 1994 ATBD, but was made in the presentation. The version 2 ATBD has a more complete validation plan, which is heavily oriented toward field correlative measurements of biophysical parameters. The review concludes that the NDVI need not be validated once the input reflectances are validated. However, validation is concerned with the outputs of an equation and not the inputs. The reflectance inputs may be highly accurate, but the equation may produce bad results. Validation also requires the assessment of a product through "independent" means, hence the reason for inclusion of biophysical parameters in the validation plan, ie., to ensure that a change in the NDVI corresponds to a "real" change in vegetation parameter. Whether or not one can say the AVHRR-NDVI product was ever validated, the MODIS-NDVI must still be validated separately.

8. One or two VIs:

The review recommends the use of one VI product, the NDVI. This is based upon (1) the lack of sufficient 'uniqueness' in the two VIs proposed, (2) the data will already be atmospherically corrected and hence no need for 'atmospheric resistance' coefficients; and (3) the idea that 4 constants and a feedback loop are too complicated for canopy background correction. These comments are mostly based on the 1994 ATBD document with no consideration of the presentation material, much of it made in response to the original ATBD review. First, the complex and lengthy MNDVI equation presented in the version 1 ATBD, has been greatly simplified. There is only one coefficient for background correction, L , and it has been validated with observational data (satellite and ground). This background adjustment factor was developed from observational data sets and not SAIL simulations and is global, not background specific (see comment 6 in response to first review).

The justification for atmospheric resistance was made at the presentation and is based on the coarse aerosol correction grid, which will leave residual aerosols given the high spatial variability in aerosol optical depths (see comment 6 in response to first review).

A repeated comment about "noise" due to heterogeneous pixels is made without clarification. Heterogeneous pixels represent 'real' spatial variations in vegetation and the NDVI should depict this heterogeneity, not mask or filter it. As mentioned in the response to the first review, the NDVI has many useful ratioing properties which were quite valuable when uncalibrated radiances were used, however, the usefulness of ratios needs to be re-assessed when we start using well-calibrated, atmospheric corrected surface reflectances as input to the vegetation index equations. We have found that many of the so called "ratioing" advantages of the NDVI are, in fact due to the non-linear compression of NDVI values. When the simple ratio, NIR / red, is applied to the same data sets, we see that the ratio does not normalize the data nor minimize noise (see e.g., Fig. 2.5). We believe that the NDVI may very well mask "noise" in heterogeneous pixels through signal compression and not through any useful "ratioing" properties.

The review report has also left the door open to a second VI. There is discussion of including the blue band for quantitative assessment of smoke, aerosols, and clouds. Long term recommendations include incorporation of field scientists and radiative transfer modelers for new state of the art VIs coupled to biophysical vegetation parameters. This has already been carried out in broadening of the team with two new Postdoctorates. We feel that the primary strength of a second (enhanced) VI is linearity and sensitivity to vegetation from deserts to dense forests and the associated scaling compatibilities. The saturation of the NDVI was not mentioned in the review report as a 'saturated' NDVI would preclude the estimation of biophysical parameters which the report stresses so highly. We agree that atmosphere and background influences should not be the major driver in implementation of a second index.

9. Final Comments:

In the version 2 ATBD we show that the non-linear transform of the NDVI from the simple ratio is primarily responsible for the loss in sensitivity at dense levels of vegetation. Most indices, including the difference vegetation index (NIR - red) and NIR/red ratio maintain sensitivity at higher levels of vegetation. Thus, there are several avenues to proceed. The simple ratio could be used as the enhanced vegetation index, or possibly some 'normalized' version of the ratio. However, the simple ratio is functionally equivalent to the NDVI (no scatter) and thus would not represent uniqueness in a second VI. The simple ratio, as the NDVI, is too sensitive to canopy backgrounds, however this could be easily corrected (or minimized) with the global adjustment factor, L . The NDVI could be similarly adjusted with the SAVI. There is concern that an ' L ' term would destroy the ratioing properties of the NDVI or simple ratio, however, we need to re-assess the importance of ratios and noise removal in atmospherically corrected, well calibrated, surface reflectance data sets. Furthermore, as mentioned above, the so called ratioing advantages of the NDVI may be due to signal compression.

The difference vegetation index (NIR - red), which is not functionally equivalent to the NDVI, similarly has a good linear range with minimal saturation problems. This index also has much less canopy background and atmosphere influences than the NDVI.

The atmospheric resistance concept in a second VI needs further research before it can be used as an operational product. We believe the concept and theory with the 'blue' band correction is sound, but is still in preliminary stages of testing. These indices are not entirely new, as the ARVI reduces to the NDVI, and the SARVI reduces to the SAVI, when the blue band correction term is removed.

Finally, the last point to consider, and related to the review panel comment about finding biophysical-specific VIs, is that an enhanced vegetation index has been found to be quite useful in canopy structural studies. Its extended sensitivity range enables better estimates of LAI and its non-saturation over canopy shadows allows one to better analyze canopy structure and roughness. The NDVI, on the other hand, could remain the primary variable in estimating fAPAR, which is supposed to saturate rather quickly as does visible reflectances in general.

Since the review panel report was released less than 4 weeks prior to the deadline for this ATBD submission, we were not able to fully incorporate and reconsider all of the comments and suggestions made in the report. We plan on revising the ATBD again following the December, 1996 review and with other peer inputs from the scientific community.